Titre: Title:	Experimental investigations on the initiation of external suffusion
Auteur: Author:	Maryam Maknoon
Date:	2009
Type:	Mémoire ou thèse / Dissertation or Thesis
Référence: Citation:	Maknoon, M. (2009). Experimental investigations on the initiation of external suffusion [Mémoire de maîtrise, École Polytechnique de Montréal]. PolyPublie. https://publications.polymtl.ca/8433/

UNIVERSITÉ DE MONTRÉAL

EXPERIMENTAL INVESTIGATIONS ON THE INITIATION OF EXTERNAL SUFFUSION

MARYAM MAKNOON

DÉPARTEMENT DES GÉNIES CIVIL
GÉOLOGIQUE ET DES MINES
ÉCOLE POLYTECHNIQUE DE MONTRÉAL

MÉMOIRE PRÉSENTÉ EN VUE DE L'OBTENTION
DU DIPLÔME DE MAÎTRISE ÈS SCIENCES APPLIQUÉES
(GÉNIE CIVIL)
JUILLET 2009

Your file Votre référence
ISBN: 978-0-494-53912-5
Our file Notre référence
ISBN: 978-0-494-53912-5

UNIVERSITÉ DE MONTRÉAL

ÉCOLE POLYTECHNIQUE DE MONTRÉAL

Ce mémoire intitulé :

EXPERIMENTAL INVESTIGATIONS ON THE INITIATION OF EXTERNAL SUFFUSION

présenté par : MAKNOON, Maryam

en vue de l'obtention du diplôme de : Maîtrise ès sciences appliquées

a été dûment accepté par le jury d'examen constitué de :

M., FUAMBA Musandji, Ph.D., président

M. MAHDI Tew-Fik, Ph.D., membre et directeur de recherche

M. BOUAZZA Zoubir, Ph.D., membre

DEDICATION

To my dear family
and friends
for their support

ACKNOWLEDGEMENTS

First of all, I would like to thank my supervisor, Professor Tew-Fik Mahdi for accepting me as his student, for his support and encouragements during my work and his confidence on me.

I would like to thank Hydro Quebec members for giving me the opportunity to participate in their work; I appreciate their professional and financial supports.

Also, I would like to thank Étienne Bélanger from hydrodynamic laboratory who patiently advised me during the assembly and the realization of the experiments. I am also thankful to the help of André Ducharme and the members of mine laboratory during the period of my studies.

Last but not least, I want to thank my family and friends for their support, specially my father, for standing beside me all the way through to this point.

RÉSUMÉ

Cette recherche présente les investigations expérimentales conduites sur le modèle construit dans le laboratoire d'hydrodynamique. Elle examine le phénomène de la suffusion externe sur l'interface de trois différentes couches du sol : argile/moraine, sable et gravier.

Cette thèse a examiné le processus de suffusion externe sur l'interface de couches du sol, en raison de l'augmentation de l'eau en amont d'une digue. En considérant les différents modèles construits comme une partie d'une digue, l'argile/la moraine a formé le noyau, le sable représente le filtre et le gravier a joué le rôle de la couche perméable.

Il y a eu plusieurs modèles avec des différences dans la géométrie ou des composants matériels qui ont été construits dans le cadre de cette recherche. Elles ont été le sujet de l'augmentation du niveau d'eau en amont jusqu'à un niveau maximal ce qui entraînera des changements de gradient hydraulique.

La première série de tests, (Sept types au totale), a consisté sur les modèles avec des géométries et des granulométries différentes au niveau du gravier dont les résultats obtenus n'ont montré aucune évidence considérable de suffusion sur l'interface argile/moraine et le sable, tandis que les données visuelles et quantitatives ont prouvé la présence de la suffusion sur l'interface de sable et le gravier.

Il a été montré que l'augmentation de la longueur de filtre ou l'utilisation des pentes en marches d'escalier ne peut pas avoir une grande influence sur l'initiation de la suffusion tandis que les grains fins de gravier ont un grand impact sur le taux d'érosion.

Le deuxième série de tests (Quatre types au totale) a été divisé en deux parties, utilisant le modèle le plus critique de première série ;

Quatre tests ont été exécutés dont deux types avec la granulométrie différente du sable. Selon quoi nous avons utilisé les grains plus fins et plus grossiers comparant avec le type critique de la série première.

Les deux suivants teste avec des graviers ayant la granulométrie différente ont été accompli par rapport du type critique de la première série qu'on peut les définir plus ou moins avec les porosités différents.

Les résultats ont révélé que les sables avec des grains plus fins se sont dilués plus facilement que les sables aux grains plus gros ayant avec un taux inférieur de suffusion. Aussi, le gravier à faible porosité peut empêcher suffusion plus facilement que la porosité du gravier plus élevées. À la suite de toutes ces données, en se concentrant sur gradient hydraulique critique au début du mouvement qu'on peut conclure que, malgré les différences dans le type de tests, le gradient hydraulique critique a environ la même valeur.

ABSTRACT

This research study presents the experimental investigations conducted on a laboratory constructed model in the laboratory of hydrodynamic, surveying the phenomenon of external suffusion on the interface of three different soil layers: clay/moraine, sand and gravel.

This work surveyed the process of external suffusion on the interface of soil layers in an embankment, caused by water augmentation in the upstream. Considering the constructed models as representing a part of an embankment, the clay/moraine formed the core, the sand was used as filter and the gravel performed the role of the pervious layer.

Several different types of models (in geometry or component materials) were constructed and subjected to a water level increase in the upstream preventing any over topping, which resulted in hydraulic gradient changes.

The first series of tests, including seven type of test, consisted of models with different geometries and gravel grain size distributions. The obtained results showed no evidence of considerable suffusion on the interface of clay/moraine and sand, while the visual and quantitative data proved the presence of suffusion on the interface of sand and gravel.

It was shown that increasing the length of the filter layer or using step like slopes may not have a great influence on the initiation of suffusion, whereas the fine-grained gravel has a great impact on the erosion rate.

The second series of tests, consisting of four types, was divided into two parts. Using the most critical test from series one, four tests were executed: two type with different sand grain size distributions, finer and coarser compared to the critical type from series one , and two test types with gravel with different grain size distributions, more and less porosity compared to the critical test type from series one.

The results revealed that types of sand with finer grains wash out more easily, and coarser sands have a lower rate of suffusion.

Also, gravel with lower porosity can prevent suffusion easier than gravel with higher porosity. With all of this data as the result, focusing on the critical hydraulic gradient on the initiation of movement, one could conclude that despite the differences in the type of tests, the critical hydraulic gradient has approximately the same value ($\approx 0.0332 \pm 0.0007$).

CONDENSÉ EN FRANÇAIS

Depuis des décennies, les digues et les barrages en terre ont été construits avec des matériaux et ou de géométrie différente pour stocker ou contrôler l'écoulement de l'eau. Généralement dans ces constructions, l'écoulement a la capacité de traverser la digue. Le passage de l'eau dans les milieux poreux pourrait créer des problèmes différents selon la stabilité ou le fonctionnement des constructions. Si ces problèmes ne sont pas reconnus et contrôlés à temps, ils pourraient nuire au bon fonctionnement du barrage.

Un aspect important de cette procédure, est le mouvement de particules du sol par l'écoulement d'eau a l'intérieure du sol, tel que mentionné par Foster et al. [1]. Cet écoulement d'eau à l'intérieure de la couche du sol est appelé « l'érosion interne ». Il est une des causes importantes de la rupture des barrages et selon les études (Foster et al. [1]) sur mille cent dix-neuf barrages, autour de quarante-six pour cent des ruptures étaient le résultat d'érosion interne.

Des barrages en terre sont construits avec des différents matériaux pour chaque couche (le noyau, le filtre et la partie perméable). Les matériaux utilisés et les méthodes de construction de chaque couche ainsi que les propriétés d'écoulement de l'eau ont tous un impact sur les mouvements de particules à l'intérieur du milieu poreux.

L'érosion interne peut être considérée comme un des phénomènes très complexe à l'intérieur des barrages. Généralement, le début de la procédure est difficile à détecter. Les premiers signes visibles de ce phénomène qui pourraient être observés se passent soit pendant la phase de progression soit durant la phase de la rupture (Mattsson et al.) [2]

Il existe toujours les possibilités de conjoncture pendant le premier entreposage des eaux ou après quelques années de fonctionnement. Pourtant, il n'est pas facile de

détecter le début du processus puisque les dégâts causés par l'érosion interne détruisent très souvent toutes les évidences.

Par conséquent, la plupart des connaissances sur ce phénomène sont basées sur les cas réels ainsi que les enquêtes effectués sur les ruptures des barrages.

Suite à de changements climatiques, la variation du niveau d'eau en amont des barrages va causer l'augmentation du gradient hydraulique. Cela entraîne un débit plus élevé de l'eau qui traverse le barrage et peut avoir un impact important sur le taux d'érosion interne.

En effet, la force dynamique créée par l'écoulement d'eau sur les particules du sol est dans la même direction que l'écoulement et le gradient hydraulique. Le mécanisme du mouvement des particules du sol donne lieu à l'apparition de quatre différents types d'érosion interne : le renard (*piping*), l'érosion régressive (*backward erosion*), la fuite concentrée (*concentrated leakage*) et la suffusion (*suffusion*). Dans ce projet, le centre d'intérêt est le phénomène de la suffusion et en particulier la forme appelée suffusion externe.

Le processus de suffusion comprend le mouvement, le réarrangement, le remplacement ou le transport de particules fines dans le squelette du sol (quand il est constitué de grosses particules) par la force de suintement [3-5]. Or, cela conduit souvent à la diminution de la densité du sol et l'augmentation de la perméabilité. Les paramètres influençant la suffusion pourraient être d'ordre géométriques ou bien hydrauliques [5, 6].

En vérifiant les propriétés géométriques, on peut expliquer si la structure des sols disposés à l'érosion est instable de l'intérieur ou pas. Par « stabilité », on se réfère à la capacité du sol d'empêcher la perte de ses particules fines lorsque l'écoulement suinte par leur squelette [7].

Selon Kovac [6], il existe deux types de suffusion distinctes : la suffusion interne et la suffusion externe. Dans le premier cas des particules fines migrent sans quitter la

couche du sol et la masse totale reste inchangée. Par la suite, selon l'accumulation ou l'évacuation des grains, la perméabilité et la porosité locale pourraient diminuer ou augmenter respectivement.

Dans le deuxième cas, la suffusion externe, des particules fines quittent la couche de sol en causant l'augmentation de porosité et perméabilité totale des sols.

Les résultats des recherches, déjà effectués sur la suffusion interne, focalisent plus souvent sur l'évaluation et la prévision du potentiel d'instabilité basé sur l'analyse de la granulométrie. Parmi les facteurs importants causant une instabilité potentielle interne, d'où se trouve le coefficient d'uniformité [8], mais aussi l'influence de la forme de la courbe granulométrie [9], [10], [11], [7], [12] et [3].

Burenkova [13] propose un diagramme divisant le sol en zones « suffusive » et « non-suffusive » . Son analyse est basée sur les changements hydrauliques et la quantité de particules fines et le changement de pression interne. Les changements de pression, l'épaisseur et la porosité du filtre [14] également la pression effective et le gradient critique hydraulique [15] ont aussi une influence importante sur la performance du filtre.

Pour des sols avec une grande quantité de particules fines, le nombre d'hydrodynamique joue un rôle important sur la quantité de matériaux dilué [16]. La baisse de pression ainsi que la diminution de contenu d'argile, augmente le taux d'érosion [4]. Wan et al. [3] estime que la plupart des critères déjà proposés pour satisfaire la stabilité de sols sont conservateurs.

La suffusion externe est une sorte d'érosion sélective de particules fines qui sont au contact avec une couche plus grosse. Dans ce processus l'écoulement emporte les particules fines vers la couche formée de particules plus grandes [17, 18].

Le suintement d'eau par un filtre granulaire (avec des pores plus larges) ressemble à l'écoulement dans un canal ouvert avec le même matériel de base. Bakker [19] propose une formule pour calculer la vitesse critique de l'écoulement dans le filtre par rapport à

d_{50} du sol. Worman [20] également conclut que la proportion de la taille de grain entre deux couches et la porosité de la couche sous-jacente ont un impact sur la suffusion. Dans le même ordre, Brauns [21] associe l'érosion avec d_{50B} et d_{wf} (la taille hydraulique effective des grain des filtres) avec un nombre de Froud constant.

Worman [22] indique également que la perte cumulative du sol pourrait être prévisible comme une fonction du temps . Son analyse est basée sur la taille des grains du matériel ainsi que le pourcentage des grains qui sont plus grand que la taille de « colmatage ». Bonelli et al. [23] ont mentionné par ailleurs que dans le sol sablonneux argileux, le volume d'argile et le gradient hydraulique influencent l'érosion interne.

Ces travaux susmentionnés focalisent sur les critères géométriques pour évaluer le potentiel d'instabilité interne, [8], [9], [10], [7], [12] et [13]. En effet, la plupart des critères proposent une classification basée sur la forme de la courbe granulométrique. Les investigations de l'effet sur le gradient hydraulique sont quasi inexistantes.

La majorité des travaux précédents indique que dans la plupart des inspections pour une érosion interne, le centre d'intérêt était les sols et les propriétés géométriques. Ces facteurs définissent le potentiel d'instabilité interne du sol. La plupart des critères mentionnés ont été définie dans la forme de la courbe granulométrique sans tenir compte d'autres facteurs, comme le gradient hydraulique. Par ailleurs, la majorité des tests ont été exécutés sur de petits échantillons de couches de sol mis sous pression et soumis à du gradient hydraulique très élevé.

Dans la présente recherche, les modèles contenant trois couches de sol ont été conçus au laboratoire hydrodynamique de l'École Polytechnique de Montréal. Elles ont été créées dans une optique de disposer des conditions aussi proche de la réalité dans laquelle les matériaux, l'argile/la moraine, le sable et le gravier, ont été choisis pour présenter le noyau, le filtre et la couche perméable, respectivement.

Les objectifs de modéliser le rôle de la charge hydraulique sur la suffusion externe dans cette série d'expériences sont les suivants :

1. Analyse du gradient hydraulique et développement de la relation pour le seuil de suffusion.
2. Développement et similitude d'un appareil construit en laboratoire avec des couches de sols pour évaluer le phénomène de suffusion.
3. Exécuter des expériences différentes pour considérer des changements de variables différentes, incluant le niveau de l'eau, les propriétés des sols, les spécifications géométriques et observer les effets sur le phénomène de suffusion.

Dans ce travail, dans les différentes séries de tests, les modèles avec des géométries différentes et des différents matériaux ont été soumis à un écoulement horizontal pour différents gradients hydrauliques.

Montage expérimental

La figure 1 présente le montage utilisé dans le cadre de ce projet. Dans un canal de 76 cm de largeur, un parallélépipède d'un mètre de long et de 50 cm de haut est construit. Il a été rempli par trois couches de sols : argile (moraine), sable et gravier, tel que montré dans la figure 2. Sous une charge d'eau donnée, l'eau s'infiltre à travers la paroi du parallélépipède pour traverser la couche de sable et de gravier.

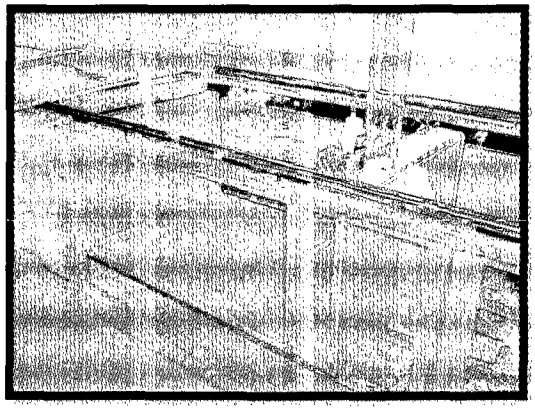

Figure 1: Cadre de montage

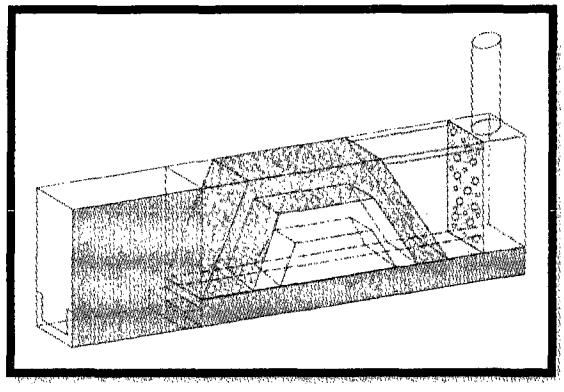

Figure 2: Assemblée expérimentale - ne pas peser

Le niveau d'eau a été varié progressivement afin de ne pas causer de variations brusques des pressions interstitielles.

Une analyse dimensionnelle permettra de limiter le nombre d'expériences à réaliser. En effet, les paramètres hydrauliques et géotechniques sont combinés en groupements adimensionnels.

Pour un niveau d'eau donné, ce dispositif expérimental permet de mesurer le débit solide érodé et le gradient hydraulique pour des conditions géotechniques (granulométrie et porosité des sols donné). Une attention particulière a été accordée au début du mouvement ce qui a permis de dégager un critère pour le début de la suffusion.

Matériel

Les sols utilisés correspondent à des constituants du Barrages d'Hydro-Québec. Il était nécessaire de vérifier les propriétés des matériaux utilisés, comme par exemple, les tests de la granulométrie, la gravité spécifique, le Proctor standard de compactage et des tests de perméabilité qui ont été effectués sur les échantillons des matériaux qui avaient été utilisés dans les différentes expériences. La figure 3 montre les courbes granulométriques des sols utilisées.

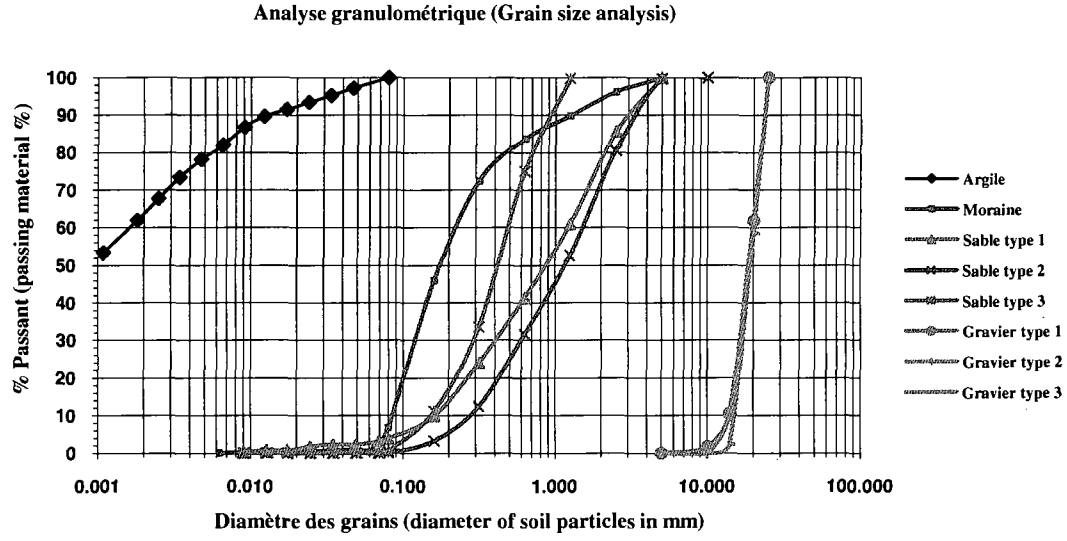

Figure 3: Analyse Granulométrique des matériaux

Manipulation

Pour remplir le réservoir en amont, l'eau a été fournie par les valves à l'intérieure du réservoir. Aussi pour stabiliser le niveau d'eau en amont de la digue, des trous de différents diamètres ont été pratiquée sur le côté de la boîte cubique.

Pour chaque test, trois couches de sédiment ont été préparées. La quantité évaluée de sol a été mélangée avec de l'eau et le mélange a été placé sous une couverture de nylon pour former un mélange uniforme.

Pour la compaction, une méthode de force statique a été utilisée, appliquant le poids mort de l'appareil de compaction sur la surface du sol pour comprimer des particules en plusieurs couches

L'argile / moraine ou le sable a été élaboré en trois étapes, pour chaque étape, une quantité suffisante a été déversée dans la boîte et elle a été compacté.

Le niveau de l'eau à l'interface sable/gravier a été mesuré grâce à 6 capteurs de pression. Deux d'entre eux sont localisés en amont et en aval de la digue pour donner les niveaux d'eau et le débit par- dessus à un déversoir rectangulaire placée en aval.

Les 4 autres sont incorporés dans le sable. Ces capteurs sont connectés à un ordinateur d'où les gradients hydrauliques sont calculés.

Le gravier a été déposé par-dessus le filtre dans une couche d'épaisseur uniforme avec une pelle. Le niveau d'eau a été augmenté progressivement pour éviter les variations rapides de pressions. Chaque étape a duré assez longtemps (15 à 20 minutes) pour atteindre un débit stable.

Les sédiments érodés ont été recueilles dans des intervalles du temps déterminé (15-20 min). La durée de cette dernière étape est prolongée de 45-60 minutes, quand le niveau d'eau atteint la crête de la digue, pour s'assurer qu'aucun déversement intempestif n'a eu lieu. Une série de récipients en aluminium a été placée en aval pour recueillir les sédiments érodés. En fin, les particules érodées ont été séchées dans le four avant d'être pesées.

Nous avons fait onze différents types d'expériences selon la géométrie du modèle, du type de sol, le noyau, le filtre et de la couche perméable (Voir la table 1).

- Dans le premier modèle, du plexiglas a été utilisé en amont, perpendiculairement à l'écoulement sur l'étendue des couches de gravier pour forcer l'écoulement dans la couche sableuse. Les résultats de ce modèle ne sont pas satisfaisants parce que la prévention d'écoulement par le gravier a causé un écoulement ascendant.
- Dans le modèle de type deux, les couches satisfont les similitudes géométriques.
- Le type 3 a été en forme trapézoïdale et le noyau a été en forme moraine.
- Le type 4 a consisté en deux sous-couches de gravier.
- Dans le type 5, les particules de diamètre supérieur à 10 mm et inférieur à 20 mm ont été utilisées dans la couche de gravier.

- Dans le type 6, la couche de sable consistait à 97 cm, le type 7 est le même que le type 6 mais avec les pentes du noyau et du filtre en marches
- Modèle 8 à 11 ont la même géométrie que le modèle 5. Les sables des modèles 8 et 9 sont différents par rapport au sable du type 5. La porosité du gravier dans les modèles du type 10 et 11 est différente de celle du type 5.

Table 1: Les spécifications d'expériences

Test	Noyau		Filtre		Géométrie	Protection			Utilité du test
	Matériel	d_{50} (mm) moyenne	Matériel	d_{50} (mm) moyenne		Matériel	d_{50} (mm) moyenne	Géométrie	
Type 1	Argile		Sable	0.85	non- isocèles, semi trapézoïdal	Gravier	18.33	$5_{mm} < d < 20_{mm}$	Effet d'un écoulement focalisé sur la suffusion
Type 2	Argile /Moraine		Sable	0.85	non- isocèles, semi trapézoïdal	Gravier	18.33	$5_{mm} < d < 20_{mm}$	Étude de la suffusion dans les digues non- isocèles avec couche de graviers bien mélangés
Type 3	Moraine	0,175	Sable	0.85	isocèles trapézoïdal	Gravier	18.33	$5_{mm} < d < 20_{mm}$	Étude de la suffusion dans les digues isocèle avec couche de graviers bien mélangés
Type 4	Moraine	0,175	Sable	0.85	isocèles trapézoïdal	Gravier	7.07 19.6	$5_{mm} < d < 10_{mm}$ $10_{mm} < d < 20_{mm}$	Étude de la suffusion s dans les digues isocèle avec deux sous couches de gravier
Type 5	Moraine	0,175	Sable	0.85	isocèles trapézoïdal	Gravier	19.6	$10_{mm} < d < 20_{mm}$	Étude de la suffusion dans les digues isocèle avec couche de gravier plus grossier
Type 6	Moraine	0,175	Sable	0.85	isocèles trapézoïdal plus longe	Gravier	19.6	$10_{mm} < d < 20_{mm}$	Étude de la suffusion dans les digues isocèle avec couche de graviers plus grossiers et une crête plus longue
Type 7	Moraine	0,175	Sable	0.85	isocèles trapézoïdal plus longe pentes en marches d'escalier	Gravier	19.6	$10_{mm} < d < 20_{mm}$	Étude de la suffusion dans les digues isocèle de pentes en marches d'escalier, avec couche de gravier plus grossier et une crête plus longue
Type 8	Moraine	0,175	Sable	0.42	isocèles trapézoïdal	Gravier	19.6	$10_{mm} < d < 20_{mm}$	Étude de la suffusion sur dans les digues isocèle digue avec couche de sable plus fin
Type 9	Moraine	0,175	Sable	1.2	isocèles trapézoïdal	Gravier	19.6	$10_{mm} < d < 20_{mm}$	Étude de la suffusion dans les digues isocèle avec couche de sable plus grossier
Type 10	Moraine	0,175	Sable	0.85	isocèles trapézoïdal	Gravier	18.8	$14_{mm} < d < 20_{mm}$	Étude de la suffusion dans les digues isocèle avec couche de gravier avec plus poreuse
Type 11	Moraine	0,175	Sable	0.85	isocèles trapézoïdal	Gravier	18.33	$5_{mm} < d < 20_{mm}$	Étude de la suffusion dans les digues isocèle avec couche de gravier avec moins poreuse

Analyse dimensionnelle

En supposant le fond mobile du canal est plat, composé de particules solides uniformes et non cohésives, se déplaçant sous l'action de l'écoulement (considéré comme uniforme et permanent), on obtient une relation fonctionnelle qui relies le gradient hydraulique au taux d'érosion.

Une analyse dimensionnelle utilisant le théorème de π, montre que le taux d'érosion E est quantifié au moyen de quatre groupes adimensionnels, le gradient hydraulique, la densité relative, le diamètre adimensionnel de la particule et la porosité (voir l'annexe II).

Le théorème de π donne une expression pour l'intensité adimensionnelle du taux d'érosion :

$$E^* = \frac{E}{\sqrt{\rho_w{}^2 g d}} = f(d_*, p, i, S_s)$$

Où E est le débit solide volumique par unité de surface. Puisque, S_s, p et d_* sont quasiment constants, l'équation s'écrit:

$$E^* = f(i) \qquad \frac{E}{\sqrt{\rho_w{}^2 g d}} = f(\frac{\Delta h}{L})$$

La forme de la relation fonctionnelle sera donnée au moyen de formules établies avec des expériences en laboratoire.

Résultats

Les résultats obtenus d'expériences qui ont inclus le suintement d'eau par trois couches différentes d'argile/moraine, le sable et le gravier montrent que :

- Le gradient hydraulique critique est quasiment le même : l'augmentation du gradient hydraulique en amont n'a pas d'influence importante sur le début de la suffusion externe entre le filtre et le noyau.
- Le maximum du taux d'érosion y est atteint à une profondeur (au dessus de la crête du filtre) égale à la moitié de la hauteur d'eau maximale (au-dessus de la crête du filtre). C'est pour le montage du type cinq et le taux d'érosion moyen le plus élevé correspondant est le plus critique.
- La figure 4,5 et 6 montre la relation entre le débit solide adimensionnelle et le gradient hydraulique. Différentes courbes sont obtenues pour les différents types d'expériences.

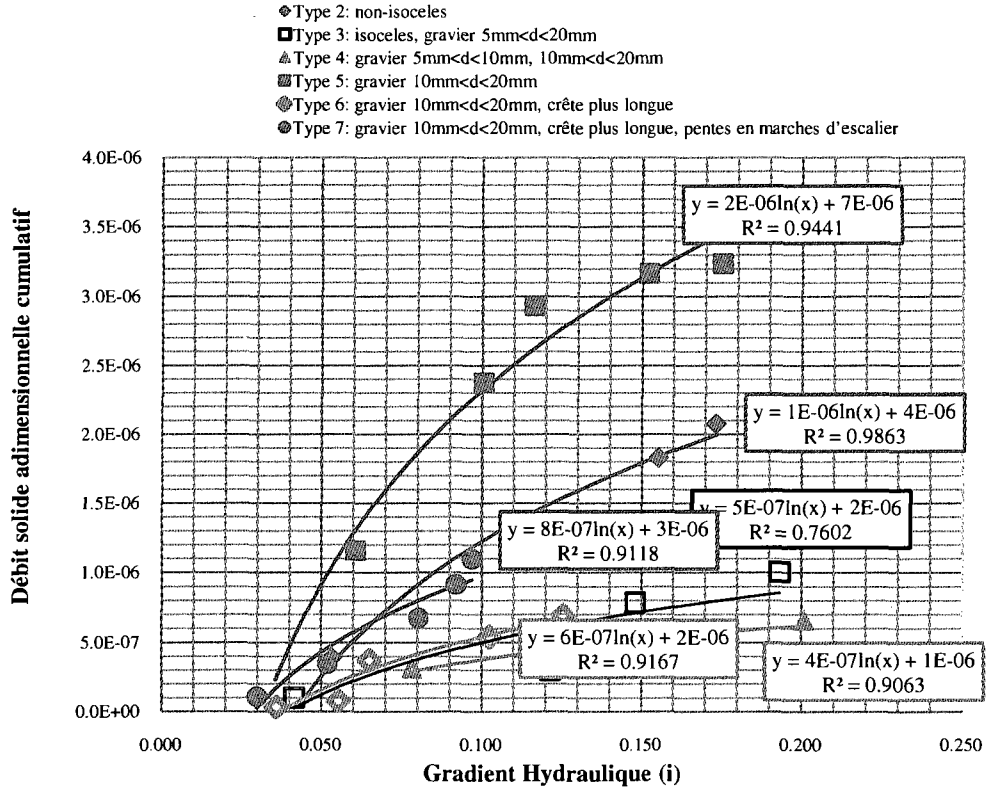

Figure 4: La relation entre le débit solide adimensionnelle et le gradient hydraulique

(Type 2-7)

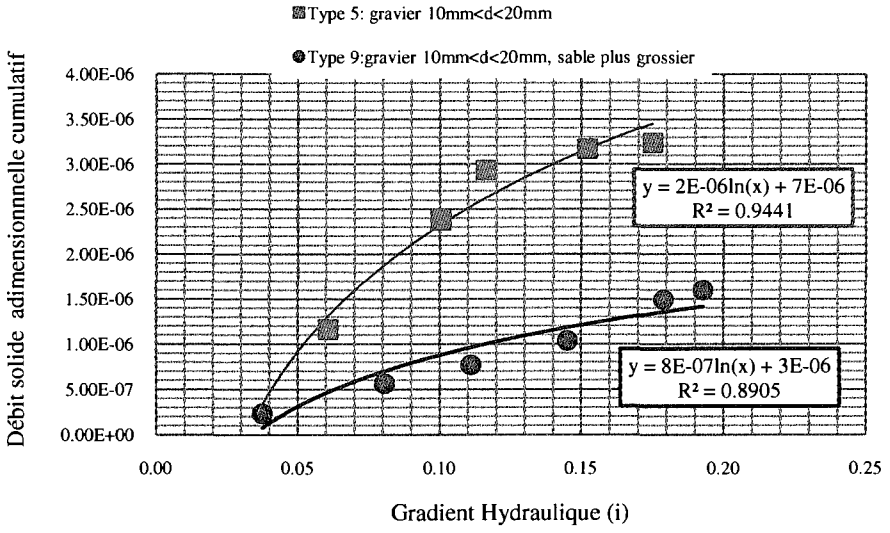

Figure 5: La relation entre le débit solide adimensionnelle et le gradient hydraulique (Type 5 et 9)

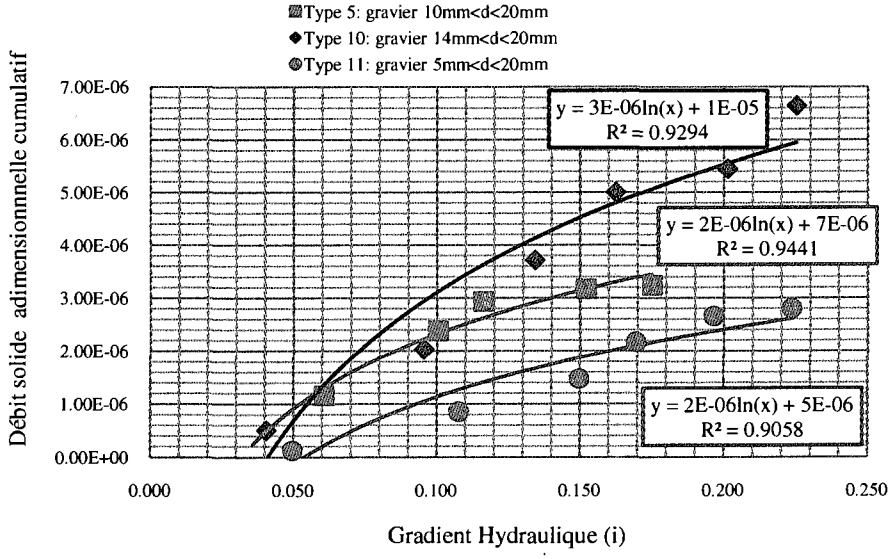

Figure 6: La relation entre le débit solide adimensionnelle et le gradient hydraulique (Type 5, 10 et 11)

- La comparaison des types 2 et 3 indique que l'eau pénétrant directement sur la couche de sable augmente le taux d'érosion pour la même couche de gravier.
- Les différences entre les tests 3 et 4 ont montré que la composition de la couche de gravier sur le filtre influence énormément la suffusion.
- Une comparaison du test 4 et 5 montre qu'il n'y a pas de différence quant à l'initiation du processus, malgré un taux d'érosion plus élevée pour le type cinq.
- La comparaison des types 5 et 6 n'indique aucune différence à l'initiation de l'érosion selon le gradient hydraulique.
- La comparaison des types 6 et 7 indique que la forme de la pente ne montre pas de changements significatifs sur l'initiation et le taux d'érosion.
- Les tests 5 et 9 montrent que l'utilisation du sable plus gros fournit un taux d'érosion inférieur.

Conclusion

- Généralement, malgré toutes les différences dans la géométrie, des propriétés des matériaux ou la différence entre les types de tests, on peut conclure que le gradient hydraulique critique a environ la même valeur.
- La forme de la pente ou la longueur du filtre ne montre pas de d'influences significatives sur l'initiation d'érosion.
- Les résultats ont révélé que la granulométrie du sable influence énormément la suffusion. Des grains plus fins se sont dilués plus facilement que les sables aux grains plus gros.
- La porosité et la granulométrie du gravier peuvent changer le taux d'érosion.

TABLE OF CONTENTS

LIST OF TABLES

LIST OF FIGURES

LIST OF SYMBOLS

C_u	Uniformity coefficient [-]
d, d_{dv}, d_{max}	Soil particle diameter [mm]
d_{wf}	Effective hydraulic grain size of filter [mm]
d_{50}	The diameter through which 50% of the total soil's mass pass [mm]
d_{60}	The diameter through which 60% of the total soil's mass pass[mm]
d_{90}	The diameter through which 90% of the total soil's mass pass [mm]
d_*	Non-dimensional diameter of the particle $\left(d\left((s_s-1)\frac{g}{\nu^2}\right)^{\frac{1}{3}}\right)$ [-]
D_H	Harmonic mean of the volume distribution of the grain diameter [mm]
D_n	Arbitrary diameter size on gradation curve [mm]
D_{n+1}, D_{n-1}	The diameter calculated from Dn
$D_{15(F)}$	The diameter through which 15% of filter material pass [mm]
$D_{85(B)}$, $D_{85(s)}$	The diameter through which 85% of base material pass [mm]
e_1	Void ratio [-]
E	Massive solid discharge by the surface unit [gram/cm^2/s]
E*	Dimensionless solid discharge [-]
F, H	Mass fraction of sediment [%]
g	Acceleration of gravity [m/s^2]
G*	Volume transport rate [-]
h', h"	Conditional uniform factor [-]
i, j	Dimensionless hydraulic gradient [-]
k	Ratio between shear velocity and pore water velocity [-]
n_b , ρ	Porosity of base material [-]
q_{cr}	Critical filter velocity [m/s]
α	Slope angle [-]
γ	Water specific weight [N/m^3]
ΔS_1, ΔS_2	percentage of sediment weight (finer than) [-]

Δ, S_s	Soil relative density [-]
ρ_s	Mass density of sand [kg/m^3]
ρ_w	Mass density of water [kg/m^3]
φ	Natural angle of repose of single grains of the base material[-]
Ψ_s	Shields parameter [-]

LIST OF APPENDICES

CHAPTER 1: INTRODUCTION

For many years, embankments and earth-filled dams have been constructed with different materials in different geometries to store or control water. In these types of constructions, usually the stored water has the ability to move and seep through the embankments.

The passage of water through porous media could establish different problems impacting the stability or function of either the construction or the foundation, and if not recognized and controlled on time could result in the embankment's failure.

One of the main issues in this procedure (water movement through the soil) is the movement of soil particles by the water flow within the soil layer, called internal erosion. [24]

The embankments are constructed with different zoning materials such as the core, the filter or transition layer and the shell or previous part. As a result of such a wide range of specifications, either related to the materials used and construction methods or flow properties, there is an impact on the movement of particles inside the porous medium.

Internal erosion is considered to be a very complex phenomenon since it occurs inside the embankments. Usually the initiation of the process is unrecognizable, and can only be documented when its progress has had a visual effect or failure occurs [2].

Most knowledge and instruction about this phenomenon is based on surveys of real cases and previous dam failures caused by this problem [1]. It should be noted that as a characteristic of this phenomenon, usually the failure or damage demolishes any existing evidence.

Depending on the manner of the soil particles' movement, the initiation of different types of internal erosion such as piping, backward erosion, concentrated leakage and suffusion are known and discussed.

The movement of soil particles starts as soon as the hydraulic gradient reaches a critical value. As a consequence of climatic changes, the variation of the water level in the upstream of dams may result in the hydraulic gradient's augmentation and a higher flow rate through the embankment. This matter may have an impact on the rate of internal erosion, especially on the interface of two adjacent soil layers - one coarser than the other - and speed up the movement of the particles of finer soil through the coarser ones, which is described as suffusion [3-5].

After reviewing the previous works and research about this phenomenon, it was apparent that in most cases investigating the phenomenon of suffusion, the focus has been on the soil and the geometric properties that define the potential of internal instability of soil and no particular attention was given to the initiation of particles movement. As a result, most clarified criteria have been related to the grain size distribution curve shape and do not consider other factors like hydraulic gradient [10], [7], [12] and [13]. Also, most of the tests have been executed on small samples of soil layers subjected to high pressures or hydraulic gradient and downward or upward seepage direction, which may not always be valid in a real situation.

In these series of experiments in this research, a relatively large model containing three soil layers was designed. Conditions were replicated as close as possible to real cases. The materials - clay/moraine, sand and gravel - were chosen as the core, filter and previous layer. The model constructed was subjected to gradually increased water in the upstream – avoiding any over topping - and the process of suffusion, in case it was to occur, was observed.

In the primary series of tests, models with different geometries were subjected to water seepage in a horizontal direction with an increasing hydraulic gradient. As the secondary series, taking into consideration the critical model of the first series as the origin, the role of sand and grain size distribution was examined.

CHAPTER 2: LITERATURE REVIEW

Internal erosion, which explains the movement of fine particles by the force of seepage through the soil and leaving behind a soil layer, as mentioned by Foster et al. [1] is an important cause for a dam's failure. In their case studies surveying 11192 dams, around 46% of dams' failures were related to internal erosion.

According to Fell et al. [17], the occurrence of internal erosion in embankments needs four initial conditions to be present:

- Existence of a seepage flow through the soil skeleton
- Presence of erodible soil materials by flow
- An exit point to allow the sediments to be flushed away
- The capability of sediments to form a roof in the case of piping

The dynamic force created by water seepage through soil over particles is in the direction of flow and hydraulic gradient. When adequately large, it can move the grain in an internal path [6].

Studying internal erosion may lead one to interesting conclusions about the nature of this event. As a process, the unrecognizable nature of its initiation is a notable point. The process is rarely recognized when it begins, and the primary visible signs that can be observed are usually either during the progress or the failure phase. Also, this procedure is not time-oriented; with no specific time that it could happen at, it is possible that it occur either during the first water storage or after few years of operating. Verifying the preliminary reasons for the process and establishing the type of internal erosion that has taken place is not always easy, according to the propensity of the event to destroy all existing evidence [2] .

A broad series of subjects may have an impact on the formation and continuation of an internal erosion mechanism. The properties of materials, limitations or weakness of the construction manner, the procedures inside the dam and the flow properties and specifications are some of such subjects.

Concerning the mechanism that initiates internal erosion, one may consider different types of internal erosion. These types are piping, concentrated leak, backward erosion and suffusion [24], which will be explained later.

In this chapter, the previous theoretical studies, laboratory experiments and research that have been done on internal erosion are reviewed and discussed. As mentioned by Schuler [5] it is difficult to interpret whether a process should be classified as suffusion or not. To clarify the boundaries between different forms of internal erosion a brief explanation about piping, concentrated leak, backward erosion and suffusion is given in this chapter.

In this work, the focus was on the phenomenon of suffusion; in particular, the aim of this laboratory research was to investigate the initiation of external suffusion caused by hydraulic gradient changes.

A brief description about soil components and the basic relations in soil, movement of water within the soil is given in the appendix I.

2.1 Piping

Piping is a form of internal erosion that starts at an exit point of water flow such as from a crack in a high permeability zone. By washing out the sediments, a tunnel is formed and developed from the downstream (exit point) to the upstream of the embankment, called the pipe. Piping can be seen in embankments as well as their foundations or from the embankment to their foundation [18, 24, 25].

Richards et al. [26] have emphasized that poor filter design or inappropriate maintenance has an impact on piping. As a general commonality, the use of filters controls the movement of soil particles and can prevent erosion and piping from cracks in its core [27] . Using a cohensionless material in the filter does not support the forming of cracks in the core, and in case of cracks in the upstream, filter grains can seal the cracks easily. Based on these explanations to prevent piping, the focus has been on the definition and description of different criteria for filter materials that can fulfill this need.

Considering the mentioned criteria by Terzaghi [28] $D_{15(F)}/D_{85\,(B)} \leq 4 \text{ or } 5$, based on the experimental investigations over the samples from glass beads in different grain size in a permeameter, Tomlinson et al. [29] concluded that filter system with $D_{15(F)}/D_{85\,(B)} \leq 8$ are safe from falling whereas $D_{15(F)}/D_{85\,(B)} \geq 12$ is susceptible to erosion, and for materials in between, only the sufficient hydraulic gradient will cause the occurrence of piping.

Lafleur [30] similarized the filter and core layer of a real dam for the investigation of a filter's operation on preventing piping using a well graded cohensionless till with maximum diameter as 38 mm under a downward seepage direction with a hydraulic gradient as high as 8. For the particles greater that 0.8 mm, no important influence on self-filtering process was observed. He found the critical combination for piping ratio $D_{15(F)}/D_{85\,(B)}$ as 8.4 in this particular case.

Skempton et al. [31] did the experiments on several samples of internally stable and unstable materials (based on criteria in [7]). Samples were subjected to the upward seepage with an increasing flow rate until piping occurred, and it was observed that piping starts with a lower hydraulic gradient compared to the critical value in unstable sandy gravel (one third to one fifth), whereas for internally stable sandy gravels the value for the initiation of piping is approximately the same as obtained by theory.

Based on an experimental investigation of Ojha et al. [25], the critical head that would lead the soil to pipe is not only in correlation with soil and flow properties but also to the length of the structure.

2.2 Concentrated leak erosion

The appropriate basis for the formation of this phenomenon is the existence of a crack, the interconnected voids in the embankment, or its foundation. Settlement, freezing, or thawing may cause a crack to form; also, the improper or poor compaction of coarser materials in a permeable zone may form voids susceptible to erosion. The flow concentrations form the erosion of the crack's walls. [24]

The amount of fine parts in the soil has the role of controlling and repairing the concentrated leak. Sherard et al. [27], performing the NEF (No Erosion Filter Test) test as the best device for defining the filter's boundary size for impervious soils, executed the different samples of soils as silts, clays and clayey and silty sands in the NEF cylinder under downward seepage flow and applying a full pressure of 413 kPa in the laboratory. The results showed that the appropriate amount of fine particles in the filter can control and seal the cracks created in impervious soils and that the proportion of fine parts for filters as $D_{15F} \leq 0.5\,mm$ seemed to be conservative for fine silts and clay soils.

Presenting the factors with influence on forming a concentrated leak as characteristics of materials (base and filter), the hydraulic, geometric and physiochemical conditions, the experimental methods of Kakuturu et al. [32] on a sample crack in clayey soil subjected to horizontal flow and a constant hydraulic head, indicated that fine content more than 85% which require $D_{15F}/d_{85B} \leq 9\,mm$, where D is the filter diameter and d relates to the base soil, is conservative, too, although this ratio not covers self-healing or progressive erosion.

Wan et al. [33] used two types of tests, HET (Hole Erosion Test) and SET (Slot Erosion Test) to investigate the relationship between erosion properties and other soil properties in an erosion crack or concentrated leak. Considering an erosion rate index (I) between 0-6 in their experiments, it was seen that index is influenced by the degree of compaction and water content. Additionally, a lower index brings up the speed of erosion.

2.3 Backward erosion

The guidance of a seepage flow to an unfiltered surface through an exit point may result in the detachment of soil particles and their being carried from the structure by flow. The continuation of this process toward the upstream may result in the formation of piping [4, 17].

Executing the experiments on the triaxial cell by Bendahmane et al. [4], on the samples of sandy-clay soils subjected to downward seepage, the results showed that an increase of hydraulic gradient over a secondary threshold value causes the erosion of sand fraction in a backward form, which is impacted by the clay content and confinement stress. In these series of tests, the hydraulic gradient range was between 5-160 m/m.

2.4 Suffusion

Mentioned by Schuler [5], the term suffusion has uncertainty even in spelling as it is used like suffusion Kovac [6], suffossion [34] and sufosion. In this study the suffusion by Kovac [6] is repeated. The process of suffusion includes the movement, rearrangement, replacement or transportation of fine particles within the soil skeleton consisting of coarse particles by the force of seepage [3-5].

The displacement of fine particles within the soil skeleton deduced the decrease of soil density and at the same time the increase of permeability. This led to the higher rate of seepage force and lower shear strength and may cause problems in the long term. As

has been mentioned by Kovac [5, 6] the parameters influencing the suffusion could either be geometrical or hydraulic conditions. While the geometrical properties are correlated to grains and their pore size distribution, their shapes and compaction, the hydraulic conditions describe the critical velocity or hydraulic gradient for the initiation of movement.

Verifying the geometrical properties, one can explain the soils disposed to erosion as internally unstable; stability refers to the capability of soils to prevent the loss of their fine particles while the flow seeps through their skeleton [7]. The necessary parameter for establishing the possibility of internal instability is the presence of a coarse particle skeleton to carry the imposed stress and the fine particles that could move within by the seepage force. In other words, in an internally unstable soil, coarse particles do not have the ability to filter the small parts as is seen in the concave upward or gap-graded gradation curves.

The division of Kovac [6] brings two different types of suffusion: internal and external . In internal suffusion, fine particles migrate without leaving the soil layer, so the total mass remains constant, and according to grain accumulation or evacuation, the local permeability and porosity might decrease or increase. However, in external suffusion, small particles leave the soil layer, causing the increasing of total porosity and permeability of the soil.

A decrease of soil density or increase of permeability brings more seepage flow through the soil that may result in lower shear strength and cause problems for the stability of the structure overlying the eroded layer [6].

In these series of tests, the emphasis was on the beginning of external suffusion where the fine and loose particles of sand were washing out in to the voids in between the gravel overlying it.

2.4.1 Internal suffusion

Reviewing previously done works shows the tendency to assess and predict the potential of instability by analyzing the gradation curve more than considering other parameters such as seepage velocity or hydraulic gradient.

Istomina [8] (mentioned in [6]) related the potential of internal instability to the uniformity coefficient.

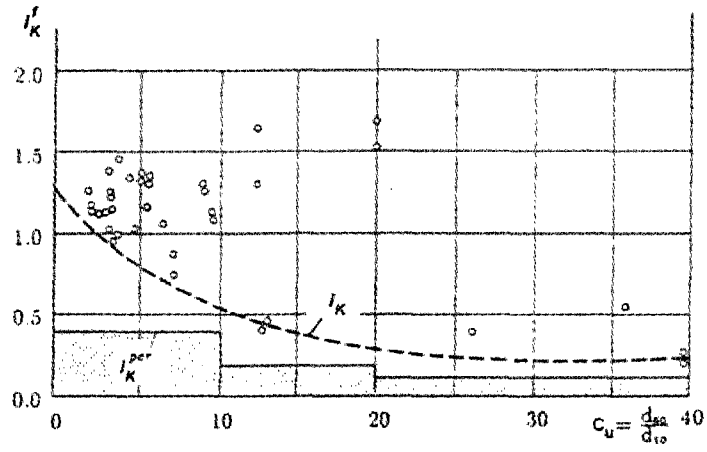

Figure 2-1: Diagram by Istomina (1957) for critical hydraulic gradient

This diagram correlates the critical hydraulic gradient to the uniformity coefficient. Istomina classified the region of suffusion as below:

For $C_U \leq 10$ there would be no erosion, soils with $C_U \geq 20$ are susceptible to erosion and the soils in between belong to transition conditions.

Lubochkov [9] suggested that shape of the gradation curve had influence on suffusion and a uniformity coefficient higher than 20 did not necessarily show the susceptibility to suffusion, as the fine particles can move inside the skeleton. In theoretical view point, he suggested that based on the grading curve, a value equal or smaller than a given limit in each grain size-interval for gradation curve slope showed the stability of the layer. Kovac [6] presented the mathematical form as below:

$$\frac{\Delta S_1 / \Delta S_2}{4} \leq 1 \quad \text{For} \quad \frac{D_{n-1}}{D_n} = \frac{D_n}{D_{n+1}} = 10$$

$$\frac{\Delta S_1 / \Delta S_2}{2.6} \leq 1 \quad \text{For} \quad \frac{D_{n-1}}{D_n} = \frac{D_n}{D_{n+1}} = 5$$

$$\frac{\Delta S_1 / \Delta S_2}{1.7} \leq 1 \quad \text{For} \quad \frac{D_{n-1}}{D_n} = \frac{D_n}{D_{n+1}} = 2.5$$

Where

- D_n : arbitrary diameter size on gradation curve
- D_{n+1} and D_{n-1} : the diameter calculated from D_n, by multiplying or dividing by 10, 5 or 2.5
- ΔS_1 and ΔS_2: difference between percentage of weight finer than, S_{n-1} and S_n , S_n and S_{n+1} respectively

Kezdi [10] has proposed a method for the determination of internal stability of a soil from the grain size distribution curve; dividing the soil at any arbitrary point on the curve into two parts: coarse and fine particles.

Assuming the filter criteria by Terzaghi [28] $\frac{D_{15f}}{D_{85s}} < 4 < \frac{D_{15f}}{D_{15s}}$, Kezdi [10] has considered coarse part as the filter for the fine parts. In which the left side of relationship ($\frac{D_{15f}}{D_{85s}} < 4$) satisfied the self-filtering, and therefore internal stability. The right part of equation ($4 < \frac{D_{15f}}{D_{15s}}$) satisfied the sufficient drainage capacity of the filter which is unrelated to the internal stability.

De Mello [11] has proposed a criterion for the internal stability of a gap-graded gradation curve. This method is similar to Kezdi [10], with a different boundary : $\frac{D_{15f}}{D_{85s}} < 5$.

Kenney et al. [7] evaluated the potential of internal instability and suffusion based on the shape of the grain size distribution curve. The soil samples of cohesionless

materials in a cylindrical cell and a surcharge pressure of 10 kPa were subjected to downward seepage and light vibration.

They proposed a graphical method for this purpose. Verifying the shape curve of the material is the key of this method. On the gradation curve, one can find the mass fraction of (F) for any particle diameter (D), and H as the mass fraction between D and 4D. The line that separates the stable and unstable materials is represented by H=F. Sufficient H and F points are plotted in a diagram to form the curve. The shape factor below the line represents the internally unstable soils. It can be seen from the graph that for narrowly graded materials ($C_u < 3$, $F \leq 0.3$) and widely graded materials ($C_u > 3$, $F \leq 0.2$) has a part or all of its shape curve below the line represented by H = F. The primarily separating line had been H = 1.3 F which was transferred to H=F after comments and discussions.

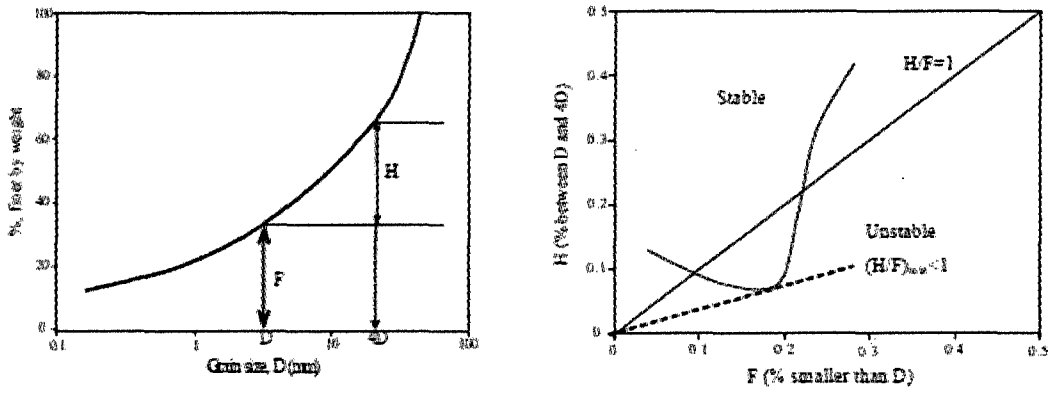

Figure 2-2: The criteria by Kenney and Lau

Lafleur et al. [12] considered the self-filtering process at the contact zone of the base filter from one side and the internal stability of base soil from the other side, executed two series of tests. For self-filtering, the screen test was conducted on samples of blended glass beads subjected to downward seepage flow under the hydraulic gradient from 2.5 to 6.5. Surveying the internal stability, compatibility tests were run on

samples in a triaxial cell with a saturation back pressure of 800 kPa. The results obtained indicate the relation between the quantity of fine particles moved and self-filtration thickness with the gradation curve. He also has represented three schematic curves for describing the internal stability.

Linear graded soils, either with a unit uniformity coefficient or uniform distribution of fine parts or soils with less than 40% coarse parts floating within finer parts are internally stable. Gap-graded soils can either be stable or unstable, while the concave upward curves show the internal instability. Talking about the gap-graded soil means the absence of an intermediate particle size from the gradation curve, and the concave upward curve describes the insufficient small sized particles.

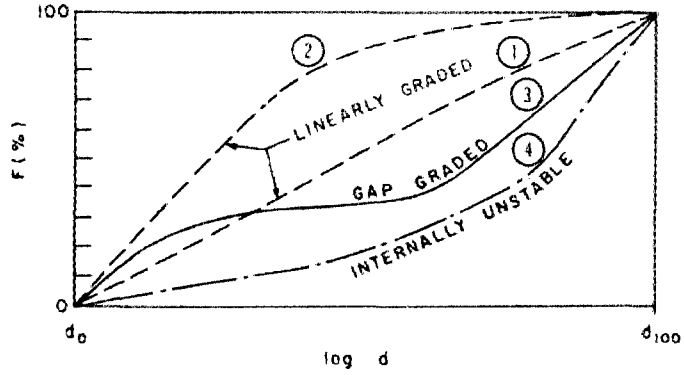

Figure 2-3: Classification of Gradation Curves of Broadly Graded Soils (Lafleur et al.)

Burenkova [13] has mentioned changes in hydraulic conditions such as the increase or sudden decrease of hydraulic forces having an impact on suffusion. Executing the tests over non-uniform soil samples, with different gradation curves and a maximum grain size of 60-100 mm and C_u=200, determined the suffosive and non-suffosive parts of the soils. Dividing the soil particles to groups from coarse to loose, and adding them step by step from coarse to fine, any increase in the volume showed the soil particles belonging to the skeleton and the inability to increase the volume describe the fraction as loose part.

Defining the conditional uniform factor as h'= d_{90}/d_{60} and h"= d_{90}/d_{15} and plotting them in a diagram represents a zone division for the ability of suffusion of soils.

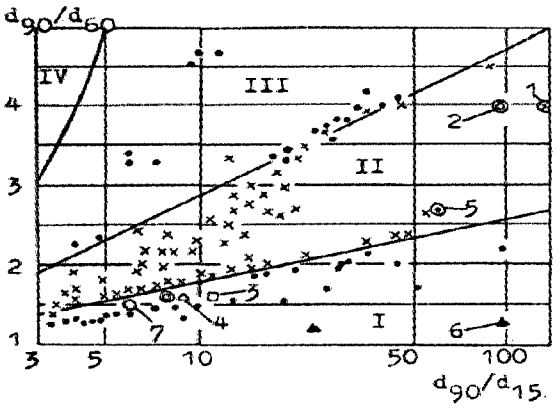

Figure 2-4: Classification of suffusive and non-suffusive soil compositions (Burenkova)

Soils belonging to zone II are non-suffosive, whereas zones I and III show the ability of a soil to be suffosive under certain hydraulic boundaries. Zone IV represents the artificial soil with an irregular gradation curve.

He has also proposed a formula to estimate the particle diameter (d_{dv}), which represents the limit between particles belonging to a loose or coarse part.

$$0.55h'^{-1.5} < {}^{d_{dv}}/_{d_{max}} < 1.87h''^{-1.5}$$

Kohler [14] has surveyed the role of changing load conditions caused by high hydraulic gradient on the performability of the filters. He suggested a filter test, putting a soil sample in a piece of equipment with two connected filter tubes, subjected to changing hydraulic gradient due to draw down effects. He suggested the increase or decrease of pressure inside the filter, thickness and the opening side between the rains in filter have important influence on filter performance against changing of load conditions.

Aberg [16] suggested that besides the Terzaghi [28] filter criteria, the base and filter materials should have grain stability with the seepage through them. He developed a mathematical formula for washing out the sediments, covering the grain and pore geometry consideration. This was clarified with laboratory tests on sand and gravel. The model covers gaps and loose grains and estimates the amount of grain washout and the decrease in volume by those washouts. It was shown that for soils with a high quantity of fine parts, the hydrodynamic number has a great impact on the amount of washed out material.

Schuler [5], having an exclusive review on the defined criteria for suffusion, has concluded there are no general valid criteria for suffusion, although some criteria are acceptable for some specific cases and conditions. He recommended checking both geometrical and hydraulic criteria to assess the susceptibility to suffusion.

Chapuis et al. [35] have studied the effect of compaction on the movement of fine particles used for the base of road pavement in a downward flow seepage test. They have concluded that when designing the criteria of base course material, permeability, filter performance and suffusion should be considered.

Moffat et al. [15], working on the hydromechanical conditions of the soils at risk of internal instability at the commencement of seepage-induced failure, proposed a new device: cylindrical specimen with 279 mm and 450 mm as the diameter and length, respectively. In a permeameter cell, samples of glass beads were subjected under effective stress of maximum 350 kPa and seepage in both the upward and downward direction with an increasing hydraulic gradient to a maximum value until internal instability occurred. He has proposed that there is a relation between effective stress and critical hydraulic gradient to cause the commencement of instability based on the gradation of each material.

Bendahmane et al. [4] having developed triaxial cells as the experimental device to characterize the erosion process of clay and sand without cracks under hydraulic gradient, have shown the type of erosion under high hydraulic gradient in clay was suffusion. With a critical hydraulic gradient of 5, decreasing the clay content to ½ caused a double increase on the rate of erosion and decreasing the pressure from 150 to 100 kPa doubled the maximum erosion.

Wan et al. [3] working on silt-sand-gravel and clay-silt-sand-gravel soil to determine the potential on internal stability, executed several tests in the laboratory. The sample device was put under downward flow with a hydraulic gradient of 8. It showed that some commonly used methods were conservative for these soils. It has been concluded that most of the proposed criteria for satisfying the stability are conservative. Soil with a steep slope on the coarser fraction and a flat slope on the finer fraction are more internally unstable. In internally unstable soils, erosion starts at a gradient lower than the critical gradient; the soil with higher porosity begins to erode with a lower gradient and plastic fines needs more gradient to erode. The gap graded needs a lower gradient that non-gap graded soil.

2.4.2 External suffusion

The form of internal erosion which involves selective erosion of fine particles from the contact with a coarser layer, for instance along the contact between silt and gravel sized particles and carry them away from soil layer is called external suffusion[17, 18].

The design of filters has been based on geometric demands. The pores in the filter material have to be smaller than the particles of the subsoil to be protected.

Bakker et al. [19], based on hydrodynamics criteria and assuming the similarity of water seepage through a granular filter with wider pores compared to the base soil, with flow in an open channel with the same base material, proposed the formula below for critical filter velocity, which relates the velocity to d_{50} of base soil and hydraulic

gradient. He tested his formula with experiments in a delft hydraulic filter box, for two layers of sand and gravel for different load components on both a horizontal and sloping bed. The maximum size of the base materials was 0.82 mm and the rate of erosion as 0.2 (gram/s/m^2) of dry sand assumed to be critical, the hydraulic gradient was increased step by step until considerable erosion was viewed.

$$q_{cr} = \frac{n}{k}\sqrt{\Psi_s \Delta g d_{50}\left(\frac{\sin(\varphi-\alpha)}{\sin\varphi}\right) - \frac{i}{\Delta(1-n_b)}}$$

Brauns [21], by executing tests over sand and gravel layers in a flume with a horizontal flow direction concluded that for $\frac{D15_f}{D85_B} \geq 20$ and a critical velocity correlated to a fraud number approximately equal to 0.7 erosion of fine particles along the interface with coarse one, exists. The erosion is also related to the d_{50B} and d_{wf} (effective hydraulic grain size of filter). He presented this correlation on the graph shown in figure 2-5.

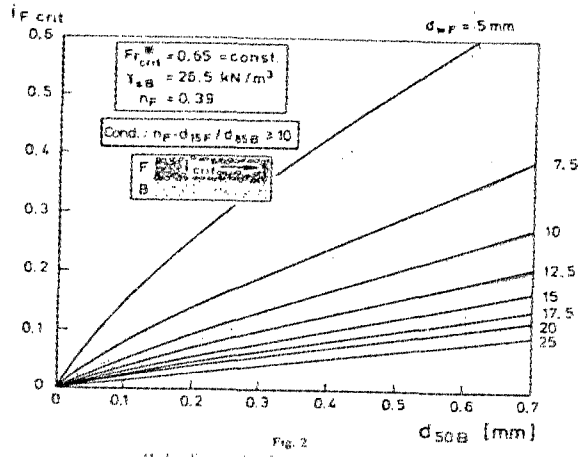

Figure 2-5: Hydraulic criterion for erosion along interface of two adjacent granular soils by Brauns 1985

Worman [20], proposing a mathematical formulation to cover the internal erosion between two layers and clarifying the formulation with experimental investigations in laboratory, he concluded the grain size ratio between two layer and the porosity of coarse layer have impact on the interfacial erosion. The seepage, buoyancy and the weight of grains force were considered in this transport relationship. Two layers of uni- sized sediments in a dimension of one, 0.3 and 0.3 for length, width and height respectively, were subjected to an increasing horizontal water flow (parallel to the interface) to clarify the formulation.

$$G^* = \left(0.56\,\frac{e_1}{8}\,\frac{1}{(S_s-1)}\,J\,\frac{D_H}{d_{85}}\right)n_1$$

Where

- 8: ratio of a_s/a_v which are surface and volume coefficient respectively
- e: void ratio
- S_s: soil specific gravity
- J: dimensionless hydraulic gradient
- D_H: Harmonic mean of the volume distribution of the grain diameter
- n_1: the mobile area fraction

Experiments on filtration of broadly graded base soil with a horizontal seepage force by Worman [22] indicated that cumulative loss of the base soil could be predictable as a function of time; presence of base filter with a small percentage of particles greater than pore size controlling the clogging of base soil, may lead to formation of a filter cake within time.

Bonelli et al. [23] suggested a framework for the phenomenon of suffusion in clayey sand, considering the clay/water interface erosion on a microscopic scale. They concluded the clay volume fraction and the hydraulic gradient have the impact on internal erosion.

Conclusion

Comparing the amount of work done in internal and external suffusion indicates that less attention was paid to the phenomenon of external suffusion.

A general review of the previous works shows that dealing with the problem of suffusion, the focus has been on the geometric criterion to evaluate the potential of internal instability of soil grains that lead to suffusion. Therefore, most of the criteria classified the shape of gradation curve such as [10], [7], [12] and [13].

The experimental investigations that have proposed the suffusion in correlation with hydraulic gradient or effective stresses seem inadequate [36], [20], [26]. The comparison also shows that in most cases, the samples were subjected to downward or upward seepage direction and only a few of them were subjected to horizontal flow direction such as [19] and [21]. Most of these samples were generally placed in a small specimen under approximately high pressure or hydraulic gradient, which may not be the real case in embankments.

After reviewing the previously done works it was seen that the suffusion was considered to be related to internal instability and the grain size distribution curve of soil particles [8], [9], [10], [7], [12], [13] and hydraulic gradient – as another aspect of this phenomenon- was not at the center of attention and less work has been accomplished towards the impact of hydraulic gradients on suffusion, particularly on its initiation.

CHAPTER 3: EXPERIMENTAL INVESTIGATIONS

3.1 Objectives

The aim of this work is to develop criteria for the threshold of the initiation of suffusion in an adequately large model under increasing hydraulic gradient, and survey the critical hydraulic gradient threshold.

The objectives of modeling the role of hydraulic head on external suffusion in these series of experimental investigations are the following:

1. Analyzing the hydraulic gradient and developing the relationship for the threshold of suffusion.
2. Development and similitude of a constructed laboratory device to model the embankment with layers of soil for testing the suffusion phenomenon.
3. Perform different experiments to consider changes in different variables including water head, sediment properties, geometrical specifications, and observe the effects on the phenomenon of suffusion.

In this chapter, first a comprehensive explanation about the selected materials and related property tests for each is given. Then the experimental design, consisting of apparatus setting and soil material, is discussed. At the end, the experiment's procedure and the specifications of each experiment type are described.

3.2 Experimental design

3.2.1 Introduction

Physical scale modeling of the external suffusion on the interface of sand and gravel was carried out in the hydrodynamic laboratory at École polytechnique de Montréal. The schematic model is shown in Figure 3-1.

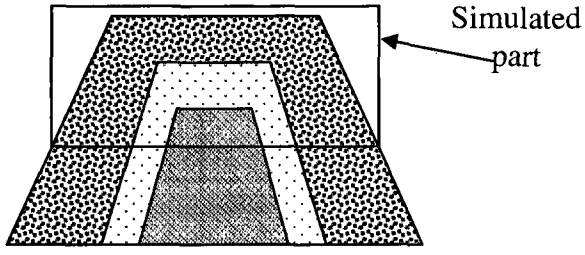

Figure 3-1: Relationship of experiments to field conditions

As the specifications of real cases were not accessible, the initial model was designed taking into consideration the sufficient length and height for the filter and the other layers. Afterwards, considering the results obtained, modifications were prepared on the assembled model in order to focus on the most critical combination.

During this work, eleven series of laboratory experiments were carried out. In these series of tests, the flow direction was considered horizontal (Figure 3-2). Horizontal flow through sediment layers represents a situation close to field conditions. These tests were performed to identify the procedure of external suffusion on the interface of the sand and gravel layers.

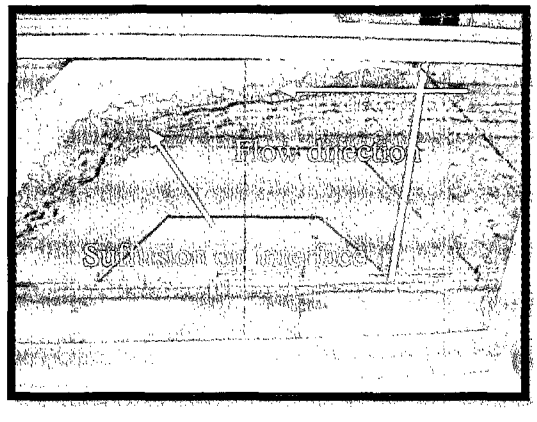

Figure 3-2:Sample laboratory experiment

Different models, in geometry and executed materials, were subjected to the experiments in order to observe the correlation between suffusion phenomenon, geometry and the properties of materials.

Particular attention was given to the beginning of the movement. This allowed developing a criterion connecting the above-mentioned parameters giving the threshold of suffusion.

3.2.2 Soil materials

To execute these series of tests, three different types of sediments were chosen to form the different layers of the model.

Each model consisted of three layers: clay/moraine to represent the core material, sand for performing the filter layer and gravel as the shell, from bottom to top, respectively. The gradation of material falls within the proper gradation limits of materials in Hydro-Quebec Dams. As the material for the core, clay was applied at the beginning and later was replaced by moraine because of a demand from Hydro-Quebec for a more realistic situation.

3.2.2.1 Experiments

Before starting any experiment it was necessary to verify the properties of the materials used. To fulfill this need, property tests were executed on samples of the materials that were used in the series of experiments.

The characteristic experiments included gradation (grain size distribution) for all sediments, specific gravity, and standard proctor compaction and permeability tests for sand.

3.2.2.1.1 Grain size distribution

Grain size distribution was determined using sieve and hydrometer tests in accordance with ASTM: D422-63 (D421 - D422 - D1140 - D2217 - E11).

In this method, to determine the relative proportion of different grain sizes within a soil sample, two methods were conducted. For the coarse part (a grain size larger than No. 200 sieve, 75 μm opening size), sieve analysis was used. First, the sand sample was passed through a No.10 sieve. A sufficient amount of material (approximately 500 grams) was washed through the No. 200 sieve. Remaining soil on the sieve was put in the oven for 24hrs to be completely dried. Then, the mass of dry soil retained on the respective sieves was determined.

For materials that passed through sieve No. 200, the hydrometer test was used. To prepare the sample required, a sufficient amount of soil (approximately 60 grams) was placed in a beaker and 125cc of a deflocculating agent was added to it (a solution of sodium hexametaphosphate). The mixture was left for 8 to 12 hours. Afterwards, the hydrometer readings were determined in specified time intervals.

As clay consisted of a notable amount of fine particles, only a hydrometer test was executed on it. For sand and moraine, both sieve analysis and hydrometer tests were executed. For gravel, due to the absence of fine parts in the material, only sieve analysis was done. The grain size distribution of clay and moraine is shown in Figure 3-3.

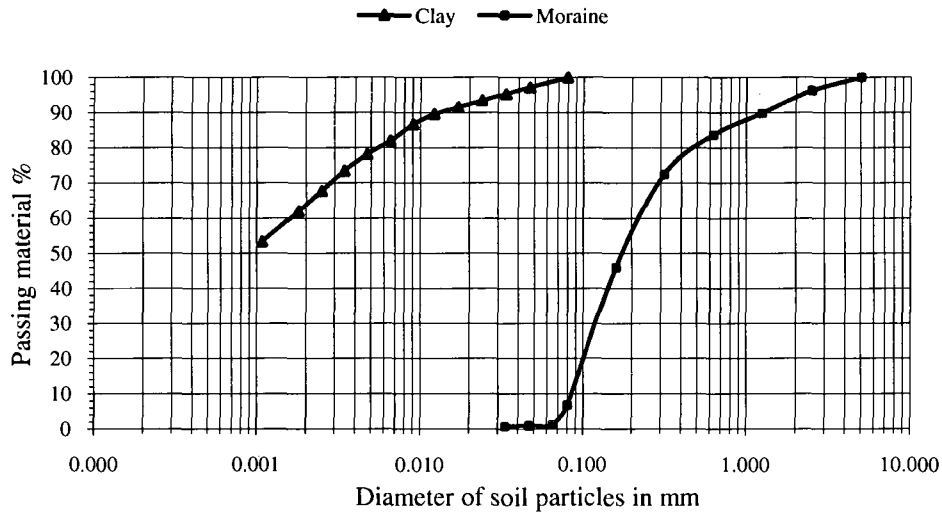

Figure 3-3: Grain size distribution curves of Clay and Moraine

For sand material, the tests were executed on two or three different samples to find out the range of grain size distribution. In these series of tests, sand was used with three different grain size distributions. Figures 3-4 to 3-6 show the grain size distribution curve for sand type one, type two and type three.

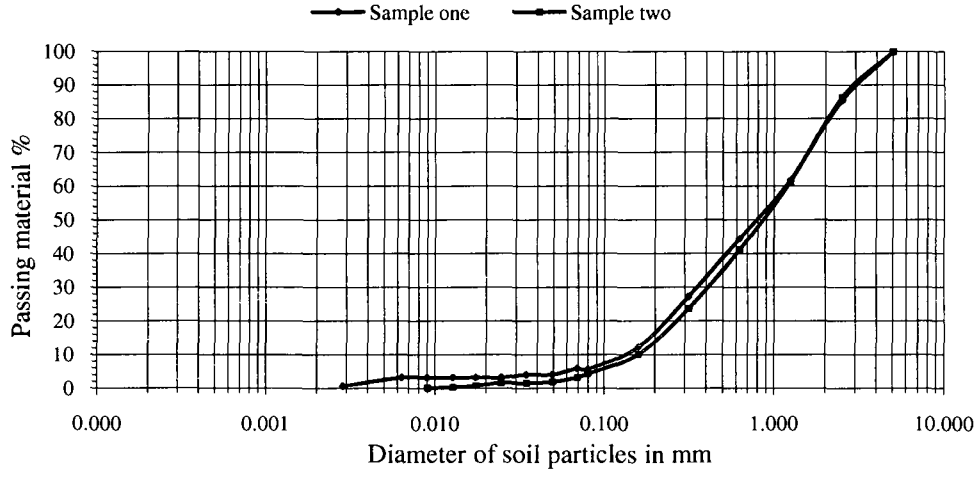

Figure 3-4: Grain size distribution curves of sand type one

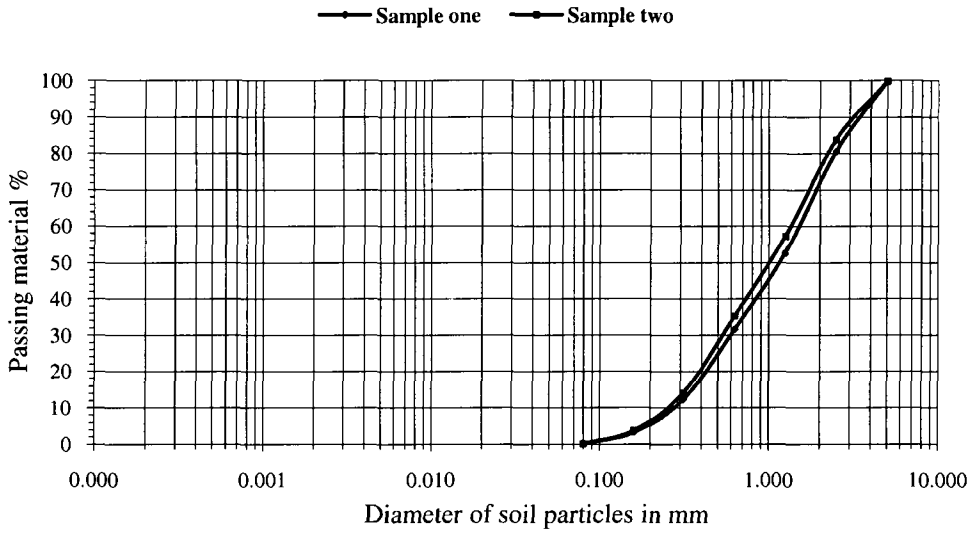

Figure 3-5: Grain size distribution of sand type two

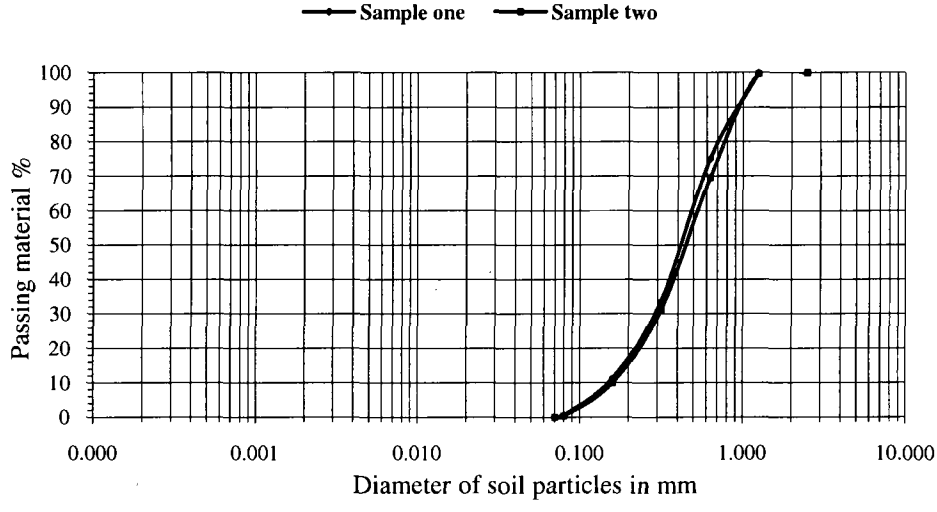

Figure 3-6: Grain size distribution curves of sand type three

The d_{50} and uniformity coefficient of each type is shown in Table 3-1.

Table 3-1: Mean diameter and uniformity coefficient of sand

Sand type	d_{50} mm	C_u
Type one	0.85	8.01
Type two	1.20	6.01
Type three	0.42	2.89

As the pervious shell, the St-Sophie gravel was used with different gradation and porosity. One type with the diameter of 5 to 20 mm, a second type with a diameter between 10 to 20 mm, and the last type with a diameter of particles inferior to 20 mm and superior to 14 mm. For all experiments, one type of gravel was used to shape one layer of gravel over the filter layer, except in tests type four, in which a combination of two types of gravel was used. The gravel that contained particles with a diameter of 5<d<10 mm shaped the first layer, and were covered with gravel particles with a diameter of 10<d<20 mm as the second layer. The grain size distribution for gravel is shown in Figure 3-7.

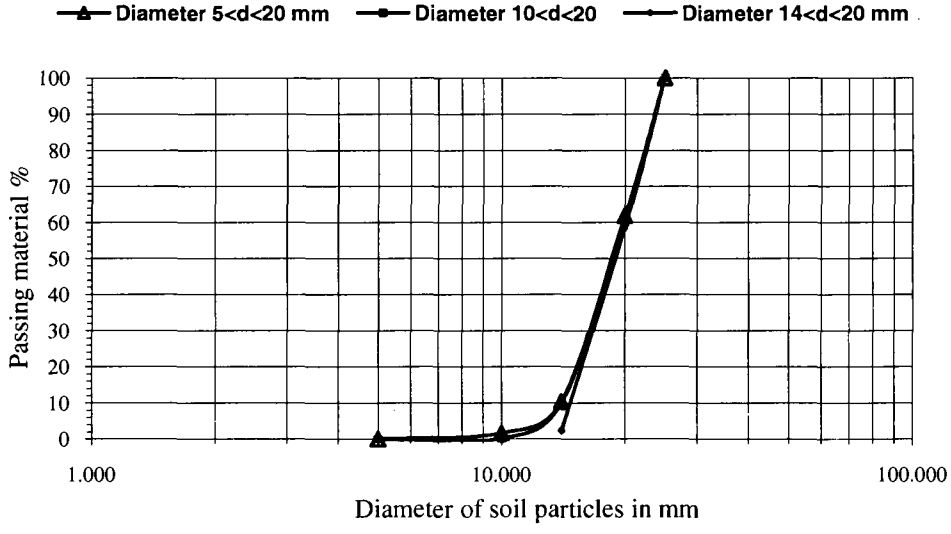

Figure 3-7: Grain size distribution for gravel

The properties of the types of gravel are shown in Table 3-2.

Table 3-2: d_{50} of gravel type

Gravel Diameter (mm)	d_{50} mm
5 < d < 20	18.33
10 < d < 20	19.16
14 < d < 20	18.80

3.2.2.1.2 Compaction test

To verify the maximum dry unit weight and optimum water content of the soil sample, one can execute the compaction test. The compaction degree may affect some of the soil properties, like strength, permeability and compressibility. Strength of soil decreases whereas permeability increases with the water content more than optimum. A standard proctor compaction test was conducted on the sand material in accordance with ASTM D698-00a.

Standard compaction tests were carried out on each of the soil samples. To execute the test, first, samples of sands with increasing water content capacities were prepared. In a mold with a diameter of 4 in (101.6-mm), three layers of sand in three steps were placed and each layer was compacted with a rammer of 24.4 N, dropped from a height of 12 in. (305 mm) twenty-five times. After measuring the compacted sample weight in the mold, it was placed in the oven to be dried. The resulting dry unit weight was determined afterwards. This process was done for all samples prepared and the curvilinear relation between the dry unit weight and the water content for the sand was drawn. Figures 3-8 to 3-10 show the results for the different sand types used in these series of experiments in this research.

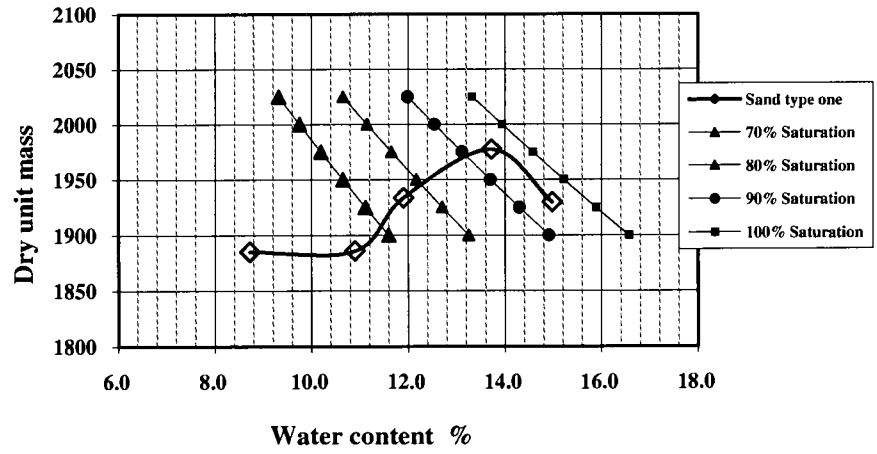

Figure 3-8: Compaction curve for sand type one

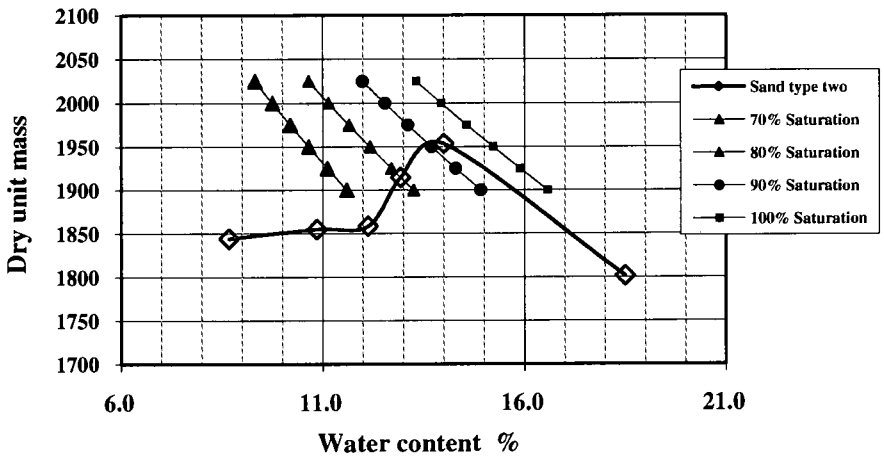

Figure 3-9: Compaction curve for sand type two

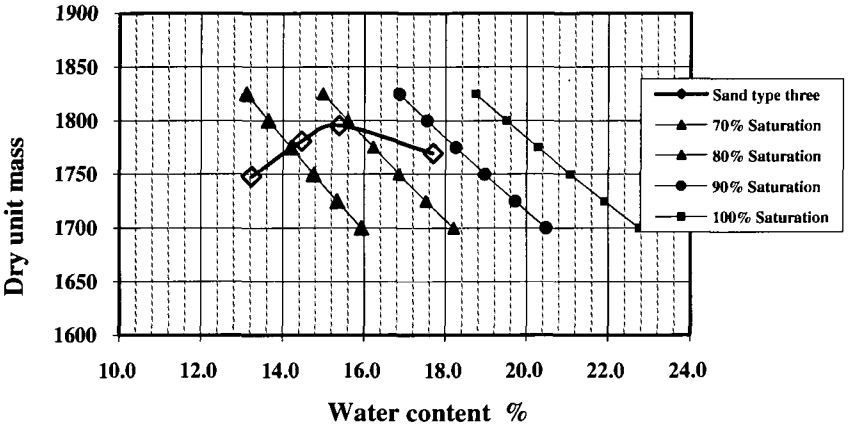

Figure 3-10: Compaction curve for sand type three

The values obtained for the dry unit mass, void ratio and optimum water content is shown in Table 3-3.

Table 3-3: Dry unit mass, void ration and optimum water content of sand types

Sand type	Dry unit mass (kg/m^3)	Void ratio	Optimum water content (%)
Type one	1977.2	0.40	13.7
Type two	1953.5	0.42	14
Type three	1795.5	0.54	15.4

3.2.2.1.3 Specific gravity test

Specific gravity is the ratio of the weight of a soil volume at an acknowledged temperature to the weight of distilled water of equal volume at a stated temperature.

Specific gravity tests were conducted in accordance with ASTM: D-854-02. This test determines the specific gravity of soil particles that pass sieve No. 4 (4.75-mm). The resulted specific gravity may be used in calculating the phase relations of soils, such as the void ratio and degree of saturation. The pycnometers are used as the apparatus of this test. The pycnometers are calibrated: a mixture of sand and water is added to the

pycnometer and the sample is vacuumed. The pycnometer is filled with water and is put into an insulated container. The specific gravity of the sand material obtained in these series of experiment is 2.773.

3.2.2.1.4 Permeability

The test of permeability of granular soil (constant head) is in accordance with ASTM-D2434-68). In the constant-head method, the flow is considered to be laminar. The purpose is to find the discharge through the specimen under a specific head of water. A permeameter with specimen cylinders is used for this purpose. The minimum internal diameter is approximately 8 to 12 times the maximum particle size according to Table 3-4.

Table 3-4: Cylinder Diameter

Maximum particle size Lies between sieve openings	Minimum cylinder diameter			
	Less than 35% of total soil retained on sieve opening		More than 35% of total soil retained on sieve opening	
	2.00mm(No.10)	9.5mm (3/8-in)	2.00-m (No.10)	9.5-mm (3/8 in.)
2.00-mm (No.10) and 9.5-mm (3/8 in.)	76mm (3in.)	...	114 m (4.5in.)	...
9.5-mm (3/8 in.) and 19.0-mm (3/4 in.)		152 mm (6 in.)	...	229 mm (9 in.)

The soil sample is compacted with compaction equipment, which has a 51 mm diameter circular face, weight of 100 grams to 1 kilogram (for soil with large gravel particles) and a height of fall of 102 mm. Drainage bade and cap are placed in the mold. The movement of particles is prevented by porous discs. The prepared sample and mold should be connected to a suitable water reservoir capable of supplying water to the permeameter under constant head. The head difference between top and bottom are measured in a specific time interval. The results obtained for the sand used in these series of tests were between 7.84E-02 and 7.42E-02 cm/s.

3.2.3 Apparatus setting

3.2.3.1 Main apparatus

Figure 3-11 presents the assembly designed within the framework of this work. In a channel of 76 cm width, a rectangular parallelepiped with 100 cm length and 50 cm depth was built. This parallelepiped box had three sides of wood, two sides of glass and one side in the vicinity of air. The glass sides permitted the observation of suffusion in case it happened.

To establish a reservoir in the embankment's upstream, a cubical box was constructed with a Plexiglas cylinder on top to protect and hold the water hoses. The dimensions of the cubical box were 76, 50 and 14 cm for the width, depth and length, respectively. For water evacuation from upstream, a metal pipe and its tap were fixed to the lower part of the cubical box (Figure 3-12). The parallelepiped box was filled with three layers of sediments: clay (moraine) as the core layer, sand as the filter layer and gravel as the pervious layer.

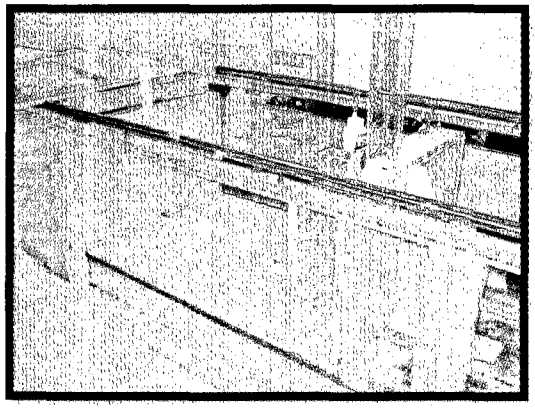

Figure 3-11: Framework assembly

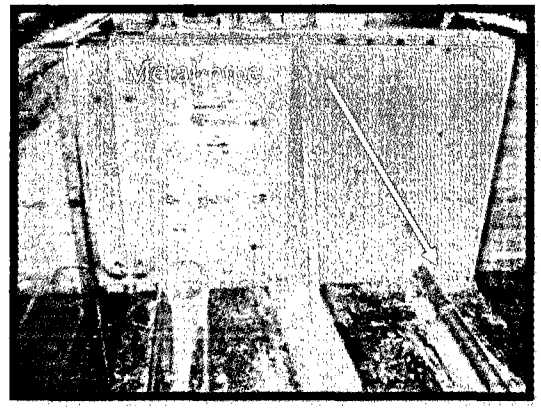

Figure 3-12: Water evacuation in upstream

3.2.3.2 Incoming flow

The necessity of an excessive amount of water during the test procedure did not allow the utilization of a constant head tank or a similar apparatus.

To fill the upstream reservoir, water was supplied manually from water valves which were connected to hoses and pipes placed in the laboratory. Through the Plexiglas cylinder, water was entered into the upstream box (Figure 3- 13 and 3- 14).

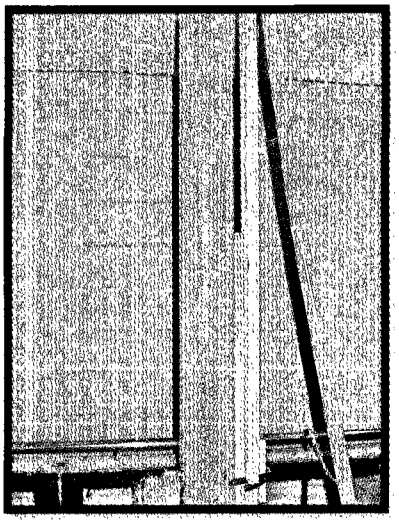

Figure 3-13: The hoses in cylindrical box

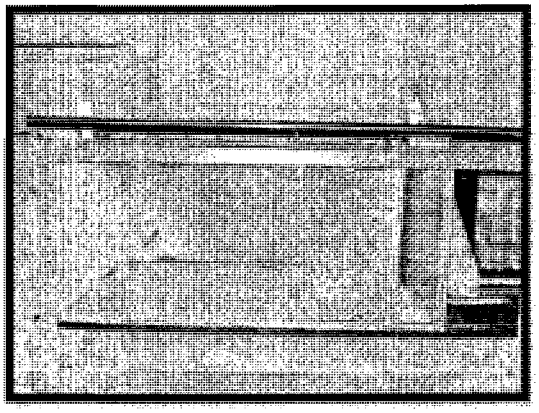

Figure 3-14: Upstream box

The side of the cubical box, in the vicinity of the model, had holes in different diameters on it, to present a porous media (Figure 3- 15) and to ensure a more uniform water pressure on the upstream of the embankment.

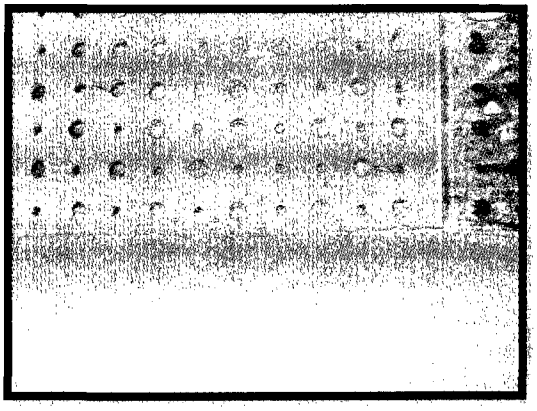

Figure 3-15: Upstream box's wall

The water inserted infiltrated through the wall and crossed the sediment layers.

In the beginning, the water was supplied in a low rate, as the presence of leakage was insignificant in downstream. Water passage above the filter layer, reaching the gravel part, increased the rate of the outgoing flow in downstream. In that situation, more water pressure was needed for water augmentation in the upstream. Therefore, the water was supplied at a higher rate.

The rate of incoming flow was captured by a Turbo US-PC2 signal converter with a measuring range of 0-5 lit/sec, supply 120 V and 60 HZ (Figure 3-16) and a glass-tube meter for the water valve and water tab, respectively. The values of discharge were in IGPM and GPM for the tab and valve, respectively.

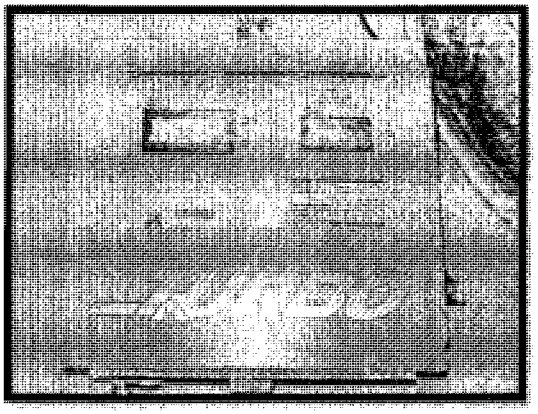

Figure 3-16: Turbo US-PC2

The volume of water inserted was controlled manually. During time intervals, the valve was opened in a manner to provide an acceptable rise in the water head upstream. Each step lasted long enough to perform a uniform flow rate upstream. One pressure transducer was located in the bottom of the cubical box, to collect the water head fluctuation and record it on the acquisition card.

3.2.3.3 Hydraulic head

To measure the water level during the passage of flow over the filter layer, pressure transducers were utilized. To reach the value of the water level in upstream, one pressure transducer was placed in the upstream box, in the downstream one was placed near the weir.

Over the filter layer, depending on the length of the filter, four or six pressure transducers were embedded at different dimensions in the filter to capture the water level fluctuation over the filter layer. All of these transducers were either connected directly to a data acquisition card and a personal computer, or to a series of piezometers (Figures 3- 17 and 3-18).

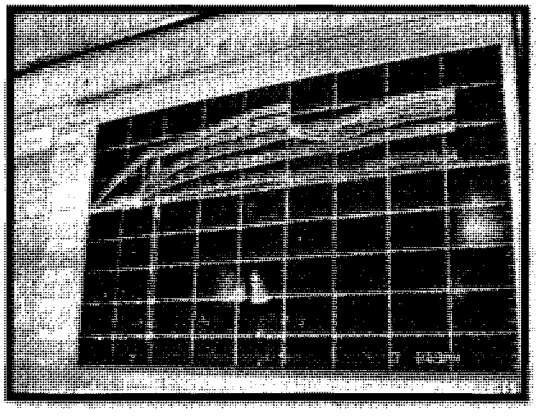

Figure 3-17: Pressure transducers connected to personal computer

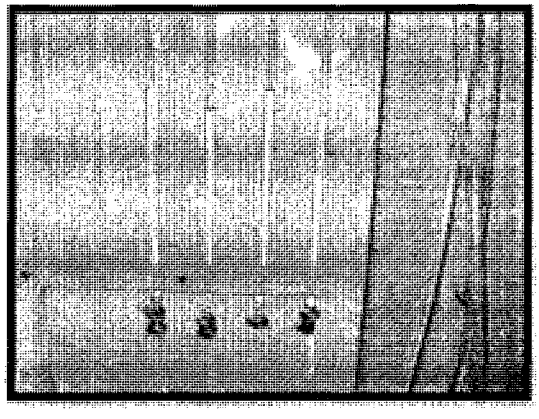

Figure 3-18: Pressure transducers connected to piezometers

In the case of a direct connection to the accusation card and the computer, the data was recorded automatically at regular time intervals and for the piezometers; the data was manually collected in time intervals.

3.2.3.4 Sediment collection

This experimental device allowed the measurement of the sediment erosion rate and its correlation to the hydraulic parameters (water level, hydraulic gradient and incoming discharge) and geotechnical parameters (grain size distribution and porosity). The existence of internal erosion caused the affected sand to be washed out from the sample and a collapse of the gravel on the surface might be observed.

In downstream, to comfortably collect the eroded sediments and outgoing flow, a lengthening slot had been established on the bottom of the wooden side (Figure 3- 19). A series of aluminum pans were placed underneath the slot to collect the eroded sediments. To guide the sediment particles inside the aluminum pans, wooden pieces were stuck to the borders of the slot (Figure 3- 20).

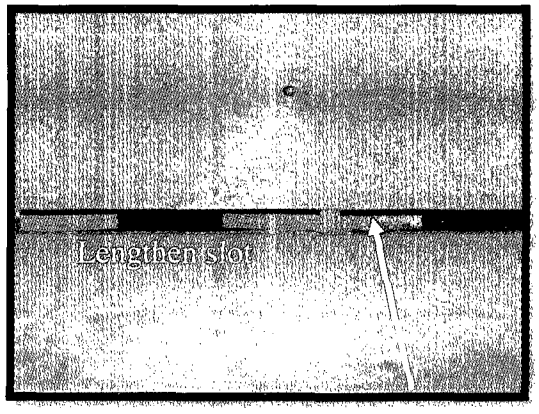

Figure 3-19: Downstream slot

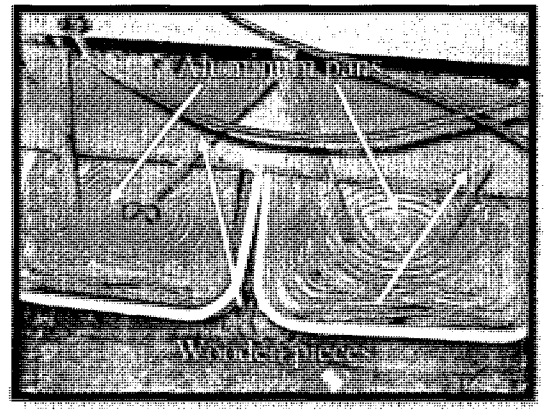

Figure 3-20: Pans for collecting eroded sediments

3.2.3.5 Outgoing flow

At the far end of downstream, a rectangular weir was located. There was a gap between the downstream wooden side and the weir. The free space of the canal in between was filled with water, tangent to the weir crest. That was the initial condition for all tests (Figure 3- 21). The weir had been calibrated in a water canal with a parabolic weir in an upstream reservoir. One pressure transducer was located on the crest in the downstream (Figure 3- 22).

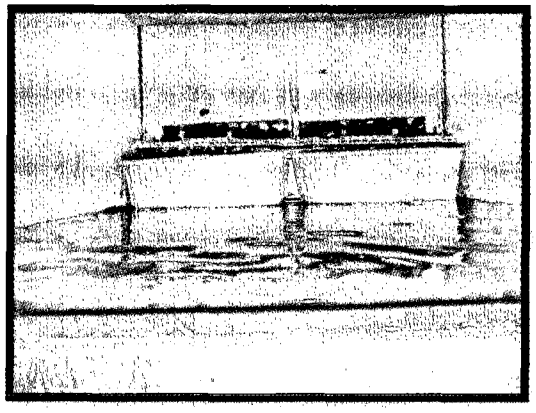

Figure 3-21: Free space in-between filled with water

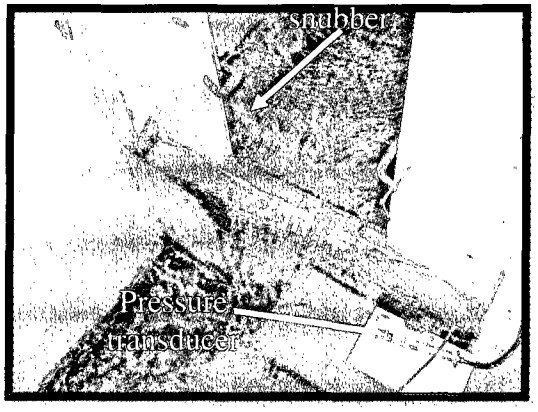

Figure 3-22: Pressure transducer for weir

3.3 Procedure of the experiments

The predefined geometry of each model was marked on the exterior of the channel walls on both sides and in the bottom of the box, and construction was made based on that. For each test, the preparation of the model took three to five days (depending on the size and geometry of the model).

3.3.1 Sample preparation

The first step was the preparation of the clay/moraine layer. For this purpose, the estimated required amount of clay/moraine was mixed with an appropriate amount of

water to form the optimum water content. The clay/moraine was placed under a nylon cover from a few hours to one day to form a monotonous mixture.

For the compaction method, a static force method was used. That is, applying the deadweight of the compaction device on the soil surface and compressing the soil particles. This compaction is limited to upper soil layers and to fulfill the desired compaction, soil is compacted in several layers. For these series of tests, the soil was compacted in three layers.

The clay/moraine core was then prepared in three steps. For each step, the sufficient pre-calculated amount of clay for the desired dry density was spilled in the box and then was compacted with a handmade compaction device (Figure 3-23).

Each layer was compacted enough to give it a well-knit body, without any visible holes or cracks. The final layer was trimmed and the slopes were formed, with the help of different devices such as a metallic ruler and trowels (Figure 3-24 and 3-25).

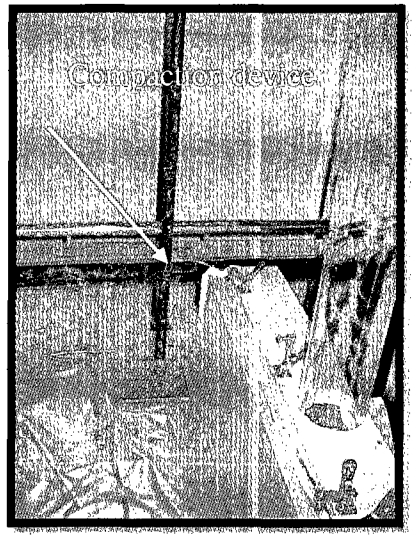

Figure 3-23: Handmade compaction device

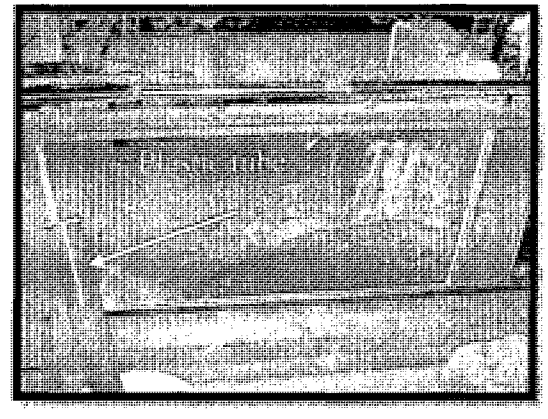

Figure 3-24: Clay core preparation

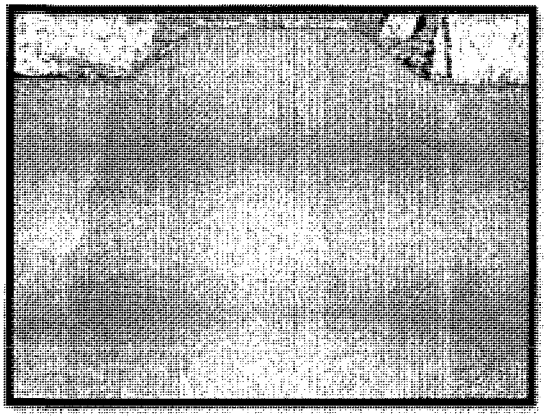

Figure 3-25: Finalized moraine core

At the end, two different samples were taken from the whole depth of the layer, with the help of a plastic tube (Figure 3-24). These samples were placed in the oven to figure out the water content of the constructed model. With the help of the water content, total mass and the occupied volume the compaction percentage of the layer was calculated. The places of removed samples were refilled and the final height was taken by using a point gauge (Figure 3-26).

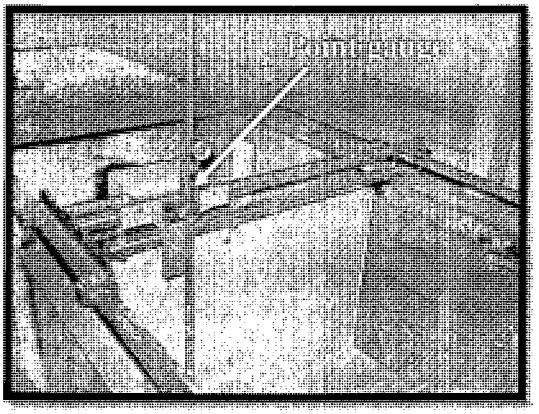

Figure 3-26: Point gauges for height evaluation

After finishing the core layer, the filter (sand) layer was prepared. The same procedures as the core were executed. To achieve the desired water content, the appropriate amount of sand and water mixture was protected under a nylon cover for a day to form a uniform mixture.

Like the core, the filter layer was placed in three different phases. In each step, the adequate quantity of sand was poured into the box and was compacted. Sand compaction was assessed by a handmade compaction device and considered adequate when an inflexible response to applied pressure was felt without the creation of a shear in the sand (Figure 3-27).

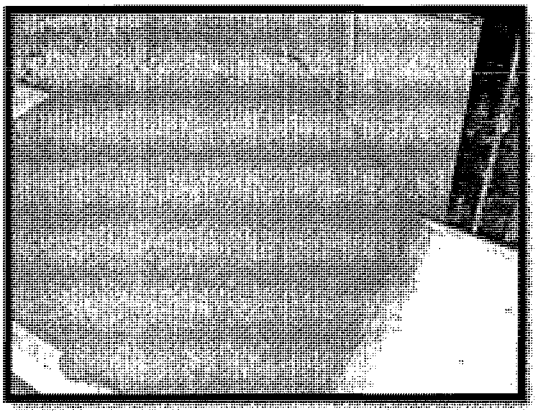

Figure 3-27: Preparation of sand layer

Before finalizing the sand level, pressure transducers were posed in the sand on the horizontal surface of the filter. The pressure snubbers were visible on the filter surface (Figure 3-28 and 3-29).

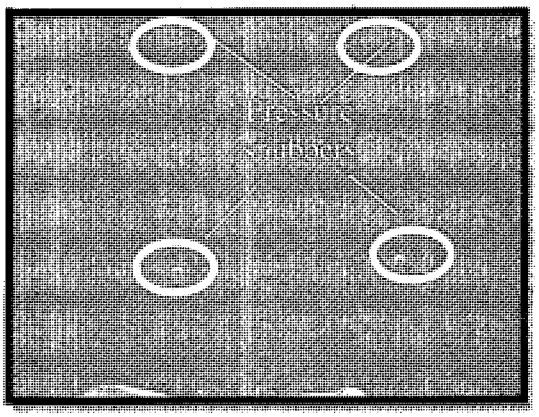

Figure 3-28: Pressure snubbers

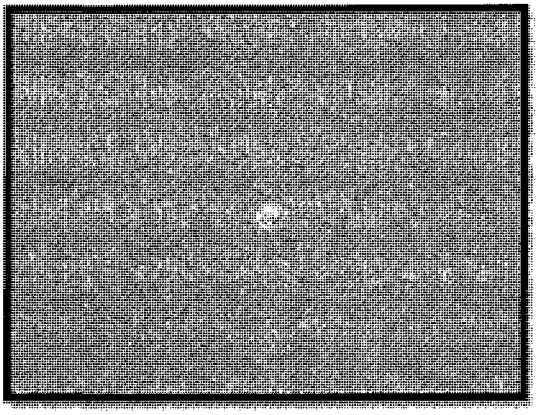

Figure 3-29: Pressure snubber on the filter surface

The snubbers were connected to the wires related to pressure transducers. The wires were placed beneath the sand, both in horizontal and sloped directions and were passed through the small holes in the downstream wooden wall (Figure 3-30). Pressure transducers were located on a wooden shelf at the same level as the snubbers in the filter (Figure 3- 31).

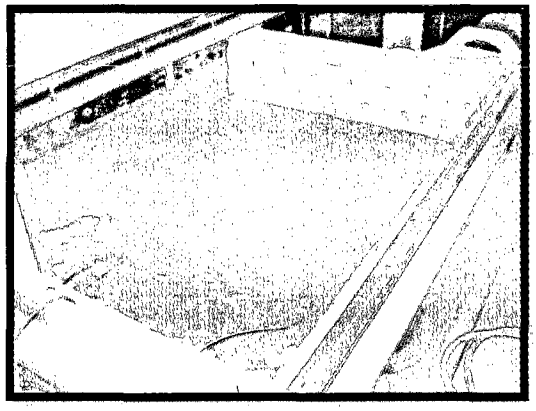

Figure 3-30: Pressure transducer's wires

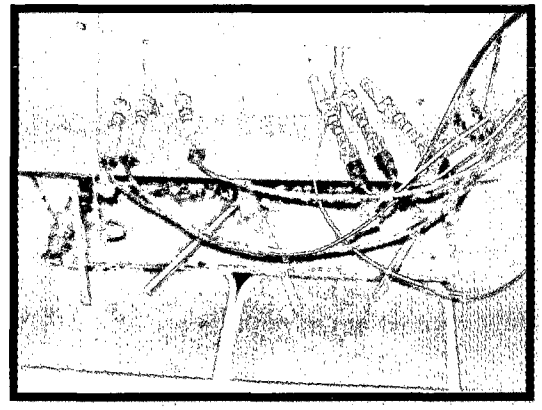

Figure 3-31: Pressure transducer on a wooden shelf

The snubbers were posed in a shallow depth from the filter surface and the dimensions and height of their surface from the bottom of the box were measured by a centimeter tape and a point gauge, respectively. After finishing this part, two samples were removed from the whole layer depth with the help of a plastic tube, and were used for calculating the actual water content after drying the samples in the oven. Then the final layer was poured, trimmed and smoothed. The slopes were shaped using wooden or metallic rulers and trowels (Figure 3-32 and 3-33). Test models were prepared at 85% ± 2% of the standard maximum dry density of the soil sample.

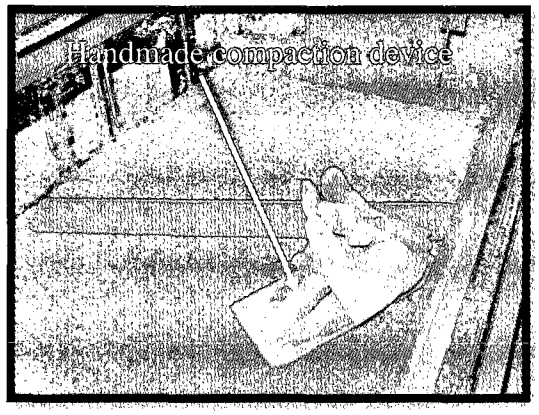

Figure 3-32: Handmade device for compaction

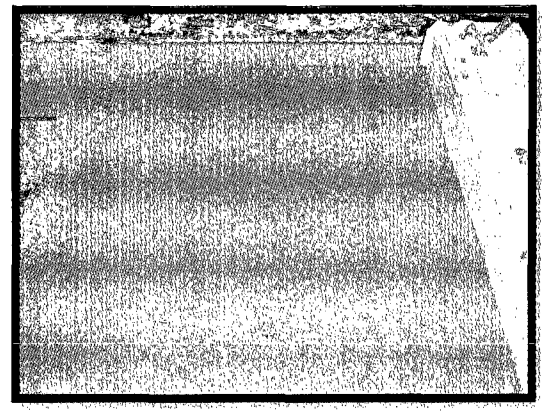

Figure 3-33: Finalized sand layer

After placing the core and filter layer, the gravel was deposited with a shovel over the filter layer in a uniform thickness. The procedure started by placing gravel in the bottom of box, forming the slopes gradually and then the crest of the embankment in a slow manner so as not to affect the filter of the final layer (Figure 3-34).

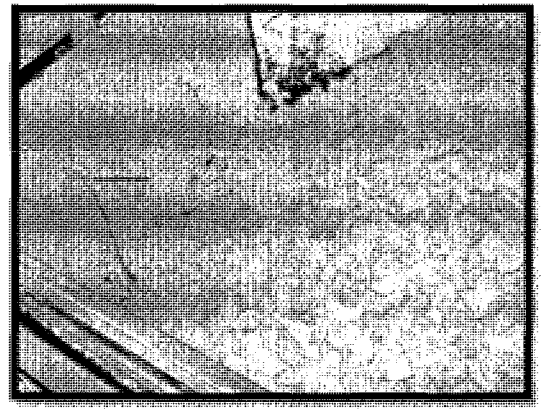

Figure 3-34: Placing the protection layer

As the continuum of the flow through porous media often affects some parameters such as the permeability, in order to reach an approximate constant permeability after the sample preparation, the water head was increased in the upstream gradually until it was a bit below the interface of sand and gravel. The sample was allowed to be in that situation for few hours to one day to obtain the maximum possible saturation.

When starting the test, the initial water level in the upstream was tangent to the interface of sand and gravel. The water level was gradually increased to prevent rapid variations of the pore pressures. Each step (15 to 20 minutes) lasted long enough to reach a stable flow rate on the model. The maximum water head in upstream was as high as possible to avoid any overtopping (Figure 3-35 and 3-36).

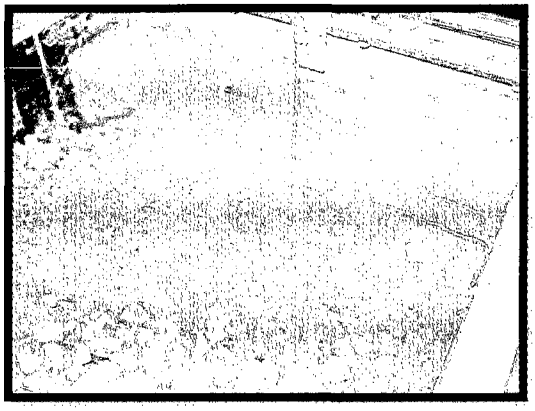

Figure 3-35: Water storage in upstream

Figure 3-36: Max upstream level

After each augmentation and reaching the steady flow, before any raise and going on to the next level, the eroded sediment, if any, was collected in the aluminum pans placed under the slot in the downstream and were put in the oven to dry. At the final position, when water reached the maximum level, tests were usually carried out for forty five minutes to one hour until the flow rate became steady, and the color of outgoing flow became clear, indicating that erosion, if any, had been completed. After the test was over, the gravel layer was removed slowly so any visible changes on the interface could be observed (Figure 3-37).

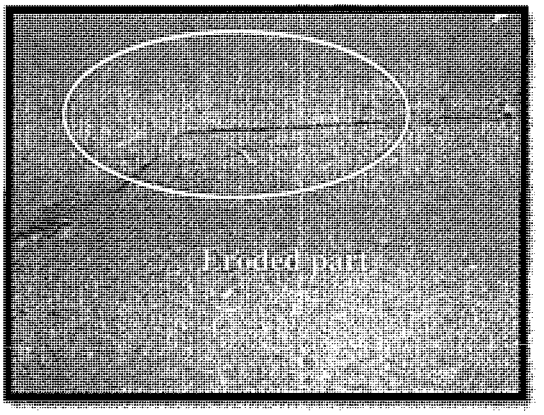

Figure 3-37: Erosion observation

Observation of the water flow passageway and the movement of sediments during the tests were recorded with a digital camera in the form of photographs and film (Figure 3-38).

Figure 3-38: Capturing the water passage and sediment erosion by camera

A schematic view of the whole apparatus is illustrated in Figure 3-39.

3.4 Measurements

3.4.1 Time

To keep the total time of the experiments and time intervals, one or two monometers were used.

3.4.2 Discharge

As mentioned in the chapter three, incoming discharge was collected using a Turbo US-PC signal converter device and a glass-tube meter device. The rate of incoming discharge was recorded in time and data was converted to m^3/s afterward. For outgoing discharge, the calibrated weir and the water head above its crest gave the outgoing flow rate.

3.4.3 Hydraulic gradient

Referred to the chapter three, the water head measurements above the filter layer were recorded by the pressure transducers in time spans. The head drop over the distance between the beginning of the filter layer and the farthest pressure transducer could be calculated. The head above the filter layer was collected by pressure transducers connected to piezometers. The distance between these points were measured with centimeter tape and the head drop over the distance gave the hydraulic gradient.

3.4.4 Erosion rate

During the execution of the experiments, in known time intervals, the eroded sediments were collected in the aluminum pans in the downstream and were put in the oven to dry. Scaling the quantity of washed sediments after drying was used to figure out the rate of erosion. Depending on the necessity unit, the rate of erosion could be presented either in $gram/cm^2$, $gram/cm^2/s$ or $kg/m^2/s$. The area (cm^2- m^2) was the

surface of the filter layer which was passed by the water and the time (s), was the duration of the specific time interval.

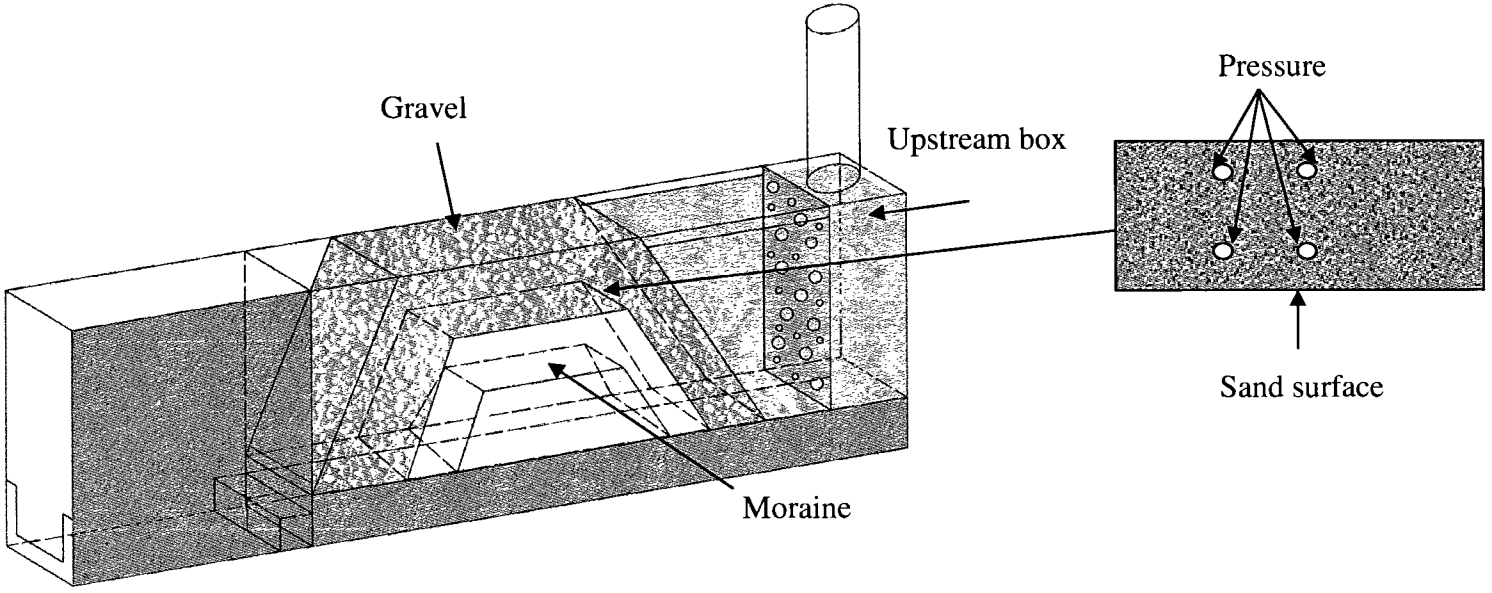

Figure 3-39: Experimental assembly - not to scale

3.5 Experiment type

As described earlier in this chapter, the properties of real models were not clear; therefore, an initial model was designed and based on the results obtained and some modifications were done on the samples to reach the critical conditions for suffusion. Seven different types of tests were done to fulfill this purpose. Afterwards, four series of tests were executed on the critical model of series one with different types of materials, two types with different gradation for filter material and two with different gravel gradation. A short description for each type is presented as follows.

Table 3.5 outlines the conditions examined in these tests. In all the experiments, the slopes of the embankments were 1:1 except the test one that was 1:1.2 and 1:1.7 for clay and sand, respectively. The width of layers was fitted to the canal width (76 cm), the length of filter crest was approximately 39- 40 cm for all tests except test six and seven with a filter crest of 98-99 cm. The height of filter layer was fluctuating between 15 to16 cm.

Three initial tests were done to examine the accuracy and output of the assembled parts. The procedure of the tests was monitored and the existing problems were fixed. The results of these tests were not usable for the final analysis.

3.5.1 Type One

This model was formed as a non- isosceles trapezoid feature (Figure 3-40) with a core consisting of compacted clay and a filter layer from compacted sand. Additionally, the gravel occupied all of the space over the sand. Plexiglas was placed above the gravel and steel beams on top of that to represent the role of a gravel shell and to fulfill the sufficient dead weight over the filter layer, as the depth of the gravel layer was not enough to perform this requirement.

In this model, some Plexiglas was placed in the upstream next to the cubical box's wall, perpendicularly to the flow direction all along the gravel layer, to force drainage through the filter layer. The purpose of this test was to see the role of seepage on the suffusion).

The results from this model were not satisfying as the prevention of water seepage through the gravel caused the sand to move upward instead of in lateral movements (Figure 3-41). Specifications of this model are summarized in Table 3-5. The gravel used had a range in dimensions between 5 to 20 mm.

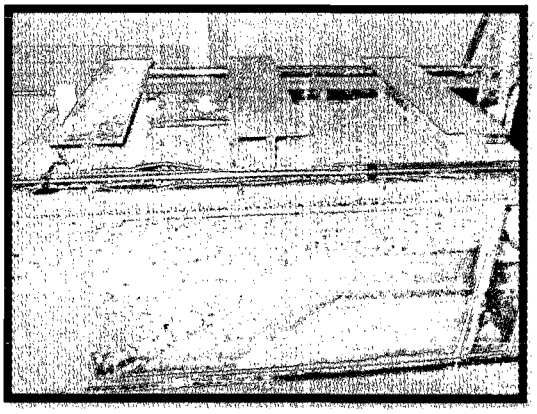

Figure 3-40: Test type one

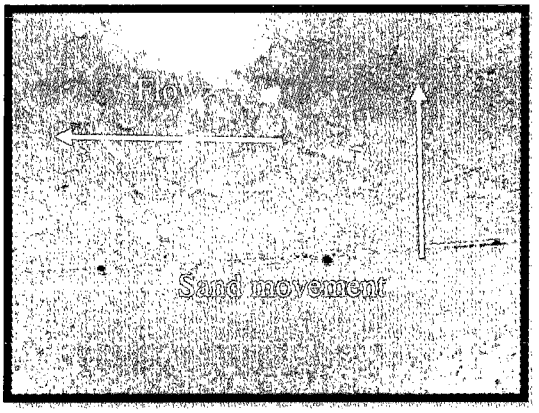

Figure 3-41: Sand movement in upward

3.5.2 Type Two

This type had the same characteristics as the first type, except:

- The layers satisfied the geometry relations and sand thickness = 0.6 thickness of gravel.
- As the dead weight over the filter was satisfied, the steel beams were removed (Figure 3-42).

The purpose of this test was to study the suffusion on non-isosceles embankment with well mixed gravel.

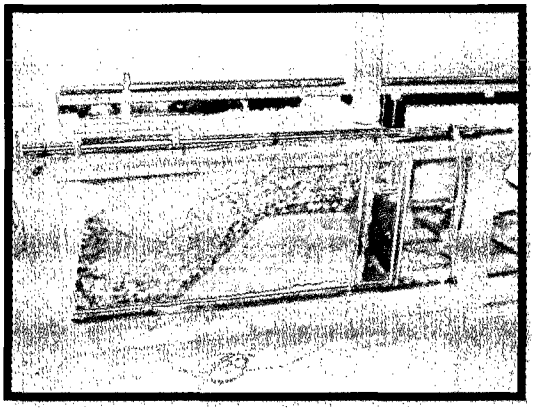

Figure 3-42: Test type two

3.5.3 Type Three

This was like type two except that:

- The model had transformed into an isosceles trapezoid (Figure 3-43).
- The core layer was formed by moraine of the grading curve represented before.
- To prepare an isosceles model, the length of the box was increased (Figure 3-44).

The purpose of this test was to study the suffusion on isosceles embankment with well mixed graved.

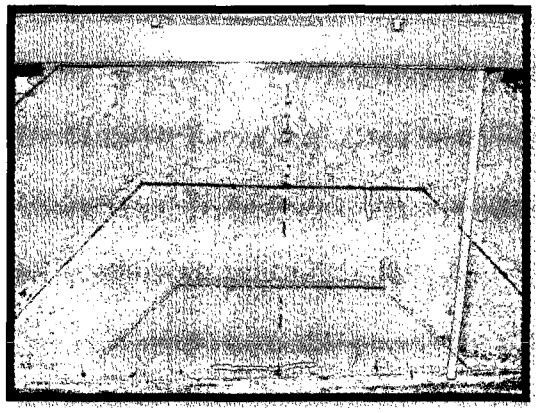

Figure 3-43: Test type three

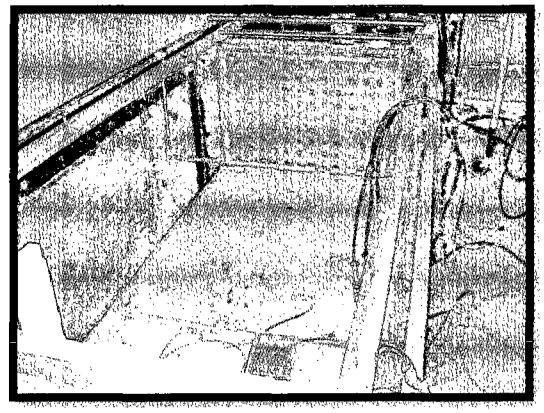

Figure 3-44: Preparation of box

3.5.4 Type Four

This type has the same characteristics as type three except that:

- The gravel layer was replaced by two sub layers:
  - The first layer with a thickness of 7 cm and of $d_{50} = 7.07$
  - The second layer with the thickness of 18 cm and of $d_{50} = 19.16$.

The purpose of this test was to study the suffusion on isosceles embankment with two layer gravel to see the role of sub layers on the phenomenon of suffusion. Figure 3-45 shows a typical assembly of type four.

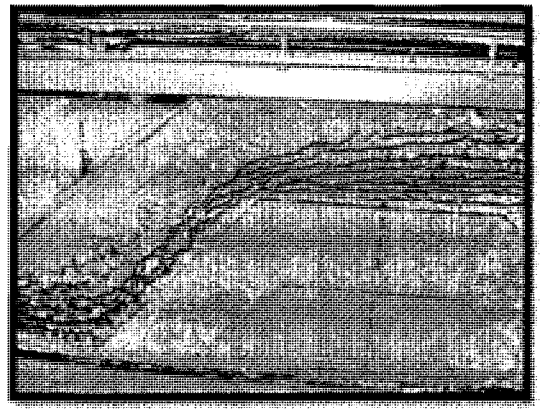

Figure 3-45: Test type four

3.5.5 Type Five

This type has the same characteristics as type four except:

- The gravel layer contained only particles of the diameter superior to ten mm and inferior to twenty mm with the same setup and materials.

The purpose of this test was to study the suffusion on isosceles embankment with coarser particles of gravel. A view of the model is shown in Figure 3-46.

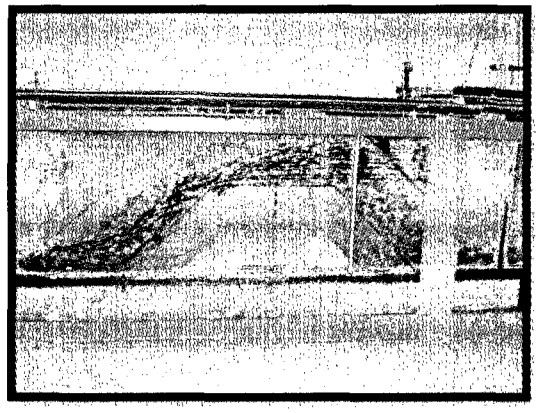

Figure 3-46: Test type five

3.5.6 Type Six

The present model had a sand layer of the surface length of 97 cm, almost twice in length as the previous model. The materials used were similar to type five.

The purpose of this test was to study the suffusion on an isosceles embankment with the same gravel porosity as type five but with a longer crest to develop the role of filter length on the suffusion. Figure 3-47 presents a view of the constructed model.

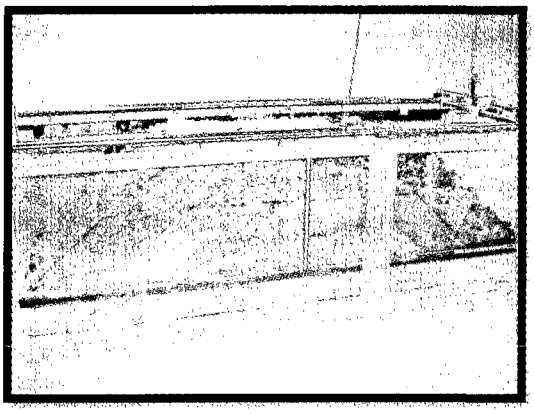

Figure 3-47: Test type six

3.5.7 Type Seven

In this model, the same materials were used as in models five and six. The length of the filter layer was similar to type six except that the slopes of the core and the filter were executed in a stair shape.

To actualize the stair forms, on the core layer, the additional moraine was removed and cut with trowels and metal rulers; as a cohesive material, the stairs were formed easily. For the filter layer, the first step was performed using a sheet of Plexiglas to form the external parapet of the stair. When it was compacted and finalized, enough gravel was placed behind the Plexiglas to support the stair and then the Plexiglas was removed. This method was used for the formation of all stairs.

The purpose of this test was to study the role of stairs like slopes on the phenomenon of suffusion, on isosceles embankment. Figure 3-48 describe this in more detail.

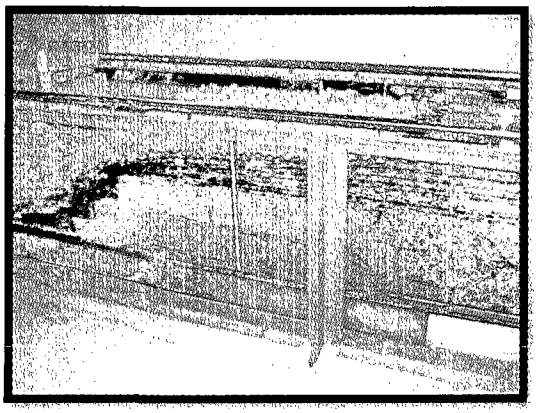

Figure 3-48: Test type seven

3.5.8 Type Eight

This type had the same characteristics of model type five, except:

- The sand layer was formed by sand type three. This type of sand had a particle size inferior to 1.25 mm.

The purpose of this test was to study the role of filter grain size on suffusion, on isosceles embankment. Filter was consisted of particles with a less d_{50} compared to type five. Figure 3- 49 presents the model constructed.

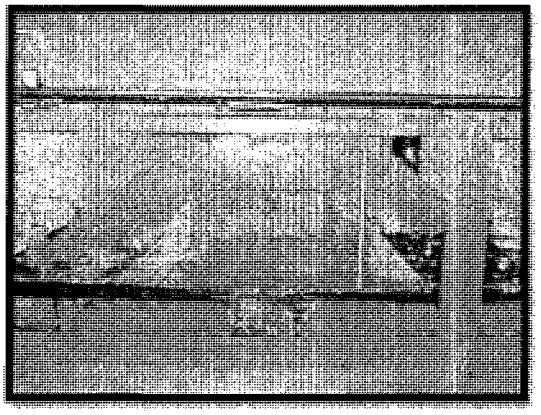

Figure 3-49: Test type eight

3.5.9 Type Nine

This type had the same characteristics as model type five, except:

- The sand layer was formed by sand type two. This type of sand contained the particle size retained on the sieve with voids of 315 mm.

The purpose of this test was to study the role of filter with a higher d_{50} compared to type five, on the suffusion in an isosceles embankment. Figure 3- 50 describe this in more detail.

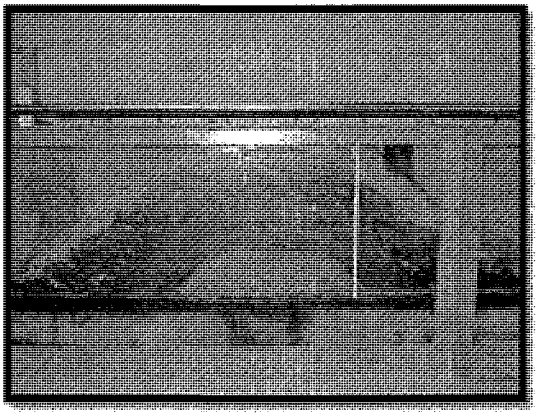

Figure 3-50: Test type nine

3.5.10 Type Ten

This type had the same characteristics as model type five, except:

- The gravel layer was formed with gravel with particles superior to fourteen mm and inferior to twenty mm.

The purpose of this test was to study impact of using more porous gravel on the phenomenon of suffusion. Figure 3-51 describe this in more detail.

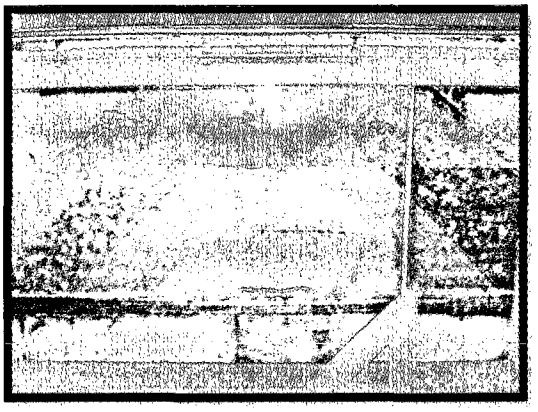

Figure 3-51: Test type ten

3.5.11 Type Eleven

This type had the same characteristics as model type five, except:

- The gravel layer was formed by gravel with particles superior to five mm and inferior to twenty mm.

The purpose of this test was to study the impact of gravel with more porosity on the suffusion. Figure 3-52 describe this in more detail.

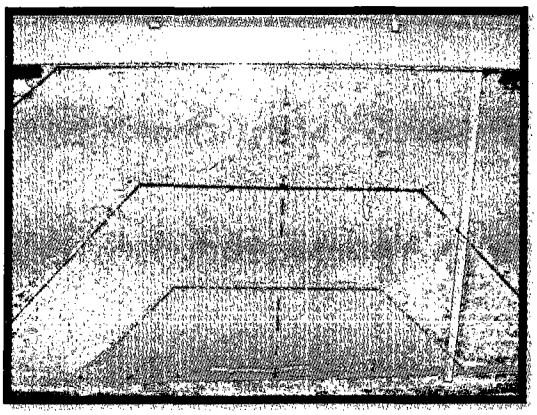

Figure 3-52: Test type eleven

3.5.12 Successive tests

In some of the tests, two or three successive tests were executed on the same model. In this procedure, after the first try, the incoming water was reduced and stopped and the water level in the upstream was decreased below the filter level. The situation was kept for one or two hours and the tests were repeated again. These types of tests were carried out to show the influence of water fluctuation on the suffusion.

Table 3-5: The experiment's specifications

Test type	Base Material			Filter Material			Geometry	Protection Material				Utility of the test
	Material	d_{50} (mm) average	Upper Length (cm)	Material	d_{50} (mm) average	Upper Length (cm)		Material	d_{50} (mm) average	Particle size	Upper Length (cm)	
Type 1	Clay		35	Sand	0.85	40	non- isosceles trapezoid plexiglas beam on top	Gravel	18.33	$5_{mm}<d<20_{mm}$	100	Study the effect of seepage on the suffusion
Type 2	Clay /Moraine		30	Sand	0.85	40	non- isosceles trapezoid	Gravel	18.33	$5_{mm}<d<20_{mm}$	60	Study of suffusion on non- isosceles embankment with well mixed gravel
Type 3	Moraine	0.175	30	Sand	0.85	40	isosceles trapezoid	Gravel	18.33	$5_{mm}<d<20_{mm}$	60	Study of suffusion on an isosceles embankment with well mixed gravel
Type 4	Moraine	0.175	30	Sand	0.85	40	isosceles trapezoid	Gravel	7.07 19.16	$5_{mm}<d<10_{mm}$ $10_{mm}<d<20_{mm}$	60	Study of suffusion on an isosceles embankment with two layer of gravel
Type 5	Moraine	0.175	30	Sand	0.85	40	isosceles trapezoid	Gravel	19.16	$10_{mm}<d<20_{mm}$	60	Study of suffusion on an isosceles embankment with coarser particle of gravel
Type 6	Moraine	0.175	84	Sand	0.85	99	isosceles trapezoid longer	Gravel	19.16	$10_{mm}<d<20_{mm}$	120	Study of suffusion on an isosceles embankment with coarser particles of gravel and a longer crest
Type 7	Moraine	0.175	84	Sand	0.85	99	isosceles trapezoid longer stairs slopes	Gravel	19.16	$10_{mm}<d<20_{mm}$	120	Study of suffusion on an isosceles embankment with slopes in stairs, coarser particle gravel and a longer crest
Type 8	Moraine	0.175	30	Sand	0.42	40	isosceles trapezoid	Gravel	19.16	$10_{mm}<d<20_{mm}$	60	Study of suffusion on an isosceles embankment containing finer particles filter
Type 9	Moraine	0.175	30	Sand	1.20	40	isosceles trapezoid	Gravel	19.16	$10_{mm}<d<20_{mm}$	60	Study of suffusion on an isosceles embankment with coarser particles filter
Type 10	Moraine	0.175	30	Sand	0.85	40	isosceles trapezoid	Gravel	18.8	$14_{mm}<d<20_{mm}$	60	Study of suffusion on an isosceles embankment with coarser particles of gravel
Type 11	Moraine	0.175	30	Sand	0.85	40	isosceles trapezoid	Gravel	18.33	$5_{mm}<d<20_{mm}$	60	Study of suffusion on an isosceles embankment with mixed particles of gravel

CHAPTER 4: RESULTS AND DISSCUSSIONS

4.1 Introduction

This section presents the analysis of results obtained during the experiments. The analysis aims to identify the factors that may influence the initiation of suffusion in the interface of two different layers of sediments.

4.2 Results

4.2.1 Suffusion in the interface of clay/moraine and sand

By executing the experiments of various types, there was no visible erosion on the interface of moraine/clay and the sand. By the grain size distribution of eroded sediments, no tracks of clay or moraine were observed.

4.2.2 Suffusion in the interface of sand and gravel

The measured data during the experiments are presented in tables 4-1 and 4-2

Table 4-1: Measured data during experiments (2-7)

	Time	Eroded sediment -gr	water head drop - inch	Gradient
Type two	0			
	1860	20.4	0.6	0.0535
	960	23.1	1.3	0.1110
	1140	18.5	1.9	0.1554
	2640	18.2	2.1	0.1734
Type three	0			
	2550	7.2	0.4	0.0415
	1110	6.2	1.6	0.1216
	1200	16.3	2.0	0.1481
	3240	20.1	2.5	0.1932
Type four	0			
	2160	19.0	1.0	0.0784
	1080	3.7	1.9	0.1432
	900	3.3	2.2	0.1698
	2820	7.4	2.7	0.2009
Type five	0			
	1140	37.0	0.8	0.0607
	1280	43.7	1.3	0.1004
	880	13.7	1.5	0.1163
	1200	7.9	2.0	0.1521
	2700	5.3	2.3	0.1751
Type six	0			
	1441	3.1	1.2	0.0360
	5445	16.8	1.9	0.0554
	813	16.2	2.2	0.0651
	735	8.4	3.5	0.1025
	1740	17.9	4.3	0.1255
Type seven	0			
	1780	13.1	1.6	0.0460
	900	14.8	2.5	0.0735
	720	16.2	2.8	0.0805
	960	15.9	3.2	0.0929
	3060	38.1	3.7	0.1078

Table 4-2: Measured data during experiments (9-11)

	Time	Eroded sediment -gr	water head drop - inch	Gradient
Type nine	0			
	1380	10.6	0.5	0.0376
	1020	11.1	1.0	0.0807
	900	6.1	1.4	0.1112
	1140	10.0	1.8	0.1452
	960	14.5	2.2	0.1791
	2400	8.3	2.4	0.1930
Type ten	0			
	900	12.7	0.5	0.0406
	1020	43.5	1.2	0.0955
	1080	51.0	1.7	0.1342
	900	32.4	2.1	0.1625
	1020	12.7	2.6	0.2014
	2280	76.3	2.9	0.2253
Type eleven	0			
	1020	3.6	0.6	0.0497
	1080	22.1	1.4	0.1077
	900	15.7	1.9	0.1498
	900	17.4	2.2	0.1694
	1440	19.6	2.6	0.1965
	2160	8.9	2.9	0.2236

It should be noted the width of filter surface for all tests was 40 cm. the length of the crest was 40 cm for all tests except 97 cm and 98 cm for test six and seven respectively. The length of water path was 30.5 cm for test 2, 33.5 cm for tests 3, 4 and 5, 87 cm for test 6, 88 cm for test 7, 31 cm for test 9 and 33 cm for tests 10 and 11.

4.3 Discussion

4.3.1 Suffusion in the interface of clay/moraine and sand

From the results obtained, one may conclude that the variation of the water head in upstream has no important influence on the suffusion between the layers of core and filter. One can say during the head augmentation, the core layer stays stable. Figure 4-1 shows some samples of clay/moraine and sand interface after the test's execution.

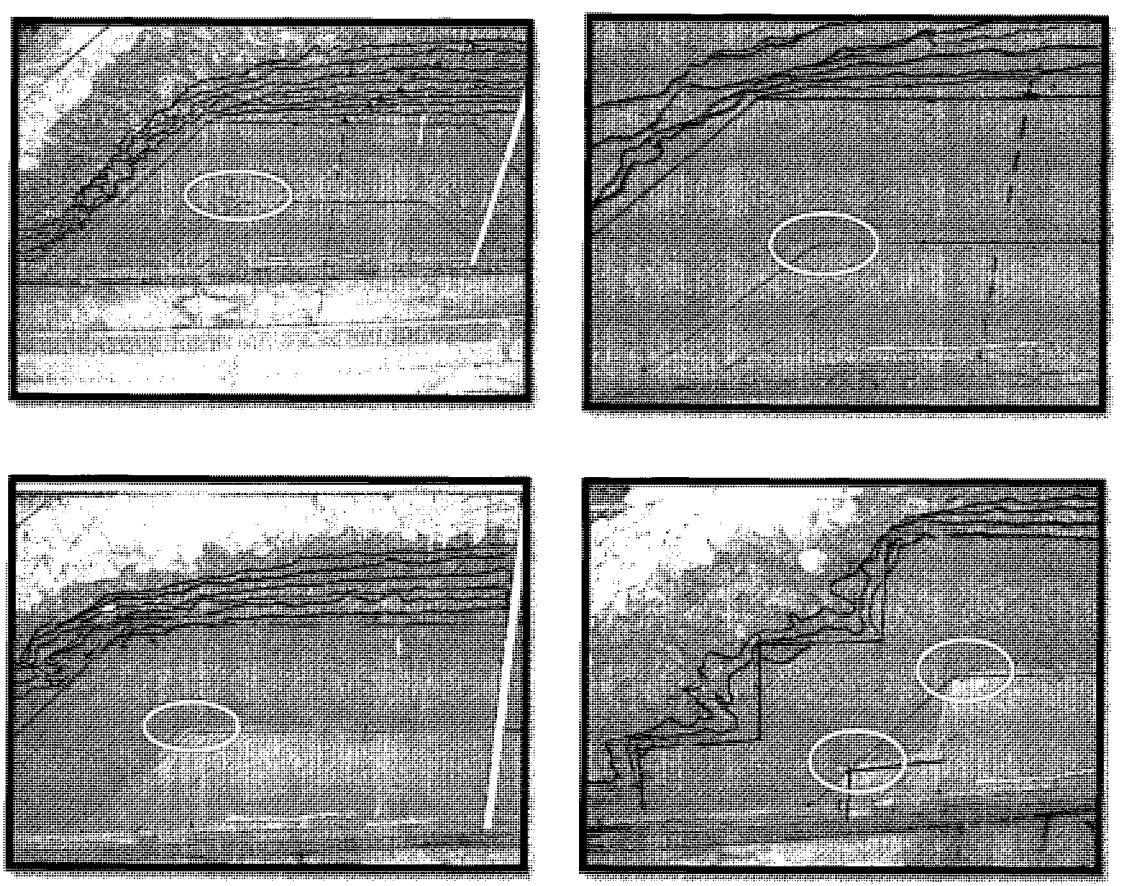

Figure 4-1: Some sample of the clay/moraine and sand interface after tests

4.3.2 Suffusion in the interface of sand and gravel

4.3.2.1 Visual comparison

Comparing the photographs taken during different tests (Figures 4-2 to 4-8), they indicate that the most visible suffusion took place during the tests of the types 5, 6 and 7. The common specification of these tests was the arrangement of gravel, which contained the particles inferior to twenty mm and superior to ten mm. It shows the porosity of the pervious layer has a great influence on the formation of external suffusion on the interface of sand and gravel layers.

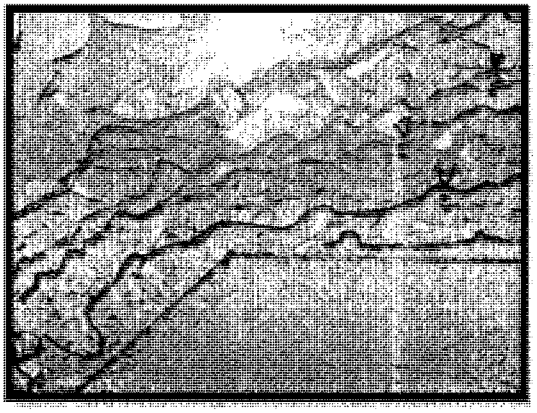

Figure 4-2: Suffusion in a sample of test type 2

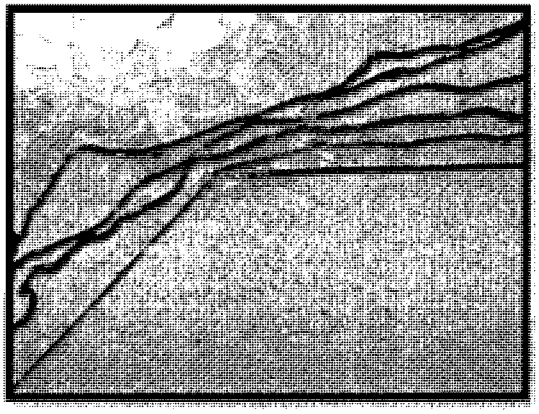

Figure 4-3: Suffusion in a sample of test type 3

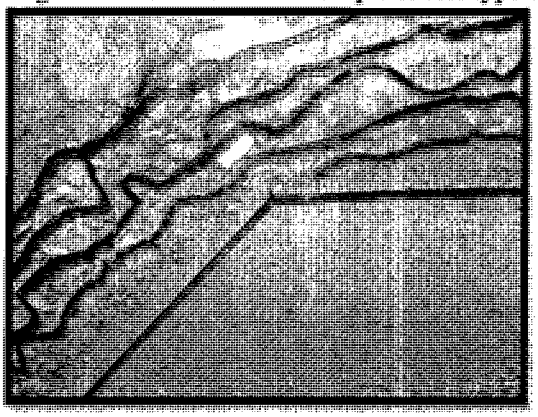

Figure 4-4: Suffusion in a sample of test type 4

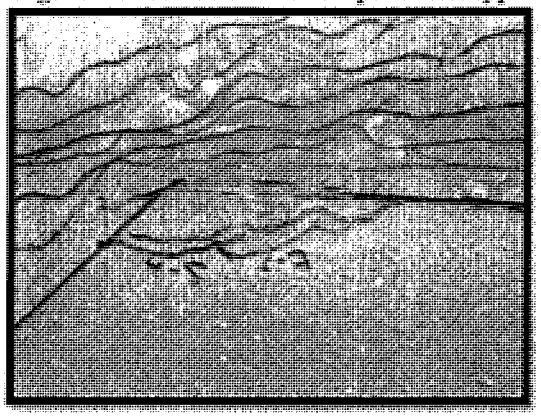

Figure 4-5: Suffusion in a sample of test type 5

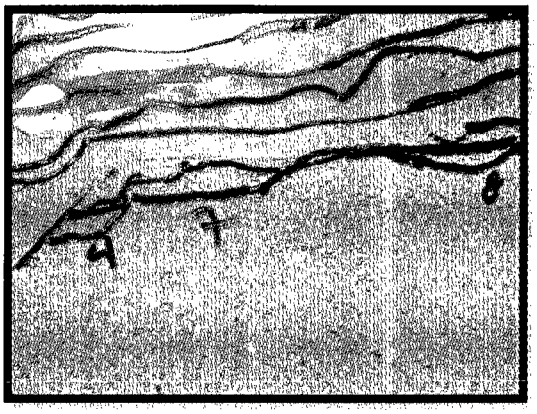

Figure 4-6: Suffusion in a sample of test type 6

Figure 4-7: Suffusion in a sample of test type 7

4.3.2.2 Solid discharge by unit of surface

Alternatively, as far as it is known, in order to reduce the number and complexity of the experiment's variables that affect a physical phenomenon and to find out the relationship between them, one can use the method of Buckingham's π [37] (for more details check appendix II).

Supposing that the mobile bottom of the channel, consisting of uniform solid particles (with diameter d and specific volume weight γs), and no movement of cohesive particles the effect of seepage, the properties of fluid, cohesionless particles and the seepage have impact on this phenomenon.

Using the theory of π for a dimensional analysis shows the rate of erosion E is quantifiable by means of four non-dimensional groups:

Hydraulic gradient: $i = \frac{\Delta h}{L}$

Relative density: $S_s = \frac{\gamma_s}{\gamma}$

Non-dimensional diameter of the particle: $d_* = d\left((S_s - 1)\frac{g}{v^2}\right)^{\frac{1}{3}}$

Porosity: ρ

Where Δh is the difference between the upstream water level and filter crest's water level, γ is the volume of the weight of water, L is the length upstream to the pressure transducer placed in the sand and υ is the kinematic viscosity of water. The theory of π gives an expression for the non-dimensional intensity of the rate of erosion:

$$A = f_A\left(d_*, p, i, S_s, \frac{E}{\sqrt{\rho_w{}^2 g d}}\right)$$

$$E^* = \frac{E}{\sqrt{\rho_w{}^2 g d}} = f(d_*, \rho, i, S_s) \qquad (4\text{-}1)$$

Where, E is the massive solid discharge by the surface unit. As Ss, ρ and d* are almost constant, the equation above says:

$$E^* = f(i) \qquad \text{Or} \qquad \frac{E}{\sqrt{\rho_w^2\, g\, d_{50}}} = f\left(\frac{\Delta h}{L}\right)$$

The form of functional relation gives the average established formula with experiments in the laboratory and in nature. The solid discharge during different tests was calculated by determining the relation 4-1. The result for each test is shown and discussed below.

As mentioned in chapter three, the results for test type one was not considered through the final analysis as the existence of Plexiglas in front of the gravel layer made the soil particles move in a vertical direction.

The results mentioned below, are representative of average value. The amount of errors calculated are described in appendix I. the results obtained for each test were pointed out on the coordinate system and the trend lines were drawn.

Tables 4-3 and 4-4 show the calculated values for the dimensionless solid discharge in different types of experiments.

Table 4-3: Measured data during experiments (2-7)

	Time	E* non cumulative
Type two	0	
	1860	3.920E-07
	960	8.579E-07
	1140	5.803E-07
	2640	2.455E-07
Type three	0	
	2550	1.005E-07
	1110	2.001E-07
	1200	4.842E-07
	3240	2.215E-07
Type four	0	
	2160	3.134E-07
	1080	1.226E-07
	900	1.308E-07
	2820	9.393E-08
Type five	0	
	1140	1.160E-06
	1280	1.217E-06
	880	5.544E-07
	1200	2.361E-07
	2700	6.995E-08
Type six	0	
	1441	1.160E-06
	5445	1.217E-06
	813	5.544E-07
	735	2.361E-07
	1740	6.995E-08
Type seven	0	
	1780	1.070E-07
	900	2.393E-07
	720	3.279E-07
	960	2.416E-07
	3060	1.814E-07

Table 4-4: Measured data during experiments (9-11)

	Time	E* - non cumulative
Type nine	0	
	1380	2.322E-07
	1020	3.308E-07
	900	2.062E-07
	1140	2.663E-07
	960	4.569E-07
	2400	1.048E-07
Type ten	0	
	900	5.054E-07
	1020	1.524E-06
	1080	1.685E-06
	900	1.284E-06
	1020	4.459E-07
	2280	1.194E-06
Type eleven	0	
	1020	1.245E-07
	1080	7.292E-07
	900	6.210E-07
	900	6.916E-07
	1440	4.851E-07
	2160	1.471E-07

Type two and three

As was described type two was constructed as a non-isosceles trapezoid whereas type three was an isosceles trapezoid. Comparing the results of type two and three in figure 4-8, shows a higher rate of suffusion for type 2. This may indicate that water entered directly onto the sand layer, for the same gravel layer, can increase the rate of solid discharge.

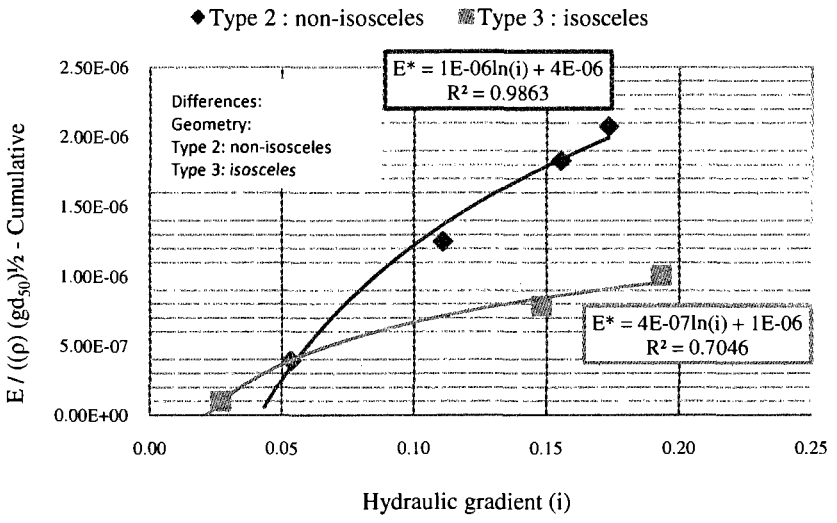

Figure 4-8: Hydraulic gradient versus dimensionless solid discharge (type 2 and 3)

Figure 4-9 shows the schematic view of test type two and three. As the condition of test type three is closer to a real situation, the test geometry was transformed to type three to establish a more realistic condition.

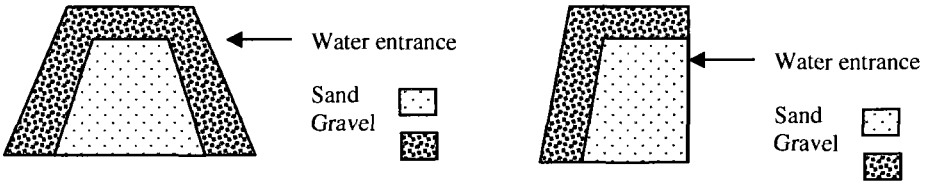

Figure 4-9: schematic view of water entrance, left: type three, right: type two

Type three and four

The differences between tests type three and four are the properties of the gravel layer. The experiments' results (figure 4-10) show a higher rate of solid discharge for type

three compared to type four. It can be concluded that the overlying gravel layer on the filter greatly influences the suffusion.

Indeed, in test type four, the gravel layer consists of two sub layers. The lower layer was formed by particles of diameter (5 mm $\leq$d $\leq$ 10 mm); the voids between particles were smaller compared to the mixture of gravel particles from size 5mm to 20 mm so the solid discharge was much lower because voids were smaller and could be more quickly sealed by the grains of sand.

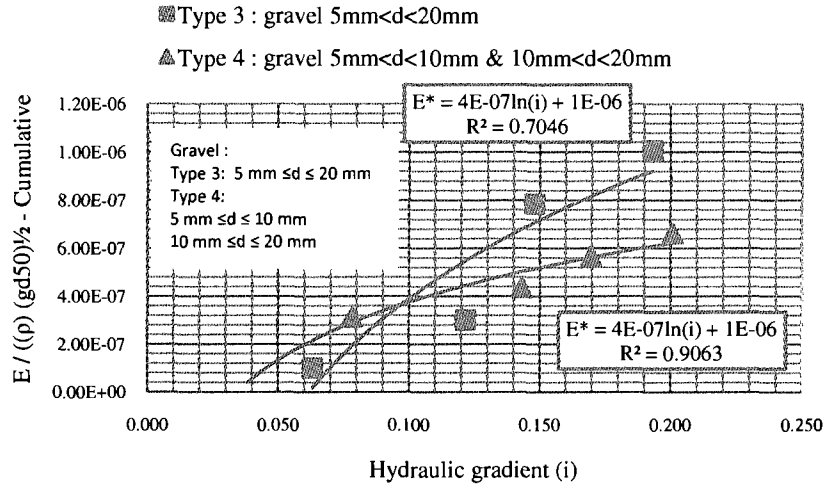

Figure 4-10: Hydraulic gradient versus dimensionless solid discharge (type 3 and 4)

Type four and five

In test type five, the gravel particles inferior to 10 mm were eliminated from the gravel layer. A comparison of test five and four in figure 4-11 demonstrates that the trend line curve of type five has a sharper slope. The conclusion can be that a higher porosity of gravel results in a higher rate of suffusion, and a small increase in a hydraulic gradient produces increases in the rate of solid discharge.

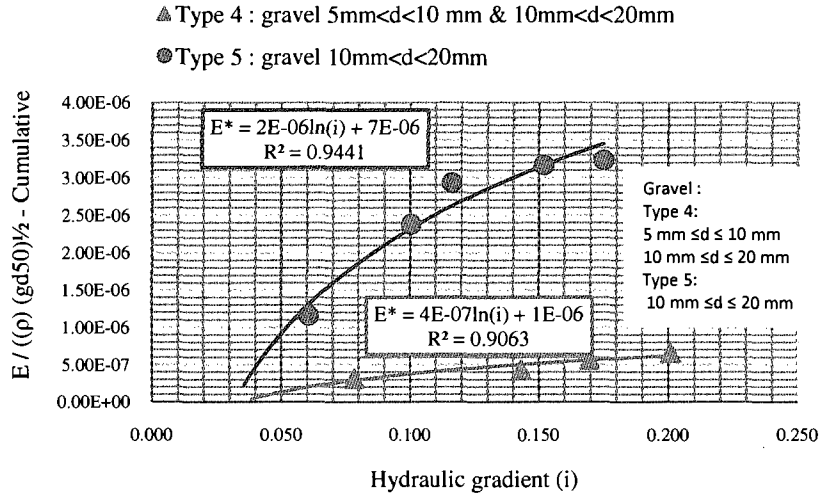

Figure 4-11: Hydraulic gradient versus dimensionless solid discharge (type 4 and 5)

Type five, six and seven

The comparison of the curves of test type five and six in figure 4-12, with the same gravel layer and a length of a crest twice as large, shows that with a longer filter crest the suffusion starts with a lower hydraulics gradient. On the other hand, with the increase of the hydraulic gradient, the solid discharge slope is milder in the case of a crest twice as long.

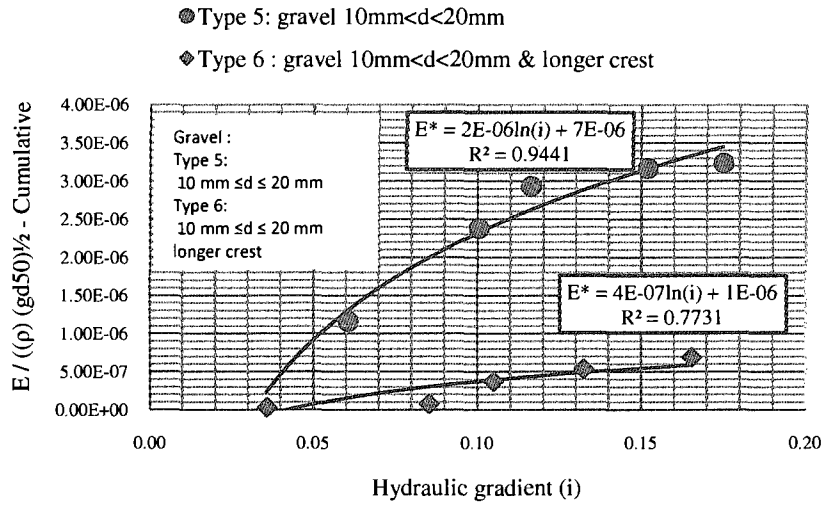

Figure 4-12: Hydraulic gradient versus dimensionless solid discharge (type 5 and 6)

The comparison of the curves of the type six and seven tests in figure 4-13, with the same geometry and material except the form of the slope, does not show any significant changes in the initiation of movement and the solid discharge rate according to hydraulic gradient. Though after the initiation, in the same range of hydraulic gradient, type seven shows more suffusion.

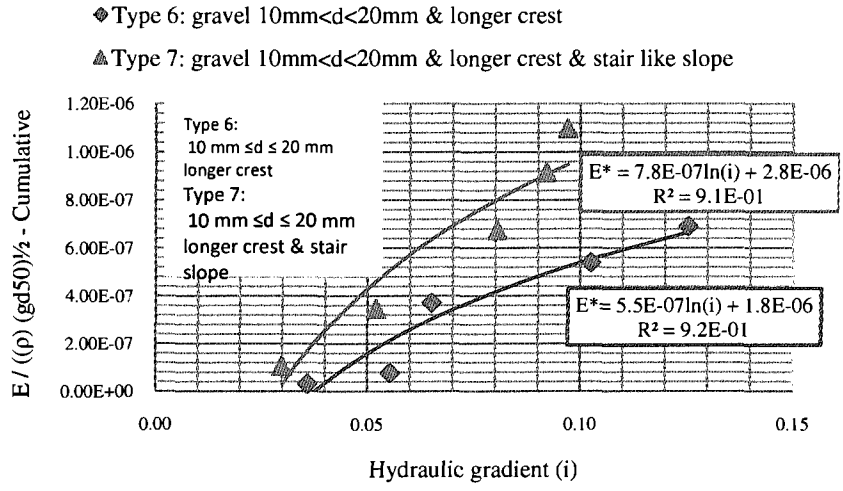

Figure 4-13: Hydraulic gradient versus dimensionless solid discharge (type6 and 7)

Considering the filter level as an origin, the relationship between the upstream water level and the water level in maximum erosion during the test is shown in Figure 4-14.

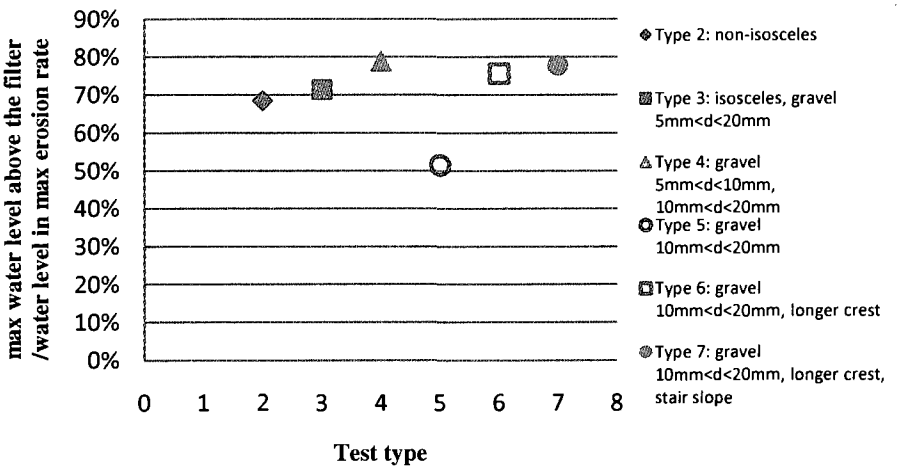

Figure 4-14: Relationship of maximum water level above the filter to water level at maximum solid discharge

During the test type 5, the maximum solid discharge is reached when the water level in upstream is approximately in the middle of the maximal water level. So, the test with gravel with a diameter varying between 10 mm and 20 mm is the most critical.

Type five, eight and nine

Tests type eight and nine were executed with a lower and higher d50 of sand compared to test five. All of the model's specifications were identical to test type five, as it proved to be the most critical situation. In test type eight, the suffusion started as the water passed through the filter layer and without any augmentation in the water level in the upstream; most of the sand was washed out in few minutes. It was so rapid that there was no chance to measure the hydraulic gradient. Figure 4-15 and 4-16 show this phenomenon.

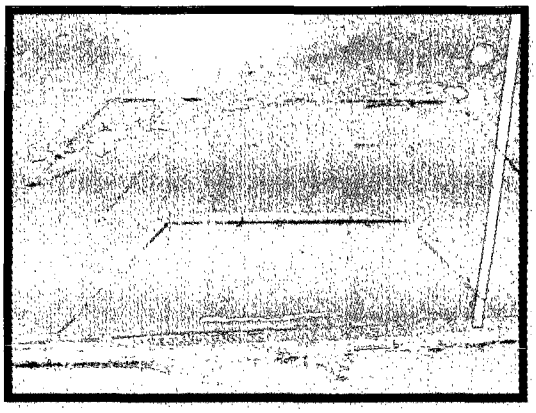

Figure 4-15: Initiation of rapid suffusion in type eight

Figure 4-16: Washing out of sands in few minutes

Figure 4-17 presents the comparison of the cumulative solid discharge rate curves in type five and nine.

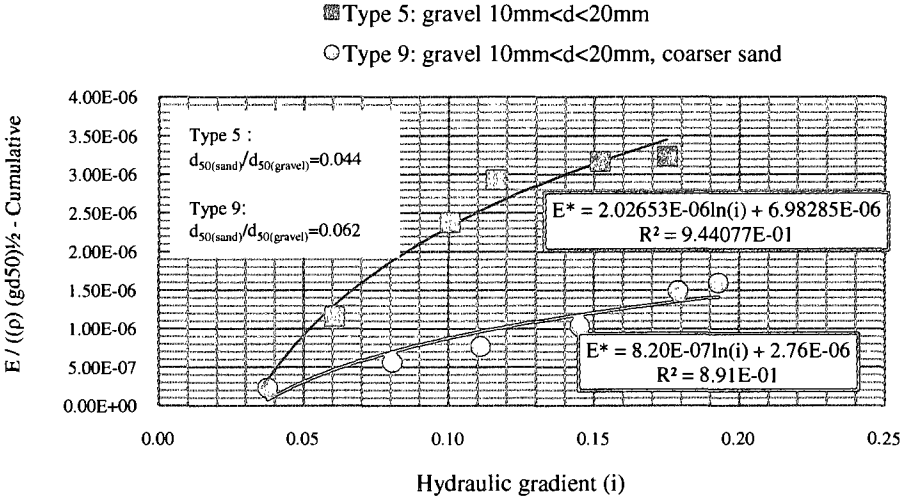

Figure 4-17: Hydraulic gradient versus dimensionless solid discharge for sand with different gradation (type5 and 9)

This shows that using coarser sand provides a lower erosion rate at approximately the same hydraulic gradient. In other words, the slope of the erosion rate is less for coarser sand.

Type fine, ten and eleven

Assuming the test type five as the primary try, test ten and eleven were conducted with gravel with different porosity. The porosity of gravel in test type ten (gravel particles $14 \leq d \leq 20$ mm) and in type eleven (gravel particles $5 \leq d \leq 20$ mm) were higher and lower compared to test type five (gravel particles $10 \leq d \leq 20$ mm), respectively. Figure 4-18 shows the erosion rate of these three types in comparison with each other.

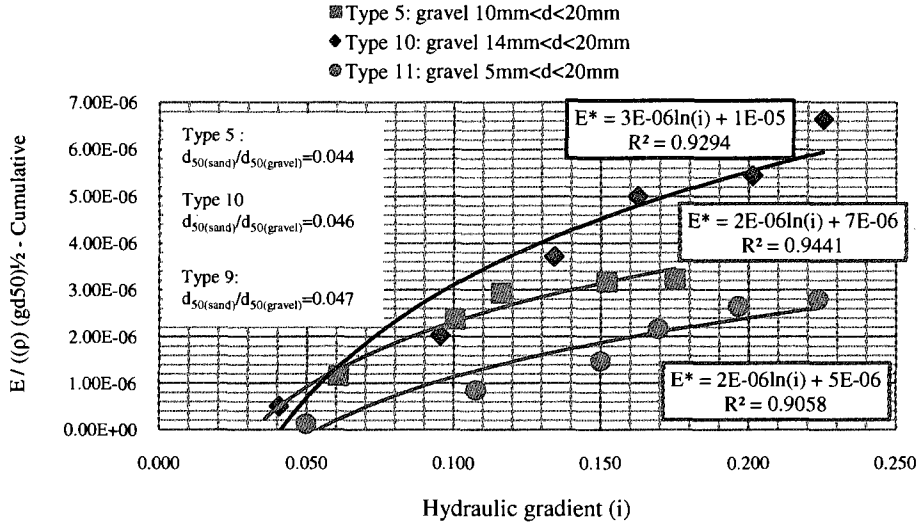

Figure 4-18: Hydraulic gradient versus dimensionless solid discharge for gravels with different gradation (type5, 10 and 11)

The results obtained indicate that by reducing the porosity of gravel overlying the filter layer, within the region of the same hydraulic gradient a smaller rate of internal erosion is observed. In other words, with bigger voids between the gravel particles, the sand grains wash out easier. Smaller vacancies in between the gravel particles fill with filter particles more rapidly.

Summery

Figure 4-19 represent the graphs related to test type two to seven.

Based on the results obtained, for each test a trend line curve was generated and by extrapolation the critical hydraulic gradient for the beginning of suffusion was estimated. As it is known the inaccuracies of the experimental data can affect the results. In appendix I the absolute error values are shown. To estimate the relative errors for erosion rate and hydraulic gradient the errors of influenced parameters are added. Focusing on the initiation of suffusion, the estimated relative error for each test is shown in table 4-5.

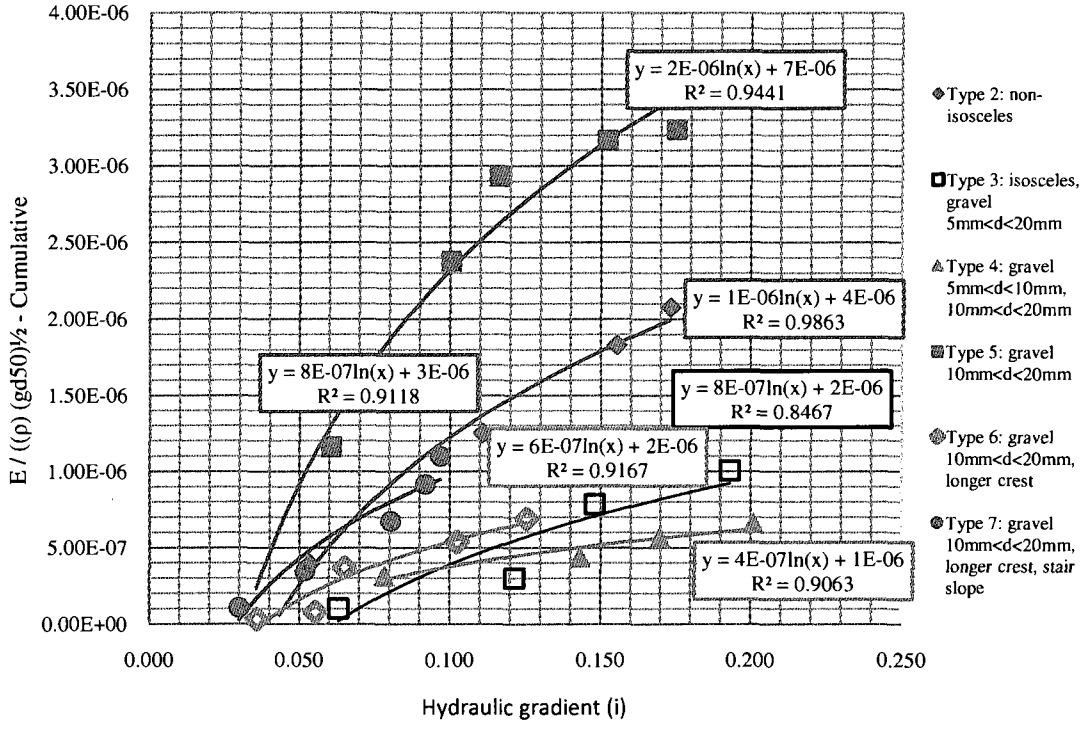

Figure 4-19: Hydraulic gradient versus dimensionless suffusion rate (Type 2-7)

Table 4-5: Estimated critical hydraulic gradient

Test type	Estimated value	R squared related to curves
Type 2	0.0418±0.0008	0.9863
Type 3	0.0249±0.0008	0.7602
Type 4	0.0344±0.0009	0.9063
Type 5	0.0319±0.0008	0.9441
Type 6	0.0376±0.0004	0.9166
Type 7	0.0289±0.0004	0.9118
Type 9	0.0343±0.0008	0.8905
Type 10	0.0412±0.0008	0.9294
Type 11	0.0539±0.0009	0.9058

Based on the results, the average critical hydraulic gradient for type two to seven is 0.0332 ± 0.0007 which means despite the differences in geometry or material properties in the experiments, the critical hydraulic gradient for suffusion is approximately located in a small zone.

4.3.3 Errors estimations

Measurements Errors

An important consideration in the experimental investigations is the way in which the obtained results can be interpreted. During the experimental testing of research, inaccuracies can affect the results. The absolute errors related to the measurement devices and tools are presented in table 4-6. To estimate the relative errors for erosion rate and hydraulic gradient the relative errors for connected parameters were added.

Table 4-6: Measurements errors

Measured quantities	unit	Absolute uncertainty (error)
Length	m	±0.0005
Water head	inch	±0.05
Mass of eroded soil	gr	±0.05
Time intervals	s	±0.5
Solid discharge *	$gr/cm^2/s$	(3.1890E-10) – (3.4388E-08)
Hydraulic gradient *	m/m	0.0002- 0.0013

*: Quantities obtained by calculation

The relative errors for different types of tests are shown in figure I-1and I-2. It could be noted that the error related to solid discharge is too small to be seen on the graph and the relative error of hydraulic gradient seems to be more important. Graph 4-20 and 4-21 indicate that as the hydraulic gradient increases, the absolute error increases as well.

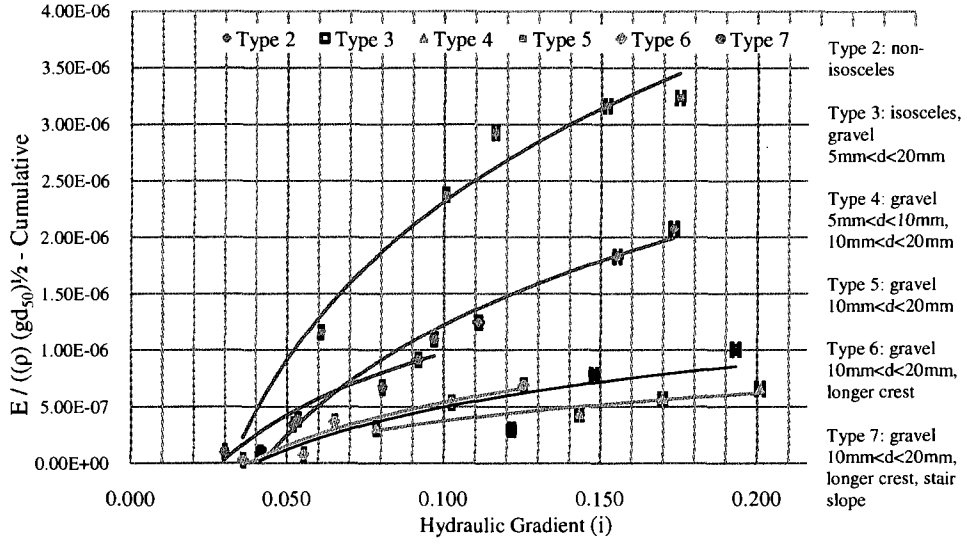

Figure 4-20: Estimated error for hydraulic gradient for test type 2 to 7

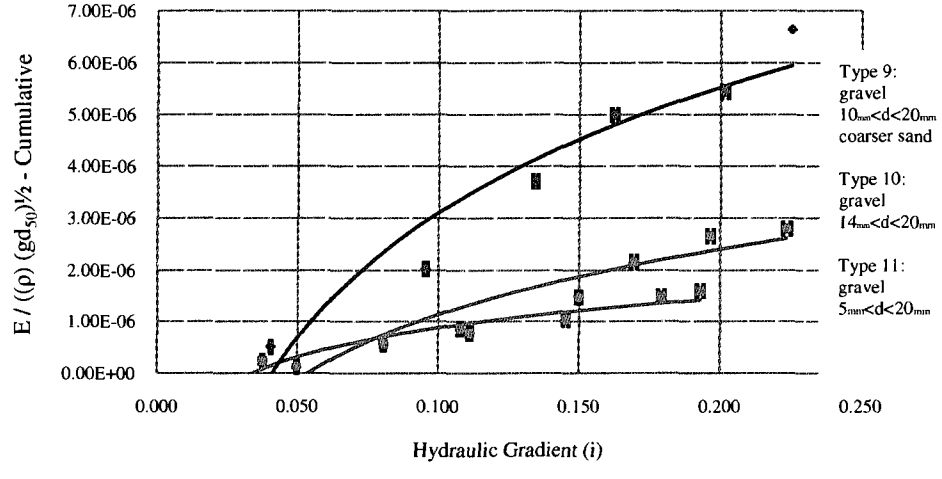

Figure 4-21: Estimated error for hydraulic gradient for test type 9 to 11

Constructions Errors

Some of the tests types were more than once. In some cases the model was re-constructed completely and in some the model was repaired. The comparison of these two showed that for having more accuracy the model should be re-constructed considering the same compaction. Figure 4-22 and 4-23 represents this comparison.

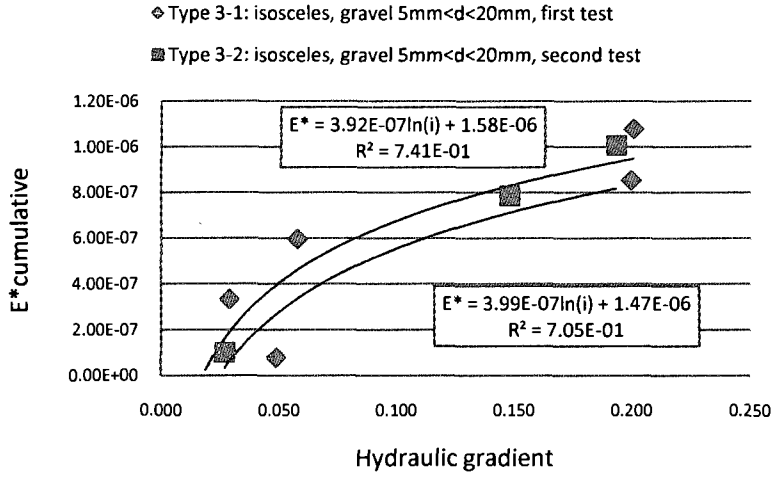

Figure 4-22: Comparison of two tests with re-construction

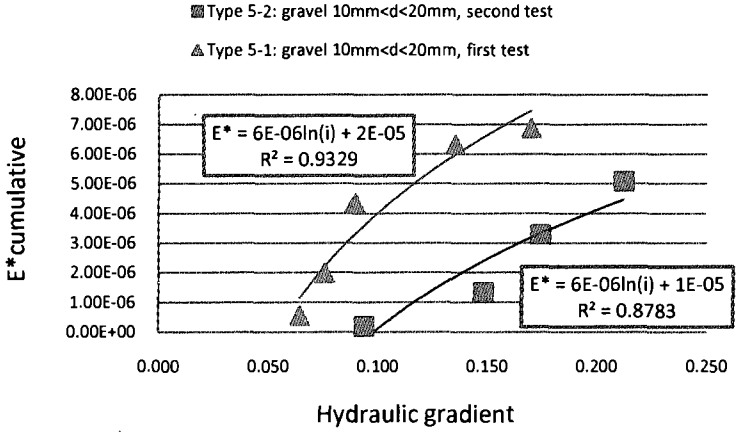

Figure 4-23: Comparison on two tests with model reparation

4.3.3.1 Successive experiments on the same model

Another phenomenon examined was the impact of repeating the procedure of water level augmentation on the upstream. In three tests, one from type five and two from type seven, after finishing the first try, water in upstream was decreased to the filter level and the experiments were redone after one or two hours. The results are shown in Figure 4-24. Reviewing the results indicate that there may not be a relationship between the successive tests, but results show that repeating the test brings about a lower erosion rate.

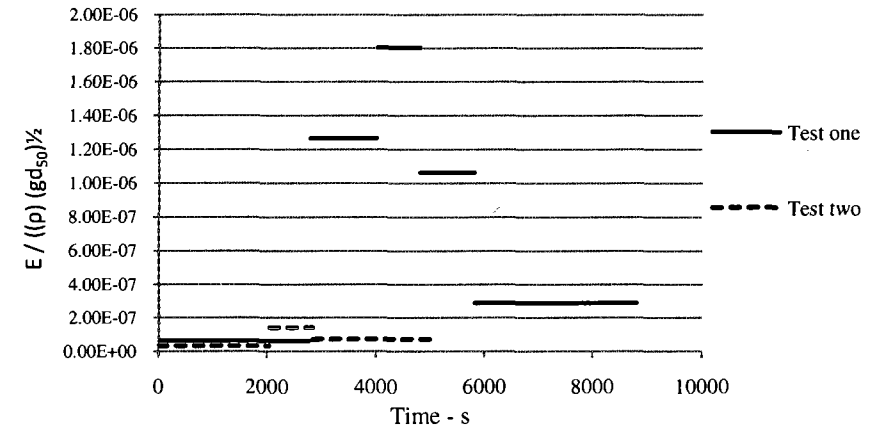

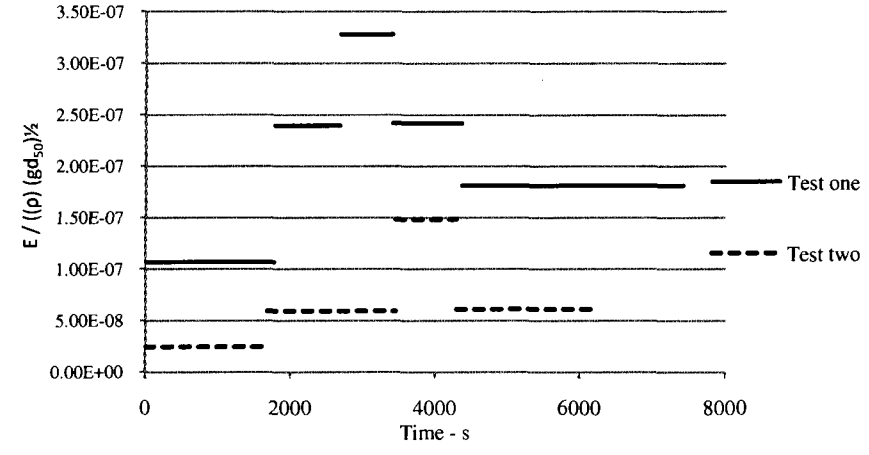

Figure 4-24: Dimensionless solid discharge in successive experiments

CHAPTER 5: CONCLUSION AND RECOMMENDATIONS

CONCLUSION

Series of different tests were executed in the Laboratory of Hydrodynamics at École polytechnique de Montreal. These studies focus on the initiation of external suffusion phenomenon due to water augmentation in the upstream. The results obtained from experiments that included the seepage of water through three different layers of clay/moraine, sand and gravel show that:

- Despite all of the differences between the experiments, the initiation of the hydraulic gradient of erosion approximately has the same value.
- The shape of the model, either increasing the filter crest length or stair like steps does not show significant changes in the initiation of the suffusion because of hydraulic gradient.
- The grain size distribution of the sand used as filter has a great impact on the suffusion. As the particles are finer, the rate of erosion is higher.
- Porosity and the particle size of gravel result in changes in the rate of suffusion. As the free space between particles increases, the rate of erosion increases as well.

SUGGESTONS

- Determining a relation between nonpermanent flow and the velocity.
- Determining a correlation between the critical hydraulic gradient and soil properties as porosity and grain size distribution.
- Executing more experimental investigation on both the models constructed from sands with different gradation while having identical gravels and the models consisted of gravel with different gradation and identical sand gradation to reach a more general result.
- Working with numerical modeling for a better understanding of particle movement.

Table 5-1: The experiment's specifications

Test type	Base Material		Filter Material		Geometry	Protection Material			Utility of the test	icr
	Material	d_{50} (mm) average	Material	d_{50} (mm) average		Material	d_{50} (mm) average	Particle size		
Type 1	Clay		Sand	0.85	non- isosceles trapezoid plexiglas beam on top	Gravel	18.33	$5_{mm}<d<20_{mm}$	Study the effect of seepage on the suffusion	0.0418
Type 2	Clay /Moraine		Sand	0.85	non- isosceles trapezoid	Gravel	18.33	$5_{mm}<d<20_{mm}$	Study of suffusion on non- isosceles embankment with well mixed gravel	0.0249
Type 3	Moraine	0.175	Sand	0.85	isosceles trapezoid	Gravel	18.33	$5_{mm}<d<20_{mm}$	Study of suffusion on an isosceles embankment with well mixed gravel	0.0344
Type 4	Moraine	0.175	Sand	0.85	isosceles trapezoid	Gravel	7.07 19.16	$5_{mm}<d<10_{mm}$ $10_{mm}<d<20_{mm}$	Study of suffusion on an isosceles embankment with two layer of gravel	0.0319
Type 5	Moraine	0.175	Sand	0.85	isosceles trapezoid	Gravel	19.16	$10_{mm}<d<20_{mm}$	Study of suffusion on an isosceles embankment with coarser particle of gravel	0.037
Type 6	Moraine	0.175	Sand	0.85	isosceles trapezoid Longer	Gravel	19.16	$10_{mm}<d<20_{mm}$	Study of suffusion on an isosceles embankment with coarser particles of gravel and a longer crest	0.0289
Type 7	Moraine	0.175	Sand	0.85	isosceles trapezoid longer stairs slopes	Gravel	19.16	$10_{mm}<d<20_{mm}$	Study of suffusion on an isosceles embankment with slopes in stairs, coarser particle gravel and a longer crest	0.0343
Type 8	Moraine	0.175	Sand	0.42	isosceles trapezoid	Gravel	19.16	$10_{mm}<d<20_{mm}$	Study of suffusion on an isosceles embankment containing finer particles filter	0.0412
Type 9	Moraine	0.175	Sand	1.20	isosceles trapezoid	Gravel	19.16	$10_{mm}<d<20_{mm}$	Study of suffusion on an isosceles embankment with coarser particles filter	0.0539
Type 10	Moraine	0.175	Sand	0.85	isosceles trapezoid	Gravel	18.8	$14_{mm}<d<20_{mm}$	Study of suffusion on an isosceles embankment with coarser particles of gravel	0.0418
Type 11	Moraine	0.175	Sand	0.85	isosceles trapezoid	Gravel	18.33	$5_{mm}<d<20_{mm}$	Study of suffusion on an isosceles embankment with mixed particles of gravel	0.0249

REFERENCES

1. Foster, M., R. Fell, and M.C.a.a.U.R.S.N.S.A. Spannagle, *Statistics of embankment dam failures and accidents.* Canadian Geotechnical Journal, 2000. **37**(5): p. 1000-1024.

2. Mattsson, H., J.G.I. Hellstrvm, and T.S. Lundstrvm, *On internal erosion in embankment dams: a literature survey of the phenomenon and the prospect to model it numerically.* 2008.

3. Wan, C.F. and R. Fell, *Assessing the potential of internal instability and suffusion in embankment dams and their foundations.* Journal of Geotechnical and Geoenvironmental Engineering, 2008. **134**(3): p. 401-407.

4. Bendahmane, F., D. Marot, and A. Alexis, *Experimental parametric study of suffusion and backward erosion.* Journal of Geotechnical and Geoenvironmental Engineering, 2008. **134**(1): p. 57-67.

5. Schuler, U., *How to deal with the problem of suffosion.* Research and Development in the Field of Dams, Swiss National Committee on Large Dams, 1995: p. pp. 145-159.

6. Kovac, G., *Seepage Hydraulics.* 1981: Elsevier Scientific Publishing Company, Amesterdam. 730.

7. Kenney, T.C. and D. Lau, *INTERNAL STABILITY OF GRANULAR FILTERS.* Canadian Geotechnical Journal, 1985. **22**(2): p. 215-225.

8. Istomina, V.S., *Filtration Stability of Soils.* Gostroizdat, Moscow-Leningrad, 1957.

9. Lubochkov, E.A., *Graphical and analytical methods for the determination of internal stability of filters consisting of non cohesive soil.* Izvestia, vniig, 1965. **78**: p. 255-280.

10. Kezdi, A., *Increase of protective capacity of flood control dikes.* Department of Geotechnique, Technical University, Budapest, Report, 1969. **1**.

11. De Mello, V.F.B., *Some lessons from unsuspected, real and fictitious problems in earth dam engineering in Brazil.* 1975.

12.Lafleur, J., J. Mlynarek, and A.L. Rollin, *Filtration of broadly graded cohesionless soils.* Journal of geotechnical engineering, 1989. **115**(12): p. 1747-1768.

13.Burenkova, V.V., *Assessment of suffosion in non-cohesive and graded soils.* Filters in geotechnical and hydraulic engineering. Balkema, Rotterdam, 1993: p. 357 360.

14.Kohler, H.J., *The influence of hydraulic head and hydraulic gradient on the filtration process.* Filters in geotechnical and hydraulic engineering. Edited by J. Brauns, M. Heibaum, and U. Schuler. Karlsruhe, Germany. October, 1992: p. 225 240.

15.Moffat, R.A. and R.J. Fannin, *A large permeameter for study of internal stability in cohesionless soils.* Geotechnical Testing Journal, 2006. **29**(4): p. 273-279.

16.Aberg, B., *Washout of grains from filtered sand and gravel materials.* Journal of geotechnical engineering, 1993. **119**(1): p. 36-53.

17.Fell, R., P. MacGregor, and D. Stapledon, *Geotechnical engineering of dams.* 2005: Taylor & Francis. Balkema, Leiden.

18.Fell, R. and J.J. Fry, *Internal Erosion of Dams and Their Foundations.* 2007.

19.Bakker, K.J., M.K. Breteler, and H. Den Adel, *New Criteria for Granular Filters and Geotextile Filters Under Revetments.* Coastal Engineering Conference, 1993. **1**: p. 1524-1524.

20.Worman, A. and R. Olafsdottir, *Erosion in a granular medium interface.* Journal of Hydraulic Research, 1992. **30**(5): p. 639-655.

21.Brauns, J. *Stability of layered granular soil under horizontal groundwater flow.* in *Proceedings 15th International Congress on Large Dams, IAUSANNE.* 1985.

22.Wörman, A., *Constitutive Equation for Filtration of Well Graded Base Soil with Flow Parallel to Base/Filter Interface.* 1996. p. 295 -304.

23.Bonelli, S., et al., *On the modelling of piping erosion.* Comptes Rendus de l'Academie des Sciences Serie II b/Mecanique, 2006. **334**(8-9): p. 555-9.

24.Fell, R. and J.J. Fry, *The state of the art of assessing the likelihood of internal erosion of embankment dams, water retaining structures and their foundations.* Internal Erosion of Dams and Their Foundations: Selected and Reviewed Papers from the Workshop on Internal Erosion and Piping of Dams and Their Foundations, Aussois, France, 25 27 April 2005, 2007: p. 1.

25.Ojha, C.S.P., V.P. Singh, and D.D. Adrian, *Determination of critical head in soil piping.* Journal of Hydraulic Engineering, 2003. **129**(7): p. 511-518.

26.Richards, K.S. and K.R. Reddy, *Critical appraisal of piping phenomena in earth dams.* Bulletin of Engineering Geology and the Environment, 2007. **66**(4): p. 381-402.

27.Sherard, J.L. and L.P.C.a.a.N.T.C.L.N.E.U.S. Dunnigan, *Critical filters for impervious soils.* Journal of geotechnical engineering, 1989. **115**(7): p. 927-947.

28.Terzaghi, K., *Soil mechanics a new chapter in engineering science: 45th James Forrest Lecture.* J. Instn Civ. Engrs, 1939. **12**: p. 106 141.

29.Tomlinson, S.S. and Y.P. Vaid, *Seepage forces and confining pressure effects on piping erosion.* Canadian Geotechnical Journal, 2000. **37**(1): p. 1-13.

30.Lafleur, J., *FILTER TESTING OF BROADLY GRADED COHESIONLESS TILLS.* Canadian Geotechnical Journal, 1984. **21**(4): p. 634-643.

31.Skempton, A.W. and J.M. Brogan, *Experiments on piping in sandy gravels.* Geotechnique, 1995. **45**(3): p. 565.

32.Kakuturu, S. and L.N. Reddi, *Evaluation of the parameters influencing self-healing in earth dams.* Journal of Geotechnical and Geoenvironmental Engineering, 2006. **132**(7): p. 879-889.

33.Wan, C.F. and R. Fell, *Investigation of rate of erosion of soils in embankment dams.* Journal of Geotechnical and Geoenvironmental Engineering, 2004. **130**(4): p. 373-380.

34.DVWK, *Merkblatter zur Wasserwirtschaft.* Heft 210, 1986.

35.Chapuis, R.P., A. Contant, and K.A. Baass, *Migration of fines in 0-20 mm crushed base during placement, compaction, and seepage under laboratory conditions.* Canadian Geotechnical Journal, 1996. **33**(1): p. 168-176.

36.Bakker, K.J., M.K. Breteler, and H. den Adel. *New criteria for granular filters and geotextile filters under revetments.* in *Proceedings of the 22nd International Conference on Coastal Engineering*. 1991. Delft, Neth: Publ by ASCE New York NY United States.

37.Buckingham, E., *On physically similar systems; illustrations of the use of dimensional equations.* Physical Review, 1914. **4**(4): p. 345-376.

38.Braja, M.D., *Advanced Soil Mechanics Second Edition.* 1997: Taylor & Francis Ltd.

39.McCarthy, D.F., *Essentials of soil mechanics and foundations: basic geotechnics.* 1988: Prenitce Hall, Engellwood Cliffs, New Jersey.

40.Howard, A.K., *Laboratory Classification of Soils: Unified Soil Classification System.* 1977: U. S. Bureau of Reclamation, Denver.

41.Lane, E.W., et al., *Report of the subcommittee on sediment terminology.* Transactions of the American Geophysical Union, 1947. **28**(6): p. 936-938.

42.White, F.M., *Fluid Mechanics, WCB.* 1999.

APPENDIX I: SOME ADDITIONAL RESULTS

Dimensionless solid discharge and hydraulic gradient versus time

Studying the changes of dimensionless solid discharge and hydraulic gradient during time intervals marked that an increase of hydraulic gradient does not necessarily cause the increase of dimensionless solid discharge. Figure 2 to 7, show dimensionless solid discharge and the hydraulic gradient relevant to it, on the same graph.

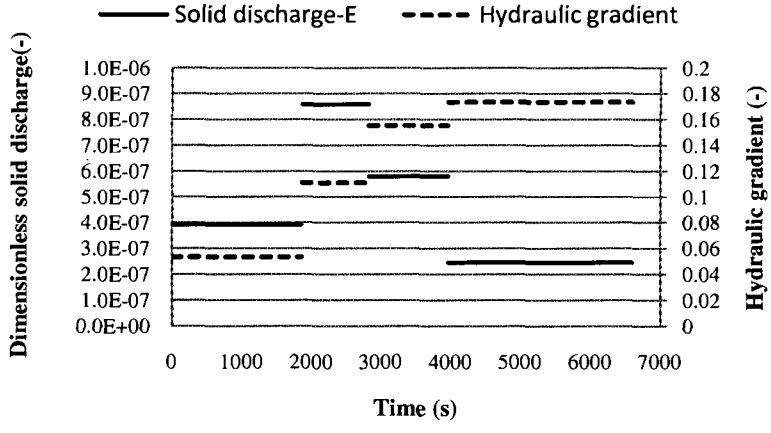

Figure 1: Solid discharge and hydraulic gradient vs. time- test type 2

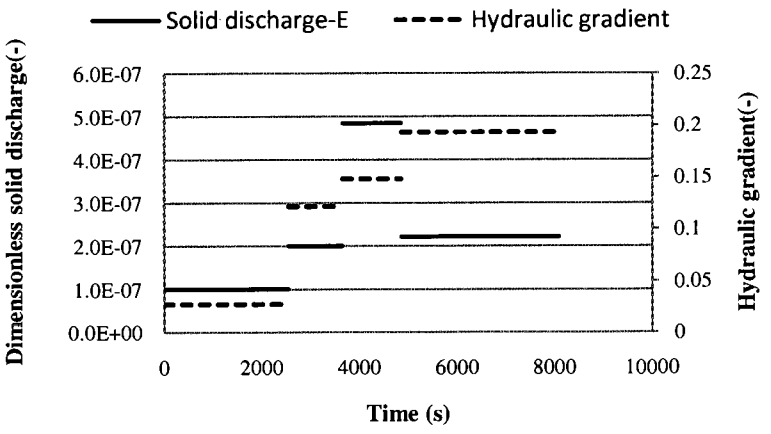

Figure 2: Solid discharge and Hydraulic gradient vs. time- test type 3

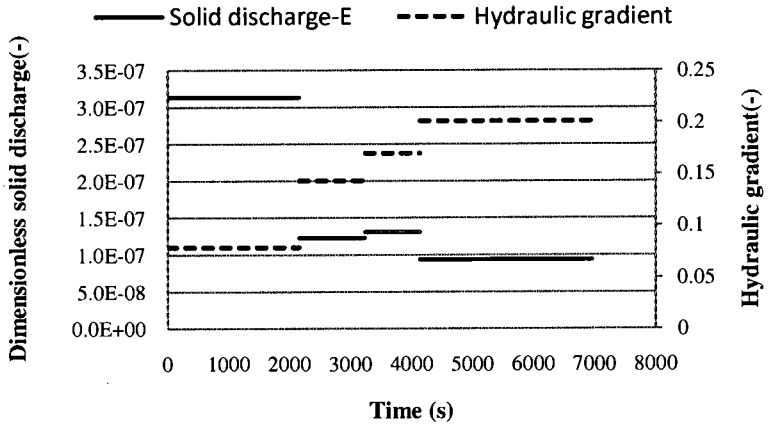

Figure 3: Solid discharge and Hydraulic gradient vs. time- test type 4

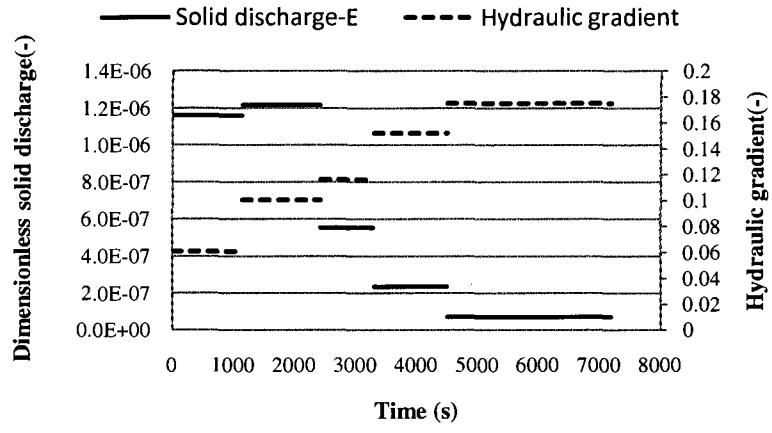

Figure 4: Solid discharge and Hydraulic gradient vs. time- test type 5

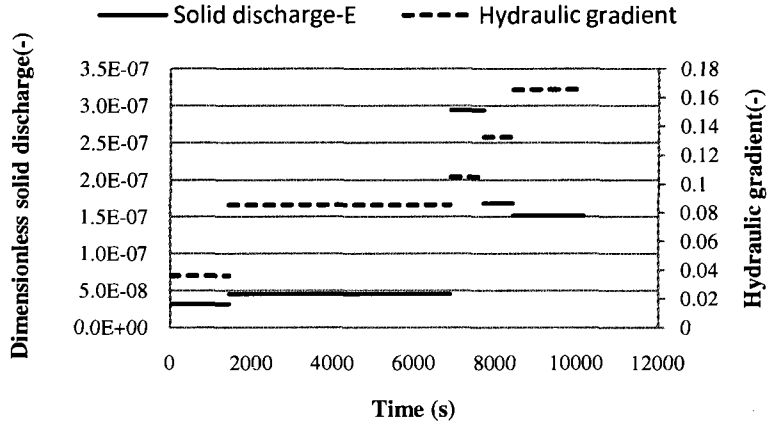

Figure 5: Solid discharge and Hydraulic gradient vs. time- test type 6

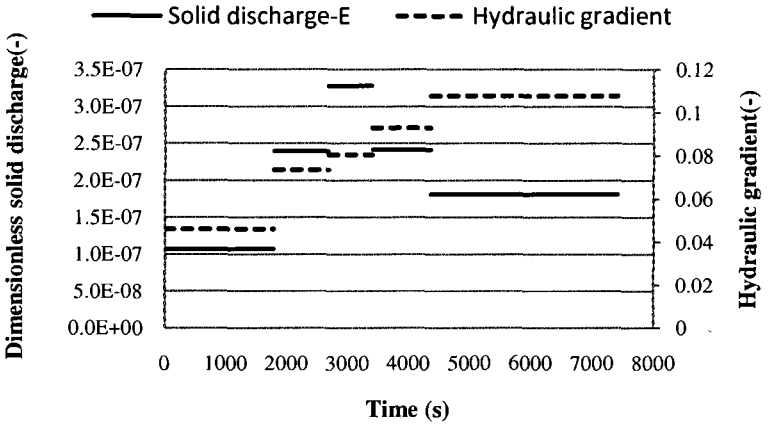

Figure 6: Solid discharge and Hydraulic gradient vs. time- test type 7

During all of the experiments, the water head was increased in the upstream to a maximum level, avoiding any overtopping, and at the same time the hydraulic gradient was raised gradually.

APPENDIX II: THEORETICAL DESCRIPTION

Man-made embankments were built from long ago for different purposes. The reserved water in upstream of embankments usually passes through them with the possibility to cause different problems during this passage.

The materials which are utilized in embankments construction are mainly soils. To survey the operation of embankments and the issues related to water flow, one need to know the soils properties and behaviors. In this part, a brief description about soil's components and the base relations which are mentioned in most soil mechanics and fundamental books such as M. Das [38], and McCarthy [39] is explained. At the end a brief discussion about the pi theorem and its usage in this work is given.

Soil weight-volume relationships, Void ratio, Porosity

The soil skeletons consist of mineral grains in different size and shapes and the void spaces existed between them; which are partly or fully filled with water or air. Solid particles, water and air perform soil as a three-phase system. Figure III-1 presents a schematic three-phase system for soil. The relationships of weight to the volume for analyzing the system are discussed below.

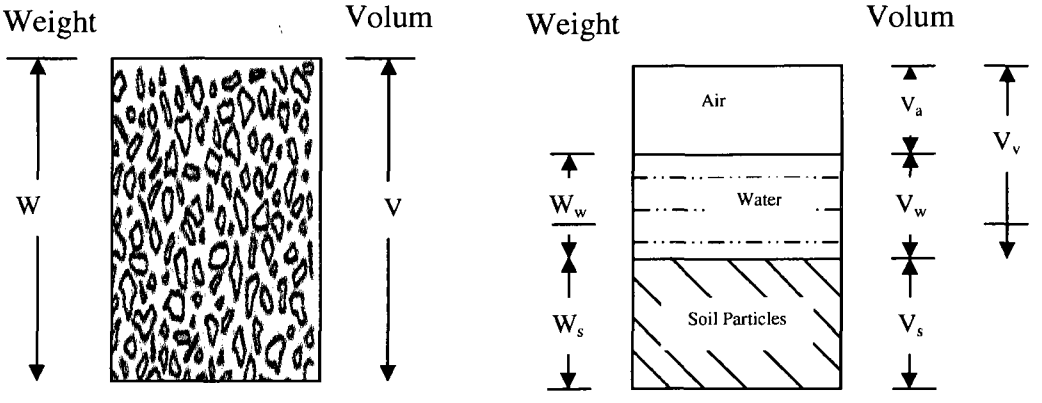

Figure 1: Weight-volume relationships for soil aggregates

A soil mass with the volume of V and weight of W on the left side and a schematic three-phase in the right size are discussed. The total weight (W) of the soil sample is equal to the weight sum of solid particles (W_s) and water (W_w). The assumed weight for the air is zero. The total volume of the soil skeleton (V) is the sum of the solid volume (V_s) and the volume of the water (V_w) and the air (V_a). The volume relations which are considered in soil studies are void ratio, porosity and degree of saturation.

The void ratio, e, describes the proportion of void's volume to the particle's volume which is expressed as a decimal.

$$e = \frac{V_v}{V_s} \quad (1)$$

Porosity, n, specifies the ratio of volume of voids to the total volume in a percentage format.

$$n = \frac{V_v}{V} \quad (2)$$

Degree of saturation and water content

Degree of saturation, S_r, is the ratio of the water volume to the void volume. It shows the portion of the void spaces filled with water as a percentage.

$$S_r(\%) = \frac{V_w}{V_v} \times 100 \quad (3)$$

Water content describes the portion of water weight to the dry solid weight as a percentage.

$$w(\%) = \frac{W_w}{W_s} \times 100 \quad (4)$$

Soil classification

As the soil is consisted of different particles, the best way to classify the soils is to determine the properties of its component grains.

Generally, the soils are categorized in to three main groups as gravel, sand, silt and clay. There exist different zone's limit divisions for these groups; nevertheless, these different size limits do not result in serious problems. Globally, in all divisions, gravel and sand are considered as coarse materials cause their grains are naturally visible and the silt and clay are called fine materials as most of their particles are not visible unaided.

One of the most popular grain size divisions is the USCS (Unified Soil Classification System) [40]. Table III-1 represents the size limits of the grain particles based on USCS.

Table 1: Unified soil Classification System

Classification	Size limits (mm)
Gravel	76.2-4.75
Coarse sand	4.75-2
Fine sand	2-0.425
Silt	0.425-0.075
Clay	< 0.075

To determine the classification of soil particles, one can utilize sieve analysis for coarse particles and sedimentation for fine particles in laboratory. The obtained results usually are explained in the form of a cumulative grain-size distribution.

Particle size distribution

The range of particle size from minimum to maximum can be determined by the sieve analysis in the laboratory. Some of the popular sieves specification, sieve number and the sized opening, is shown in table III-2 [41],[40].

Table 2: Different standard sieves and their sized opening

Sieve no.	U.S. Standard (mm)	Tyler Standard (mm)	British Standard (mm)
# 4	4.76	4.70	-
# 8	2.38	2.362	2.057
# 10	1.68	1.651	1.676
# 20	0.84	0.833	-
# 40	0.42	-	-
# 60	0.25	0.246	0.251
# 100	0.149	0.147	0.152
# 200	0.074	0.074	0.076
# 270	0.053	0.053	-
# 400	0.037	0.038	-

In the procedure of the sieve analysis, the cumulative weight of materials retained on each sieve to the total mass is calculated as a percentage. Presenting them on a semi logarithmic coordinate gives the grain size distribution curve. The horizontal logarithmic scale presents the sieve opening and the vertical arithmetic scale present the soil's cumulative weight percentage finer than a particular sieve opening size.

Relating to the range and amount of particle sizes the grain size distribution curves may be presented in different formats. Soils can be either well graded or poor graded. In case of poor gradation, two type of uniform–graded and gap-graded are imaginable. A good distribution of particles from small to large size which produce a longish straight curve presents the well-graded soil.

Soil basic parameters

Utilizing the gradation curve, three soil's basic parameters can be determined. Figure III-2 represents a sample gradation curve and the utilized parameters for basic relations are marked on the curve.

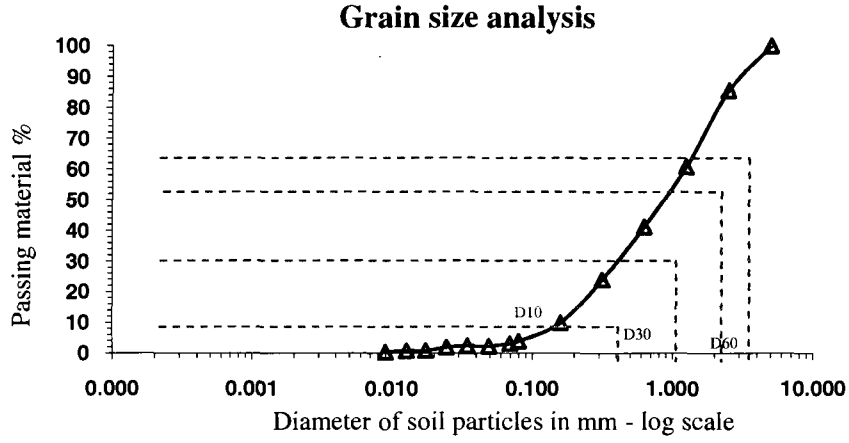

Figure 2: Grain size distribution of a sand soil sample

Effective size

D_{10}, the effective size, represents the size (diameter), through which 10% of particles are passing.

Uniformity coefficient

C_u, represents a proportional suggestion of the range of particle size.

$$C_u = \frac{D_{60}}{D_{10}} \quad (5)$$

Where

D_{60}: the diameter through which 60% of the total soil's mass pass
D_{10}: the diameter through which 10% of the total soil's mass pass

Sedimentation method

To obtain the distribution of fine particles, like clay and silt, the sedimentation method is utilized in the laboratory. Soil sample is placed in a solution with distilled water and

the settlement of soil particles in the solution is allowed. The decreasing average specific gravity during settling by using a hydrometer in different time intervals is verified. With considering stokes equation for spheres falling freely in a known fluid, the data are used to provide the diameter of particles and the weight percentage that is finer than a particular size.

Seepage

Due to different and irregular shape of soil's grains, there exist pores and void spaces between solid particles being interconnected. Water is capable of flowing through the pore spaces in the soil. It actually travels through the connected voids. Water passage through the soil may affect the properties and behavior of particles. Either the construction operation or construction's performance can be influenced by these affections.

Some of the factors that can affect the water movement through the soil are, pressure differences between two points in the water flow path (water moves from a point with a higher energy to the point with lower energy), the density and viscosity of water, size, shape and arrangement of the particles, mineral or electrochemical properties of the water and soil particles but not all the influences of these factors are clarified.

Velocity, Permeability and Hydraulic gradient

The velocity of seepage usually is very low that can be negligible. The exception is when the water velocity is great enough to start moving or eroding the grain particles. To determine the quantity of flow, an average discharge velocity is considered. The discharge velocity is the volume of flow by total area (soil and voids) normal to the flow direction in per unit time. For average seepage velocity one can divide the discharge velocity by the porosity of soil. Studying the water velocity through the soils indicate the influence of void's size and the hydraulic gradient i on it.

As a soil's property, permeability shows the tendency of the soil to let the water seep through its interconnected spaces. The factors that may influence the permeability are the water viscosity, size and shape of the soil particles, degree of saturation, and void ratio. Based on the pore size and their connectivity, values of permeability change. Soils with coarser particles have the higher permeability compare to the soil with fine particles. The dimension of permeability is the same as velocity and usually is expressed as (cm/s) or (mm/s).

Filter design

Embankment dams usually consist of different parts with special specific functions for each. The transition or shell (gravel) zone contains the pervious material and satisfy the structural strength of the embankment. The core (base) zone is the main part of the dam and usually consists of an impervious material. Its role is to prevent water passage through the dams. Filter is a porous medium, consisting of solid particles and the empty spaces between them. Filter's design purpose is to protect the base layer against erosion and piping (prevent the loss of fine particles), seepage control and authorization of water crossing the core freely.

The productivity of filter is influenced by the size and connection of voids between its particles. Filters should have sufficient discharge capacity and a higher permeability compare to the base soil, resulting in larger grain size towards core layer solid particles. It should be considered that different parameters may influence the operation of filters. Properties of the used materials including the gradation curve, particle's shape, fine part's amount and the internal stability, relative density and compaction of filter, hydraulic gradient, material's chemical properties and filter thickness are some of these factors. For design of filters, the necessary terms which should be considered are [28]:

- Piping or Stability requirement

Seepage of water from a soil with fine grains to a soil with coarse grains may wash out the fine parts into the voids in between the coarser parts. Based on the grain size relation between base and filter material, filters should be able to prevent the movement of protected soil into the filter zone.

To satisfy this necessitate, Terzaghi and Peck [28] based on experimental investigations, presented the below criteria

$$\frac{D_{15(F)}}{D_{85\,(B)}} \leq 4 \; or \; 5 \quad (22)$$

Where

$D_{15\,(F)}$: the diameter through which 15% of filter material pass
$D_{85\,(B)}$: the diameter through which 85% of protected soil pass

- Permeability requirement

  The particles should be coarse enough to allow the seepage flow pass through the filter and prevent the buildup of high pore pressures and hydraulic gradients.

  Based on Terzaghi [28] investigations relationship 23 can satisfy this need.

$$\frac{D_{15(F)}}{D_{15\,(B)}} \geq 4 \; or \; 5 \quad (23)$$

  Where

  $D_{15\,(B)}$: the diameter through which 15% of protected soil pass

For filter material as sand, to prevent bulking during the compaction, materials should be saturated as much as possible.

Buckingham's pi theorem

To decrease the number and complexity of experimental variables affecting the physical phenomenon, one can use dimensional analysis [42]. Considering a phenomenon with n dimensional variables, using the dimensional analysis can reduce

n, to k dimensionless variables and this reduction can be from one to four depending upon the problem complexity.

In a dimensional analysis the factors could be:

- Dimensional variables

  Which are variable dimensional quantities during a specified case; by being plotted in terms of each other they show data. They are transformable to dimensionless value.

- Dimensional constant

  The dimensional values those are invariable during a given run. Having the possibly of being dimensionless, they are normally used to help the process of nondimensionalizing.

- Pure constant

  Arising from mathematical manipulations, have no dimensions and never did.

- Naturally dimensionless physical variables

  By virtue of their definition as ratios of dimensional quantities

The two assumptions for dimensional-analysis method are

- The dimensional homogeneity of proposed physical relation
- Comprising of all relevant variables in the proposed relation

One of the dimensional analysis methods is the Buckingham's pi theorem which was presented by Buckingham [37]. In this method different dimensionless groups are found as the power products of affected variables, denoted by π_1, π_2, π_3, etc.

Considering a physical process with n dimensional variables which contain m primary dimensions, the relating equation will have (n-m) dimensionless groups. Finding (n-

m) =k, k scaling variables not forming a pi between themselves, is selected. Each pi group is power product of k variables plus one additional variable and dependent.

The concluding equation obtained has the form of:

$$\pi_1 = f(\pi_2, \pi_3, \ldots\ldots \pi_{n-m})$$

Pi theorem and erosion

The phenomenon of erosion, considering the mobile bottom of uniform soil particles (with diameter d, specific volume γs), can be described as uniform and permanent with three constitutes: fluid, non-cohesive particles and the seepage.

1. Fluid:
   - Density, ρ (ML^{-3})
   - Dynamic viscosity, μ ($ML^{-1}T^{-1}$)

2. Non- cohesive particle
   - Density, ρ_s (ML^{-3})
   - Grain diameter, d (L)
   - Soil volume, V (L^3)
   - Void volume, V_v (L^3)

3. Seepage
   - Δh, water head drop (L)
   - L, water path length (L)
   - Acceleration of gravity, g (LT^{-2})

So, the erosion rate of non-cohesive soil particles from a mobile bed can be defined by the following ten parameters

$$\rho, \mu, \rho_s, d, V, V_v, \Delta h, L, g, E$$

To have a more facile quantification of erosion rate some of the above mentioned parameters can be transformed to the more known variables. One can consider:

Hydraulic gradient (i) as $\frac{\Delta h}{L}$ and porosity (p) as $\frac{V_v}{V}$, could be two dimensionless groups. In this case, the erosion rate is related to eight parameters

$$\rho, \mu, \rho_s, d, p, i, g, E$$

Having eight parameters and three primary dimension (MLT) five groups of non dimensional parameters could be generated, having hydraulic gradient and porosity, the ρ, d and g are chosen as the base quantities, choosing E as the forth parameter one reaches $\left(\frac{E}{\sqrt{\rho^2 gd}}\right)$, and the group of ρ, d, g and μ ,one can reach $d\left(\frac{g}{v^2}\right)^{\frac{1}{3}}$ that is the dimensionless diameter d* . As the last group of dimensionless parameter, the relative density $\left(\frac{\rho_s}{\rho}\right)$ could be considered.

Now the rate of erosion could be expressed as

$$A = f_A\left(d_*, p, i, S_s, \frac{E}{\sqrt{\rho^2 gd}}\right)$$

In these series of experiment, using one type of sand for different tests may help in assuming that the porosity, relative density and dimensionless diameter are approximately constant, so the rate of erosion could be defined as related to hydraulic gradient.

$$E_* = f(i) \qquad \text{Or} \qquad \frac{E}{\sqrt{\rho_w^2\, g\, d}} = f\left(\frac{\Delta h}{L}\right)$$